



UNIVERSITEIT VAN PRETORIA
UNIVERSITY OF PRETORIA
YUNIBESITHI YA PRETORIA

Investigating the effect of the heavy metals cadmium, lead and chromium, alone and in combination on the components of the coagulation system

Submitted in partial fulfilment for the degree Magister Scientiae in Anatomy with specialization in Human Cell Biology

Department of Anatomy, Faculty of Health Science, University of Pretoria

Liselle Pretorius

16004273

Supervisor: Prof HM Oberholzer¹

Email: nanette.oberholzer@up.ac.za

Co-supervisors:

Dr H Taute¹

Email: helena.taute@up.ac.za

Dr M van Rooy²

Email: mia.vanrooy@up.ac.za

Department of Anatomy¹, Department of Physiology²

Faculty of Health Science

27 August 2021

Declaration

I, **Liselle Pretorius**, declare that this dissertation entitled: “**Investigating the effect of the heavy metals cadmium, lead and chromium, alone and in combination on the components of the coagulation system**” which I hereby submit for the degree **Magister Scientiae in Anatomy with specialization in Human Cell Biology** at the University of Pretoria, is my own work and has not previously been submitted by me for a degree at this or any other tertiary institution.

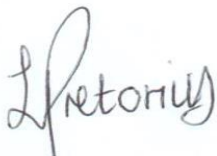
I understand what plagiarism is and am aware of the University’s policy in this regard.

I declare that this dissertation is my own original work. Where other people’s work has been used (either from a printed source, internet or any other source), this has been properly acknowledged and referenced in accordance with departmental requirements.

I have not used work previously produced by another student or any other person to hand in as my own.

I have not allowed, and will not allow, anyone to copy my work with the intention of passing it off as his or her own work.

The author, **Liselle Pretorius**, has obtained for the research described in this work, the applicable research ethics approval. The author declares that they have observed the ethical standards required in terms of the University of Pretoria’s code of ethics for researchers and the policy guidelines for responsible research.



.....

Signature

10 December 2021

.....

Date

Acknowledgements

“And whatever you do, whether in word or deed, do it all in the name of the Lord Jesus, giving thanks to God the Father through him.”

Colossians 3:17

First of all, I would like to thank God for providing me with this opportunity and giving me the wisdom and guidance to achieve my goals.

I would also like to express my deepest appreciation to my supervisor, Prof Nanette Oberholzer, for her valuable advice, constructive criticism and unwavering support. Her knowledge and guidance have inspired me to become the researcher I am today.

I am grateful to both my co-supervisors for their helpful contributions. Many thanks to Dr Helena Taute, for her assistance and guidance in the laboratory. Her knowledge and advice were of great value to me. I also wish to thank Dr Mia van Rooy, for extending her assistance in acquiring and analysis of the TEG results.

Special thanks to the staff at the Laboratory for Microscopy and Microanalysis of the University of Pretoria, for the use of their microscopes and their assistance.

I would like to acknowledge the help I received from Dr June Serem, with her assistance regarding statistical analysis.

Thanks should also go to Dr Giel Roode, Prof Prashilla Soma and the nursing staff at Prinshof Student Healthcare Clinic at the University of Pretoria, for their assistance with the phlebotomy and the volunteers for generously donating blood for this study.

Lastly, I am extremely grateful to my parents for supporting me, as the completion of my dissertation would not have been possible without their love, encouragement and unwavering support.

Investigating the effect of the heavy metals cadmium, lead and chromium, alone and in combination on the components of the coagulation system

By

LISELLE PRETORIUS

Supervisor: Prof HM Oberholzer¹

Co-supervisors: Dr H Taute¹ and Dr M van Rooy²

Department: Anatomy¹ and Physiology²

Degree: MSc (Anatomy with specialization in Human Cell Biology)

Abstract

In recent years, heavy metal exposure has become a serious concern for the health care sector as more humans are being exposed to heavy metals each day. Most of the environmental contamination and human exposure result from anthropogenic activities such as mining and smelting. The industrial and agricultural sectors also play a big role. Cigarette smoke in particular contains trace amounts of heavy metals that puts chronic smokers at serious risk. Previous studies have determined that there is a strong correlation between heavy metal exposure and the production of reactive oxygen species and nitric oxide formation.

Therefore, the aim of this study was to investigate the effect of cadmium (Cd), lead (Pb) and chromium (Cr) alone and in combination on the erythrocytes and fibrin networks of the coagulation system in human blood. In addition, the ability of these metals to produce reactive oxygen species and nitrite were also determined. The choice of metals for this study were based on a previous study that compared the levels of metals between smokers and non-smokers and found significantly higher levels of Cd, Pb and Cr in the platelet-rich fibrin of smoking individuals.

Whole blood was collected from ten volunteers (non-smokers) and exposed to x1, x10 and x100 the heavy metal concentration found in platelet-rich fibrin of cigarette smokers. The scanning electron microscopy analysis revealed that the Cd + Cr combination groups caused the highest degree of echinocyte formation and fibrin network alterations. These findings were supported by the thromboelastography® analysis that indicated a significant decrease in R-time and SP-values for the Cr-containing group, suggesting a shorter initiation time for clot formation. This may explain why considerable fibrin formation was observed in the Cr-exposed groups (alone or in combination) and support the fact that heavy metals have the ability to influence clot formation and increase the risk of thrombosis. The dichloro-dihydro-fluorescein diacetate (DCFH-DA) analysis revealed that the x10 Cd and Pb-exposed groups showed a considerable amount of reactive oxygen species production, compared to the other groups, which can potentially cause oxidative stress. No significant changes were observed in blood nitrite levels in any of the exposure groups.

Therefore, the increased production of reactive oxygen species, altered red blood cell and fibrin network morphology as well as a decrease in some of the coagulation parameters support the hypothesis that the coagulation pathway is a potential target for heavy metal toxicity.

Keywords: Cadmium, chromium, coagulation system, heavy metals, lead, reactive oxygen species, reactive nitrogen species, scanning electron microscopy, smoking, thromboelastography, whole blood.

Table of Content

Chapter 1: General Introduction	2
Chapter 2: Literature Review	5
2.1. Source and bio-accumulation of heavy metals	5
2.1.1. Cadmium.....	6
2.1.2. Lead.....	7
2.1.3. Chromium	7
2.2. ADME of heavy metals.....	8
2.2.1. Cadmium.....	8
2.2.2. Lead.....	10
2.2.3. Chromium	10
2.3. The coagulation system and heavy metal toxicity.....	12
2.4. Influence of ROS and NO on the coagulation system.....	14
2.5. Previous studies on heavy metal toxicity	15
2.6. Aim and objectives	18
2.7. Ethical consideration	19
2.8. Data management.....	20
2.9. Funding.....	20
Chapter 3: The effect of cadmium, lead and chromium alone and in combination on fibrin networks and erythrocyte morphology	22
3.1. Introduction	22
3.2. Materials and Methods	24

3.2.1.	Metal preparations	24
3.2.2.	Blood collection	24
3.2.3.	Sample preparation for SEM	25
3.3.	Results	26
3.4.	Discussion.....	37
3.5.	Conclusion	39
Chapter 4: Thromboelastography: The effect of metals on coagulation parameters		42
4.1.	Introduction	42
4.2.	Materials and Methods	43
4.2.1.	Metal preparation	43
4.2.2.	Blood collection	44
4.2.3.	Sample preparation for TEG®	44
4.2.4.	Statistical Analysis	44
4.3.	Results.....	44
4.4.	Discussion.....	51
Conclusion.....		55
Chapter 5: The effect of cadmium, lead and chromium, alone and in combination on ROS formation		57
5.1.	Introduction	57
5.2.	Materials and Methods	58
5.2.1.	Metal preparation	58
5.2.2.	Blood collection	58
5.2.3.	Sample preparation for DCFH-DA assay.....	59

5.2.4.	Sample preparation for the haemolysis assay	59
5.2.5.	Statistical Analysis	60
5.3.	Results	60
5.3.1.	The effect of heavy metals on ROS production	60
5.3.2.	The haemolytic effect of heavy metals	65
5.4.	Discussion.....	66
5.5.	Conclusion	69
Chapter 6: The effect of cadmium, lead and chromium on nitrite levels		71
6.1.	Introduction	71
6.2.	Materials and methods	72
6.2.1.	Metal preparation	72
6.2.2.	Blood collection	72
6.2.3.	Sample preparation for the Griess assay.....	73
6.2.4.	Statistical analysis.....	73
6.3.	Results	74
6.3.1.	The effect of heavy metals on nitrite formation	74
6.4.	Discussion.....	78
6.5.	Conclusion	80
Chapter 7: Concluding discussion		82
7.1.	Summarised results.....	82
7.2.	Limitations and future prospective	83
Chapter 8: References		Error! Bookmark not defined.

Chapter 9: Appendices97

9.1. Ethical clearance certificate.....97

9.2. Patient informed consent documents98

9.3. Originality report.....102

List of Tables

Table 3.1:	The concentrations and volume of whole blood exposed to different heavy metals.....	24
Table 3.2:	Summary of the changes observed in whole blood with added thrombin, exposed to metal combinations at different concentrations.	35
Table 3.3:	Summary of SEM analysis in whole blood with added thrombin, exposed to metal combinations at different concentrations.	36
Table 4.1:	Whole blood parameters, measured by the TEG®.....	43
Table 4.2:	Summary of the effects of Cd, Pb and Cr, alone and in combination, at x100 concentration found in cigarette smoke on the parameters of whole blood. ...	47
Table 4.3:	Summary of the effects of Cd, Pb and Cr, alone and in combinations, at the x100 concentration of each respective metal, on the various parameters of whole blood. The data represents the average of ten volunteers.	48
Table 5.1:	Summary of the effect of Cd, Pb and Cr, alone and in combination on ROS production at x1, x10 and x100 the concentration found in cigarette smoke ..	65
Table 6.1:	Summary of the effect of Cd, Pb and Cr, alone and in combination on nitrite production at x1, x10 and x100 the concentration found in cigarette smoke ..	77

List of Figures

Figure 2.1:	Basic flow diagram of how Cd is transported through the body, synthesis and degradation in liver and kidney tissue	9
Figure 2.2:	Diagram of the intracellular uptake and DNA damage due to Cr(VI) toxicity ..	12
Figure 2.3:	Diagram of the cell- based model for the coagulation pathway	14
Figure 2.4:	Flow diagram of the objectives of this research project.....	19
Figure 3.1:	Scanning electron micrographs of whole blood with thrombin exposed to Cd, Pb and Cr, alone and in combination at concentrations x1, x10 and x100 showing fibrin network formation together with erythrocytes	33
Figure 3.2:	Representative SEM micrographs of erythrocytes prepared from whole blood with added thrombin, exposed to metals; scale bars.....	34
Figure 4.1:	The graphical waveform representation of a normal TEG [®] tracing.....	43
Figure 4.2:	Representative TEG [®] viscoelastic traces of the control and metal groups	49
Figure 4.3:	Graphical representation of the mean and standard deviation (error bars) for the coagulation parameters	51
Figure 5.1:	The effects of Cd, Pb and Cr alone and in combination on ROS production (%) evaluated at x1 the concentration found in PRF exposed to cigarette smoke	61
Figure 5.2:	The effects of Cd, Pb and Cr alone and in combination on ROS production (%) evaluated at x10 the concentration found in PRF exposed to cigarette smoke	62
Figure 5.3:	The effects of Cd, Pb and Cr alone and in combination on ROS production (%) evaluated at x100 the concentration found in PRF exposed to cigarette smoke	63
Figure 5.4:	Effect of heavy metals on ROS production (%), evaluated at x1, x10 and x100 the concentration found in PRF exposed to cigarette smoke	64
Figure 5.5:	The haemolytic effects of Cd, Pb and Cr alone and in combination at x1, x10 and x100 the concentration found in PRF exposed to cigarette smoke	66

Figure 6.1	The effects of Cd, Pb and Cr alone and in combination on nitrite production (%) evaluated at x1 the concentration found in PRF exposed to cigarette smoke..	75
Figure 6.2:	The effects of Cd, Pb and Cr alone and in combination on nitrite production (%) evaluated at x10 the concentration found in PRF exposed to cigarette smoke	75
Figure 6.3:	The effects of Cd, Pb and Cr alone and in combination on nitrite production (%) evaluated at x100 the concentration found in PRF exposed to cigarette smoke	76
Figure 6.4:	The effects of Cd, Pb and Cr alone and in combination on nitrite production (%) evaluated at x1, x10 and x100 the concentration found in PRF exposed to cigarette smoke	77

List of Abbreviations and Acronyms

%	Percentage
ml	Millilitre
µl	Microlitre
µM	Micromolar
AAPH	2,2'-Azobis(2-amidinopropane) dihydrochloride
ADME	Absorption, distribution, metabolism and excretion
AEC	Animal Ethics Committee
Alb	Albumin
ANOVA	Analysis of variance
As	Arsenic
Asc	Ascorbate
Ca	Calcium
Cd	Cadmium
CdCl₂	Cadmium chloride
CVD	Cardiovascular disease
Cr	Chromium
CrCl₂	Chromium chloride
CLSM	Confocal laser scanning microscopy
Cu	Copper
Cys	Cysteine
DNA	Deoxyribose nucleic acid
DMD's	Dense matted deposits
DCFH-DA	Dichloro-dihydro-fluorescein diacetate
DCPIP	2,6-Dichlorophenolindophenol
ddH₂O	Double distilled water
EtOH	Ethanol

EVAC	Vacuum extraction
GSH	Glutathione
Hg	Mercury
HMDS	Hexamethyldisilazane
IARC	International Agency of Research on Cancer
isoPBS	Isotonic phosphate buffer saline
LPS	Lipopolysaccharide
MT	Metallothionein
min	Minutes
Ni	Nickel
NO	Nitric oxide
NO₂⁻	Nitrite
NO₃⁻	Nitrate
eNOS	Endothelial nitric oxide synthase
NOS	Nitric oxide synthase
NRC	National Research Council
Pb	Lead
PbCl₂	Lead chloride
PbS	Galena
ppm	Parts per million
PRF	Platelet-rich fibrin
PS	Phosphatidylserine
ROS	Reactive oxygen species
RBC	Red blood cells
SE	Standard error
SEM	Scanning electron microscopy
SD	Standard deviation
TEG	Thromboelastography

TEM	Transmission electron microscopy
TAC	Total antioxidant capacity
TF	Tissue factor
UPBRC	University of Pretoria Biomedical Research Centre
vWF	von Willebrand factor
WHO	World Health Organization
Zn	Zinc

Chapter 1

Chapter 1: General Introduction

In recent years, heavy metal exposure has become a serious concern for the health care sector as more humans are being exposed to them each day. These elements are considered dangerous because they tend to bioaccumulate in the body and increase in concentration over time (Hanfi *et al.*, 2019). Most of the human contamination originates from anthropogenic activities like mining and smelting. The industrial and agricultural sector also play a big role, along with volcanic eruptions and toxic gas emissions (Yang *et al.*, 2005).

Cigarette smoke in particular contains trace amounts of heavy metals that puts chronic smokers at serious risk (Caruso *et al.*, 2013). The metals found in tobacco smoke that are commonly associated with health effects include arsenic (As), cadmium (Cd), chromium (Cr), nickel (Ni), and lead (Pb) (Caruso *et al.*, 2013). Most of these metals are identified as carcinogenic to humans by the International Agency for Research on Cancer (Caruso *et al.*, 2013). According to a 2017 survey conducted by the Southern Africa Labour and Development Research Unit approximately 20% of South African adults are regular cigarette smokers (Vellios, 2021). It is estimated that cigarette smoking leads to 44 000 deaths per year in South Africa, equating to 121 deaths per day (Vellios, 2021). Smoking-related diseases are associated with nicotine addiction, leading to the repeated inhalation of a variety of toxins each day (Gaziano, 2005; Gidlow, 2004; Jomova and Valko, 2011).

Other sources of heavy metals include chemicals like fungicides and pesticides, medication, fuel, electrical wires and cosmetic products. Humans may also be exposed to heavy metals through occupations like welding or working in factories that use metals like Ni, copper (Cu) and Zn (Adial and Wiener, 2018). Exposure to these sources for long periods can lead to accumulation of heavy metals in the body and eventual toxicity. Metals such as Cd, Pb and Cr are essential elements required by the body for various biochemical and physiological functions (Kampa and Castanas, 2008). A concentration that is higher than the common threshold can result in a variety of diseases or syndromes (Kampa and Castanas, 2008).

Heavy metals can affect the liver, gastrointestinal tract, kidneys, brain, heart, blood, skin or eyes – depending on the route of exposure (Muhammad Waqar, 2012). Over the last couple of years, there have been an increase in the number of people diagnosed with cardiovascular diseases (CVD) such as strokes, myocardial infarctions and venous thrombo-emboli (Steven *et al.*, 2019). Various studies suggest that a wide range of heavy metals have the potential to induce erythrocyte damage, increase platelet aggregation and alter the coagulation

parameters, thereby increasing the risk of thrombosis (Gaziano, 2005; Steven *et al.*, 2019; Watt *et al.*, 2012). There is also a strong correlation between heavy metal exposure and the production of reactive oxygen species or nitric oxide in cells (Aggarwal *et al.*, 2019; Cimmino *et al.*, 2015; Simon and Fernandez, 2009).

Previous studies have used concentrations of heavy metals based on the World Health Organization's (WHO's) minimum acceptable limits in drinking water (Arbi *et al.*, 2017; Naidoo *et al.*, 2019; Venter *et al.*, 2017b). For the current study, the focus is shifted towards heavy metals present in cigarette smoke. Therefore, the aim of this study was to investigate the effect of Cd, Pb and Cr, alone and in combination on the platelets, erythrocytes and fibrin network of the coagulation system in human blood. In addition, the ability of these metals to produce reactive oxygen species (ROS) and nitrite were determined. The reason for these metals being tested alone and in combination was that exposure is often not limited to one metal at a time but a combination of different metals at various concentrations, as in the case of cigarette smoke. The literature review focussed on the bio-accumulation, absorption, distribution, metabolism, excretion (ADME) and toxicity of these heavy metals as well as the role they play in human health (Yaprak and Yolcubal, 2019).

Chapter 2

Chapter 2: Literature Review

2.1. Source and bio-accumulation of heavy metals

The use of tobacco products has steadily been increasing all over the world and in turn the rate of nicotine addiction has also increased (Muhammad Waqar, 2012). The repeated inhalation of nitrosamines, volatile organic compounds, polycyclic aromatic hydrocarbons and toxic heavy metals are the causes of many smoking-related diseases like cancer, strokes, diabetes and heart disease. The term heavy metal refers to any metallic element with a relatively high density and the ability to cause toxicity (Caruso *et al.*, 2013). These naturally occurring components of the Earth's crust enter our bodies via drinking water, food and air. Although the majority of these trace elements are essential for maintaining a healthy metabolism in the human body, higher concentrations can lead to poisoning due to bioaccumulation in the body over time (Hanfi *et al.*, 2019).

Cadmium is a class 1 carcinogen (carcinogenic to humans) and has a high transfer range (22%) into smoke compared to other components. Chromium is also considered class 1 with a transfer range of 1.74% and Pb has been elevated from class 2B (possibly carcinogenic to humans) to a class 2A (probably carcinogenic to humans) carcinogen with a transfer range of 6.3% (Muhammad Waqar, 2012). Cadmium and Pb have long (10-12 years) half-lives in the human body, which make them particularly dangerous because of its ability to accumulate in tissue. Cigarette smoke is one of the largest sources of Cd (and to a lesser extent Pb) exposure in the general population. It is estimated that through smoking one packet (20 cigarettes) each day, 2-4 µg of Cd, 1-5 µg of Pb and 1-3 µg of Cr can be deposited into the lungs of smokers and non-smokers alike (Caruso *et al.*, 2013; Muhammad Waqar, 2012).

The trace amounts of heavy metals found in tobacco can differ depending on where and how it is grown and processed. Tobacco grown in China contains higher levels of Cd and Pb compared to tobacco grown elsewhere (Caruso *et al.*, 2013). This might be attributed to environmental pollution and the type of fertilizer or pesticide used. The pH of the soil can also influence the rate of metal uptake. Other potential metal sources include humectants and flavourings used in the manufacturing process (Muhammad Waqar, 2012).

2.1.1. Cadmium

Cadmium is a rare metal that makes up about 0.1 parts per million (ppm) of the earth's crust and exist in a divalent cation (e.g. CdCl_2) (Hans-Wedepohl, 1995). This non-biodegradable metal is mainly produced as a by-product of mining, smelting and refining of Zn. Trace amounts of Cd ($\pm 10\%$) can also be produced during the recycling of iron and steel scrap (Fthenakis, 2004).

This metal is a persistent and widespread environmental pollutant that has the ability to cause diseases associated with impaired kidney function (Adams *et al.*, 2011). Studies have shown that tobacco is the dominant source of Cd exposure among smokers. Accumulated Cd found in soil is readily absorbed by the roots of tobacco plants and subsequently absorbed through the lungs when tobacco leaves are burned (Adams *et al.*, 2011). Among non-smokers, foods like leafy greens, shellfish, legumes, nuts and root vegetables are considered the most significant sources of Cd (Adams *et al.*, 2011).

Organs such as the lungs, liver and kidney as well as bone can be damaged by Cd, depending on the dose, route of administration and duration of exposure (Prozialeck and Edwards, 2012). Transmission electron microscopy (TEM) analysis found that Cd bio-accumulates in the nucleus, mitochondria and rough endoplasmic reticulum of liver and kidney cells (Venter *et al.*, 2017b). The kidney is also the organ that shows the most adverse effects with chronic exposure, resulting in the accumulation of Cd in the epithelial cells of the proximal tubules (Prozialeck and Edwards, 2012). This accumulation can be characterized by polyuria and an increase in urinary excretion of compounds such as electrolytes, amino acids, low-molecular-weight proteins and glucose (Prozialeck and Edwards, 2012). A growing number of studies suggest that children, women and individuals with health conditions such as diabetes are very susceptible to low levels of Cd exposure which can cause adverse renal effects (Prozialeck and Edwards, 2012).

The reason for Cd accumulation in the organs mentioned above is because the body doesn't have a mechanism to excrete Cd successfully (Jomova and Valko, 2011). A high incidence of toxicity as a result of accumulation over time is expected because the half-life of Cd is 25 years in tissue and it can persist for ± 75 -128 days in erythrocytes (Jomova and Valko, 2011).

2.1.2. Lead

Lead rarely occurs in its native metallic form and is therefore classified as a chalcophile. It is generally found combined with sulphur. Lead is the 38th most abundant element and makes up 14 ppm of the earth's crust. The main source of Pb is a mineral called galena (PbS), which is mined from Zn ores (El-Safty *et al.*, 2004). Lead is mostly used for the production of Pb-acid batteries. Due to the mechanical properties of Pb (high density, low melting point, ductility, and relative inertness), it is used in a wide variety of products.

Lead is used to make bullets, scuba diving weight belts and architectural metals in roofing material, pipes, paint and car parts. Most of the Pb exposure to humans is due to improper disposal of industrial waste into the air, water and soil (El-Safty *et al.*, 2004). Exposure can also occur through food or consumer products (W.H.O, 2016). Occupational exposure is a common cause of Pb poisoning in adults for example, artists that uses oil paint or welders that work with Pb are at particular risk (Bae *et al.*, 2001).

Salts containing Pb is readily absorbed by the body and 1% of it is stored in bones (Venugopal and Luckey, 2013). The rest is excreted within a few weeks of exposure in urine and faeces. Continuous exposure may result in bioaccumulation. When Pb is absorbed into the bloodstream, it is highly toxic and affects almost every organ and system in the human body. It has the ability to interfere with the proper functioning of enzymes by binding to the sulfhydryl groups and can also mimic and displace metals that act as co-factors in many enzymatic reactions (Rudolph *et al.*, 2003).

Pb can cause severe damage to the brain and kidneys. By mimicking calcium (Ca), Pb can cross the blood-brain barrier. Once in the brain, it will degrade the myelin sheaths of neurons and interfere with the neurotransmission routes (Rudolph *et al.*, 2003). Lead exposure, through the inhalation of cigarette smoke, can also lead to renal dysfunction and nephrotoxicity (El-Safty *et al.*, 2004).

2.1.3. Chromium

Chromium is the 21st most abundant element and make up 100 ppm of the earth's crust. It exists in a variety of different oxidative states and are found in the environment due to erosion of Cr-containing rocks or volcanic eruptions (Nordberg, 2009). Most of the Cr exposure to humans is due to improper disposal of industrial waste. Factories that manufacture rubber,

stainless steel, textile dyes, leather or chrome plates are the main sources that contaminate the water sources (Bakshi and Panigrahi, 2018).

Rivers downstream from these industrial factories can have more than five times the standard amount of Cr present in the water, which is highly toxic to fish because the metal is easily absorbed through their gills. From there it enters the bloodstream, cross cell membranes and bio-concentrates itself up the food chain (Bakshi and Panigrahi, 2018).

Chromium is also common in a wide variety of soil-grown foods. The Cr content can vary from 1 to 13 µg per serving depending on the soil mineral content, plant cultivar, growing season and if there is contamination during processing (Thor *et al.*, 2011). The type of cookware also plays a role as Cr has the ability to leech into food when cooked in new stainless-steel containers (Thor *et al.*, 2011). Cigarette smoke also contains trace amounts (0.246 - 14.6 mg/kg) of Cr and can be accumulated in the human body with continuous use over time (Bakshi and Panigrahi, 2018).

Cr(III) plays a role in glucose and lipid metabolism and also plays a part in the action of insulin (hormone that regulates the storage of carbohydrates, proteins and fat) (Di Bona *et al.*, 2011). Its deficiency in the body have shown to cause cardiovascular and metabolic diseases like diabetes (Di Bona *et al.*, 2011). Cr(VI) is highly toxic when inhaled and can have mutagenic effects, whereas Cr(III) is less toxic because it cannot cross cellular membranes, making it less likely to be accumulated in the body over time (Jomova and Valko, 2011).

2.2. ADME of heavy metals

2.2.1. Cadmium

The inhalation of toxic fumes or contaminated dust particles is one of the major routes of Cd exposure with around 5-50% of inhaled Cd entering the body and being absorbed through the lungs (Oliveira *et al.*, 2019). Due to the high level of Cd accumulation in tobacco leaves, cigarette smokers generally have a higher blood Cd level, compared to non-smokers. Once Cd is inhaled into the lower respiratory tract it becomes difficult for the body to excrete it and it will accumulate in several organs responsible for detoxification. Although the liver and kidneys are the primary site for accumulation, various components of the coagulation system can also be affected. Heavy metal toxicity has not only shown to change the state of relaxation and contraction of blood vessels but also found to diffuse through the alveolar wall and into the blood stream, causing widespread harm throughout the body (Stohs *et al.*, 2001). Cadmium

levels in urine samples have also been associated with other health conditions like osteoporosis, peripheral artery diseases, hypertension, diabetes mellitus and various cancers (Adams *et al.*, 2011).

After individuals are exposed to Cd via inhalation or ingestion, Cd-albumin complexes will form in the body and be transported to the liver via the blood circulation (Nordberg, 2009). A small amount of Cd is excreted into bile-bound glutathione (GSH) (Figure. 2.1). Once in the liver, the Cd-albumin complexes will dissociate and Cd will either bind to metallothionein (MT) to form a new complex or it will induce a toxic effect (Figure. 2.1) (Nordberg, 2009). The Cd-MT complex will then be transported to the kidneys from the liver via the bloodstream and will be absorbed by the proximal renal tubules via endocytosis (Figure. 2.1) (Nordberg, 2009). Lysosomes will release Cd ions from the Cd-MT complex (Figure. 2.1). The accumulation of Cd ions in the epithelial cells of the renal tubules can result in generalized re-absorptive dysfunction characterized by polyuria and low-molecular-weight proteinuria (Prozialeck and Edwards, 2012).

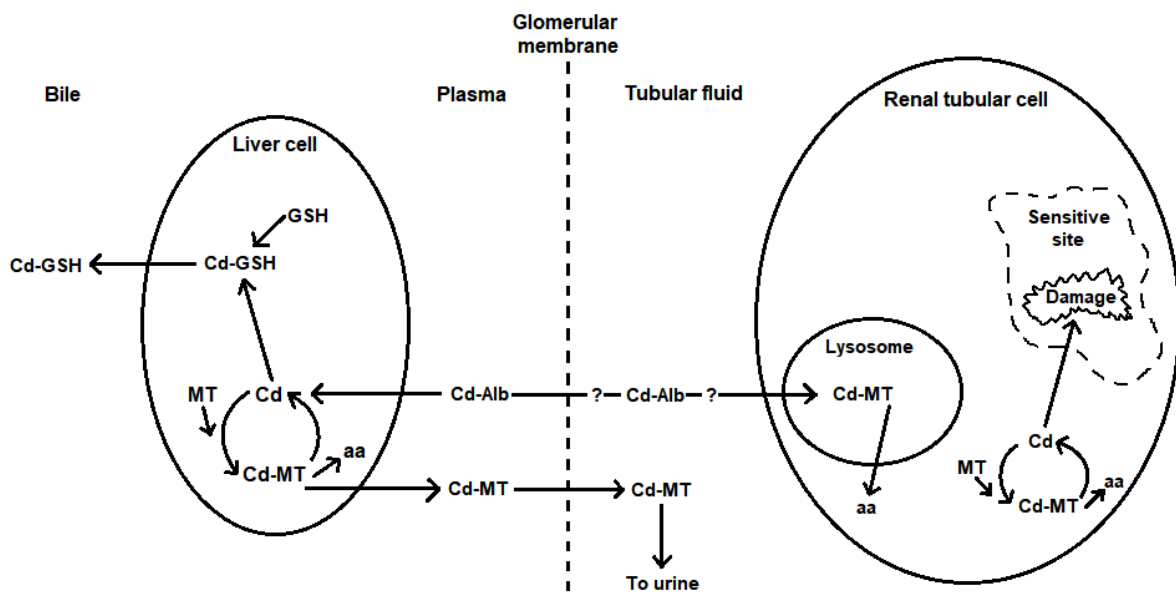


Figure 2.1: Basic flow diagram of how Cd is transported through the body, synthesis and degradation in liver and kidney tissue. Key: GSH: glutathione; MT: metallothionein; aa: amino acids; Alb: albumin. Modified from Nordberg (2009)

Although Cd accumulation in the proximal tubules is seen as the traditional reason for non-specific toxic effects in kidney cell death, evidence suggests that there may be other causes of toxicity. Early staged, Cd-induced proximal tubule injury may also be caused by specific changes in cell to cell adhesion, cellular signalling pathways and autophagic responses before the onset of necrosis or apoptosis (Prozialeck and Edwards, 2012).

2.2.2. Lead

Lead can enter the body via inhalation, ingestion or skin absorption. Its inhalation is very dangerous for young children because their bodies absorb a higher percentage than adults do. Smokers and individuals with Pb-related occupations can inhale radioactive Pb-210, which is toxic to the human body if accumulated over time (Rudolph *et al.*, 2003). In the past, the major source of exposure for children was through chewing objects that were covered with Pb-based paint. Alternatively, dry paint deteriorates over time and enter the body through hand-to-mouth contact. Lead can also be ingested through contaminated food, water or alcohol. Skin exposure may be significant for people working with organic Pb compounds. The rate of skin absorption is lower for inorganic Pb (Rudolph *et al.*, 2003).

The rate of absorption through the gastrointestinal tract depends on the physiochemical characteristics of the individual as well as the medium. Children can absorb 40-50% of water-soluble Pb, compared to 3-10% for adults (Rudolph *et al.*, 2003). Absorption mainly occurs in the duodenum. It is distributed to various organs by binding to erythrocytes in the blood. It can also be transferred from the mother to the infant via breast milk (Rudolph *et al.*, 2003).

Inorganic Pb is metabolised by forming various Pb-complexes with protein and non-protein ligands. The metabolism of organic Pb compounds occur in the liver through oxidative dealkylation facilitated by P-450 enzymes (Rudolph *et al.*, 2003). Lead is primarily excreted in the urine and faeces, independent of the route of exposure. Small amounts can also be excreted through saliva, sweat, breast milk, hair and nails (Rudolph *et al.*, 2003). The elimination half-lives for inorganic Pb in blood and bone are approximately 30 days and 27 years, respectively.

2.2.3. Chromium

There are three routes of exposure through which Cr(VI) can enter the human body: inhalation, ingestion and absorption through the skin. Inhalation via the airways and absorption through the skin are the primary routes of uptake for occupational exposure (Jomova and Valko, 2011).

When high levels of Cr are inhaled, it can become difficult to breathe and the nasal cavity may become irritated. Contact with the skin can cause skin ulcers and allergic reactions like redness and swelling in areas that were exposed to Cr (Jomova and Valko, 2011). It has been confirmed by the International Agency of Research on Cancer (IARC) that Cr(VI) is a carcinogen that affects the lung and nasal cavity and when inhaled on a frequent basis, it causes lung cancer in humans (Jomova and Valko, 2011).

Other effects like gastrointestinal problems, hypertension and hepatic and renal failure have been found in both occupational and non-occupational exposure to Cr(VI). Studies have shown that contaminated drinking water increases the metastases of somatic tumours in humans and animals. A study by Jomova and Valko (2011) also reported damage to the reproductive system and sperm production of mice when exposed to Cr(VI) (Jomova and Valko, 2011).

After oral administration, Cr(VI) is detoxified by the saliva, gastric juices and intestinal bacteria. If the Cr(VI) is absorbed by the intestines it will be reduced by GSH in the blood and liver. Only individuals with long-term exposure will show signs of genotoxicity and carcinogenicity. Thus, the risk of lung cancer will increase when the cellular defence mechanisms are overwhelmed. Normally Cr(VI) will be reduced by the cells to lower the carcinogenic potential and erythrocytes will deplete Cr(VI) by forming protein complexes (that are unable to leave the cell) to lower the oxidative states (Figure. 2.2). The risk of toxicity is not reduced because free radicals are formed through this process that are harmful. The reduction of Cr(VI) to Cr(III), which is not harmful to the human body, is accomplished by non- enzymatic reactions with ascorbate (Asc), GSH and cysteine (Cys) (Figure. 2.2) (Jomova and Valko, 2011).

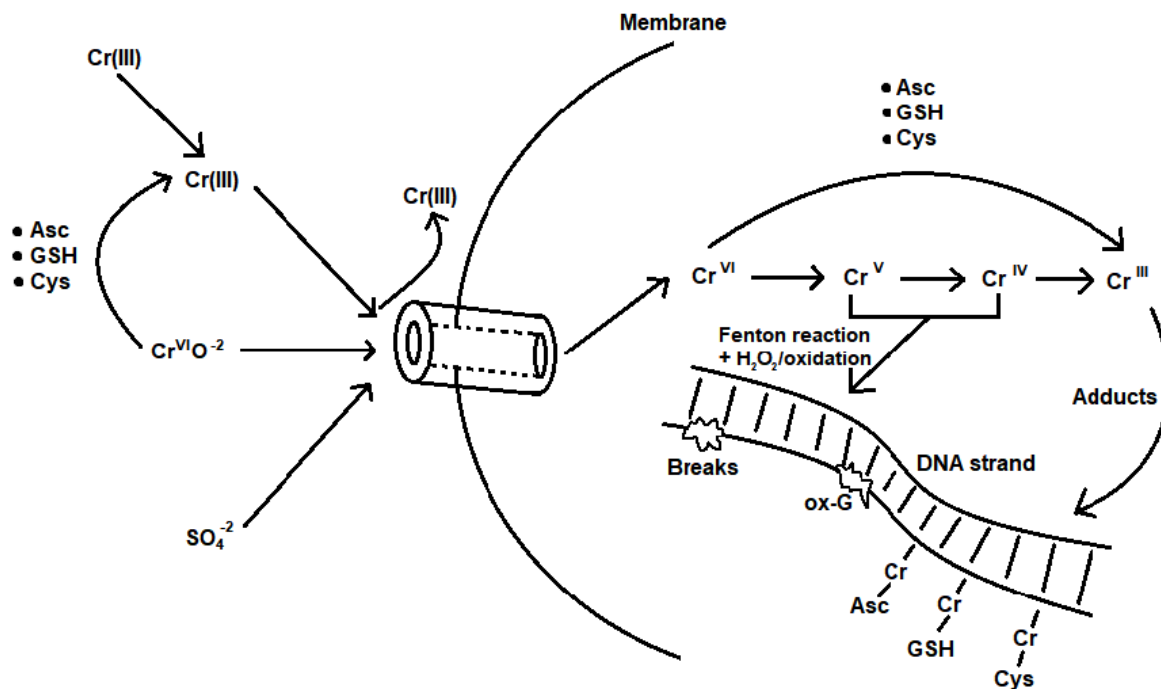


Figure 2.2: Diagram of the intracellular uptake and DNA damage due to Cr(VI) toxicity. Key: Asc: ascorbate; GSH: glutathione; Cys: cysteine. Modified from Jomova and Valko (2011).

Only Cr(III) will be detected in the urine and faeces because it can be excreted by the body. Cr(VI) will be excreted in the bile. The valence state of Cr will determine the rate of excretion, which can take from a few hours up to a few days (Jomova and Valko, 2011).

2.3. The coagulation system and heavy metal toxicity

The circulatory system allows blood to circulate and transport various different substances (oxygen, carbon dioxide, amino acids, electrolytes, hormones and waste material) to and from the different parts of the body to provide nourishment. The circulatory system also helps to fight diseases and maintain homeostasis by regulating the body's temperature and pH levels. The blood in the circulatory system is circulated by the heart and consists of four components: plasma, red blood cells (RBCs), white blood cells and platelets (Fang *et al.*, 2016). The cardiovascular system is the only system that connects all the organs of the body and is affected by heavy metals (Gaziano, 2005).

Erythrocytes are the most abundant type of blood cell in the body and its main function is to transport oxygen to the tissue via blood flow through the capillaries of the circulatory system. Haemoglobin, located in the cytoplasm of erythrocytes, is an iron-containing biomolecule that

has the ability to bind to oxygen molecules (Fang *et al.*, 2016). It is also responsible for the red colour of erythrocytes. Erythrocytes are round, biconcave-shaped cells that lack a nucleus and most organelles in order to accommodate four molecules of haemoglobin and to reduce the volume of the cell to allow it to move through the capillaries. The haemoglobin is surrounded by a plasma membrane that is composed of a double layer of phospholipids, scattered membrane proteins and cholesterol molecules (Moini, 2016). Roughly 2.4 million erythrocytes are produced in the bone marrow each second in a healthy human adult and circulates through the body for 100 to 120 days (Sender *et al.*, 2016). Approximately 84% of all cells in the human body are erythrocytes and when they die their components are digested and recycled by macrophages (Sender *et al.*, 2016). The plasma membrane of erythrocytes is vulnerable to the effects of ROS when exposed to heavy metals because of its composition and direct contact with plasma and blood of the liver, pancreas and kidney (Moini, 2016).

Haemostasis is the balance between the formation of a blood clot and the breakdown of the clot through fibrinolysis to maintain blood flow (Furie and Furie, 2005). The coagulation system is responsible for the prevention of blood loss by changing the blood from a liquid to a gel in order to form a blood clot. The mechanism of coagulation involves activation, adhesion and aggregation of platelets and the deposition and polymerisation of fibrin (Furie and Furie, 2005). Platelets lack a nucleus because they are formed from fragments of megakaryocytes (Lowe and Anderson, 2008). Fibrinogen has a centrosymmetric, tri-nodular, s-shaped structure and is cleaved by thrombin during coagulation to form fibrin fibres (Swanepoel *et al.*, 2015). Reactive oxygen species production as a consequence of heavy metal accumulation in the body that can cause irregular platelet activation. This in turn will affect the coagulation process (Swanepoel *et al.*, 2015).

Thrombin is used to regulate clotting and the balance between thrombotic (pro-coagulation) and antithrombotic (anti-coagulation) components need to be tightly regulated to maintain homeostasis and prevent haemorrhages from occurring (Van Rooy *et al.*, 2015). The cell-based model of coagulation is used to explain the clotting process in three phases, namely initiation, amplification and propagation. In the initiation phase (Figure. 2.3A) vascular endothelium and circulating blood cells are disturbed and an interaction occurs between the plasma-derived activation factor VII and tissue factor (Swanepoel *et al.*, 2015). During the amplification phase (Figure. 2.3B) thrombin activates the cofactors V and VIII and factor XI on the surface of the platelets (Swanepoel *et al.*, 2015). In the final stage (propagation phase) (Figure. 2.3C), large amounts of thrombin are produced and together with the formation of a stable buffer at the site of injury, blood loss will be prevented (Swanepoel *et al.*, 2015).

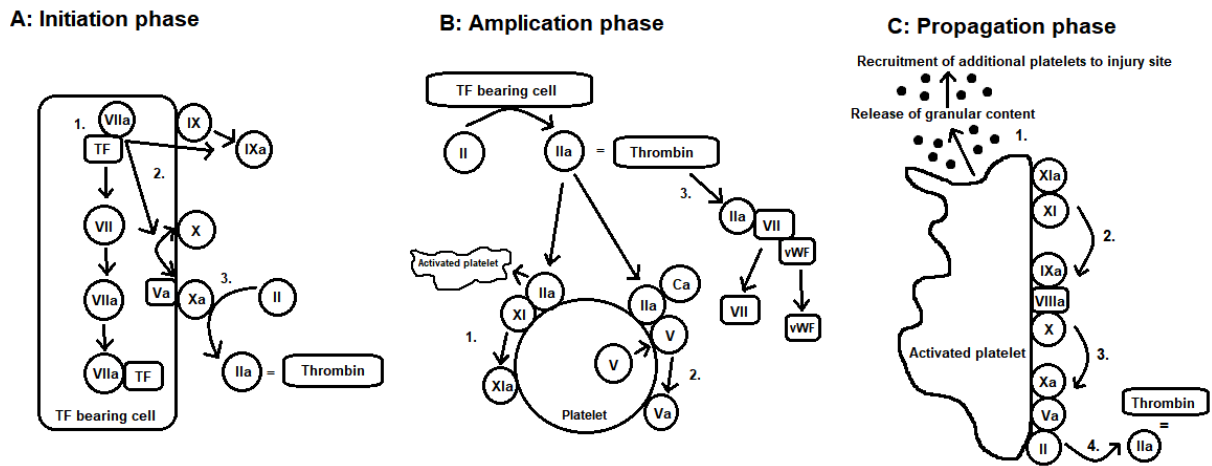


Figure 2.3: Diagram of the cell- based model for the coagulation pathway. Key: TF: tissue factor; vWF: von Willebrand factor; Ca: calcium; a: activated factor (e.g. VIIa). Modified from Swanepoel *et al.* (2015).

2.4. Influence of ROS and NO on the coagulation system

In order to maintain haemostasis and regulate thrombosis, the body requires precise interactions between the platelets, inflammatory cells, plasma proteins and the vessel wall. Integrins play one of the most important roles in haemostasis because they act as communicating elements between the different cell types mentioned above (Gregg *et al.*, 2004). Integrins help to regulate and control the adhesion and aggregation of platelets at the site of injury. Studies have shown that ROS production has the ability to transduce integrin activation signals and modulate integrin function (Barrett *et al.*, 2018). When the vessel walls are injured, platelets are recruited to stimulate blood coagulation while ROS is produced. Reactive oxygen species then change the integrin's binding affinity and function by inducing conformational changes (Gregg *et al.*, 2004).

Nitric oxide helps to increase blood flow and lower blood pressure by stimulating vasodilation, inhibiting leukocyte and platelet adhesion, as well as reducing smooth muscle cell proliferation. It can also act to prevent atherosclerosis (Abeyakirthi, 2020). Nitric oxide is produced from an amino acid called L-arginine that is transformed to L-citrulline with the help of nitric oxide synthase (NOS) in the presence of oxygen and cofactors (Adewoyin *et al.*, 2019). Nitric oxide synthase has three isoforms, of which endothelial NOS (eNOS) is constitutively expressed in endothelial cells (Bredt, 1999). Due to its unstable nature, NO usually reacts with other molecules to form more stable products. In the blood, NO is oxidized to nitrite (NO_2^-) and then further to nitrate (NO_3^-), with the help of oxyhaemoglobin. Sometimes, NO_3^- is produced as a by-product when NO reacts directly with oxyhaemoglobin to form methaemoglobin (Abeyakirthi, 2020). Previous studies have indicated that heavy metal exposure has the ability

to affect the cell signalling pathway in endothelial cells (Briffa *et al.*, 2020; Majumder *et al.*, 2008; Pritchard *et al.*, 2000; Vaziri and Ding, 2001). Majumder *et al.* (2008) found that low levels of Cd exposure (100 nmol/L) blocks eNOS phosphorylation and inhibits NO production in endothelial cells. Similarly, Pb-induced hypertension in rats have shown to increase ROS production, enhancing NO inactivation and decreasing NO bioavailability which resulted in compensatory upregulation of NOS (Vaziri and Ding, 2001).

The inhalation of heavy metals like Cd and Cr through cigarette smoke can also induce ROS production (Arbi *et al.*, 2017). These metals are associated with CVD, arteriosclerosis and thrombosis. Cadmium targets the endothelium of the vascular system and can cause inflammation, decreased endothelial migration and function, impaired NO production, as well as cell death (Arbi *et al.*, 2017).

Metal ions can cause oxidative damage in two ways: i) they act as a catalyst of the Fenton reaction by producing ROS and ii) they reduce the level of antioxidants such as GSH, by binding to enzymes that are involved in the antioxidant pathways. The bioaccumulation of ROS can lead to cellular and tissue damage. Janse Van Rensburg *et al.* (2019) studied the oxidative and haemostatic effects of three heavy metals by using scanning electron microscopy (SEM) and thromboelastography[®] (TEG[®]). The results showed reduced GSH levels and an increase in hydroxyl radical formation. They also noted erythrocyte deformation and accelerated platelet activation. Although the TEG[®] results were statistically insignificant it was clear that the heavy metal exposure adversely affected thrombus formation. It was concluded that heavy metal exposure could potentially lead to an increased risk for thrombosis (Janse Van Rensburg *et al.*, 2019).

2.5. Previous studies on heavy metal toxicity

Over the last 50 years, there has been a significant increase in the consumption of tobacco products. Cigarette smoke contains various toxic materials that is very harmful to human health when inhaled. Heavy metals like Cd, Cr and Pb can accumulate in different tissues and bodily fluids through smoking (Muhammad Waqar, 2012).

Lead is highly toxic to the body and can affect the brain, nervous system, reproduction system and RBC (Muhammad Waqar, 2012). High Pb levels have been associated with behavioural problems in children as well as decreased intelligence quotient (IQ) levels (Needleman *et al.*, 1979). A survey done on 24 middle-aged men in Brittan showed a correlation between Pb

blood concentrations and the use of alcohol and cigarettes (Shaper *et al.*, 1982). Lead toxicity is also known to reduce sperm count and motility, as well as affecting the sperm morphology and function (Gidlow, 2004).

A study was conducted by El-Safty *et al.* (2004) on male cigarette-smoking Egyptians to evaluate the effects of Pb (inhaled through cigarette smoke) on the renal proximal tubular function and structural integrity. The results showed an increase in urinary excretion in all groups that were exposed to Pb, whether they were smokers or non-smokers. In addition, there was a greater elevation among Pb-exposed smokers than among Pb-exposed non-smokers. The authors concluded that Pb exposure led to renal dysfunction and nephrotoxicity (El-Safty *et al.*, 2004).

Adams *et al.* (2011) hypothesized that cigarette smoking is associated with higher urine Cd levels in a dose-dependent manner. The authors combined urine Cd measurements of smokers and dietary data to assess the sources of Cd in a sample of healthy premenopausal females. They found that the usual consumption of Cd-rich food like leafy greens, shellfish, root vegetables and organ meats are associated with elevated levels of Cd in the urine (Adams *et al.*, 2011). A previous study also suggests that Cd and Cr accumulation through cigarette smoke can have an influence on the coagulation system (Arbi *et al.*, 2017). Pretorius *et al.* (2016) found that smokers have a higher risk of CVD and thrombus formation.

Chromium and Cd have been shown to bioaccumulate in the nucleus, mitochondria and rough endoplasmic reticulum of liver and kidney cells in chicken embryos (Venter *et al.*, 2017b). When exposed to high doses, these metals can also cause mitochondrial damage, membrane rupture, sinusoid dilation and necrosis in liver tissue of Sprague-Dawley rats (Venter *et al.*, 2015).

Arbi *et al.* (2017) investigated the effects of mercury (Hg) and Cd, alone and in combination, on the coagulation system of Sprague-Dawley rats (Arbi *et al.*, 2017). The authors exposed 24 male rats to heavy metal concentrations that were 1000 times that of the WHO water limits, for 28 days. Using SEM, they determined that both Cd and Hg caused platelet activation. Chromium increased the average thickness of fibrin fibres and allowed aggregation and formation of dense matted deposits (DMDs) (Arbi *et al.*, 2017). A similar study was done by Naidoo *et al.* (2019) to investigate the structural changes in lung tissue. Scanning electron microscopy confirmed that there were structural and morphological changes to the alveoli and bronchioles. Fibrosis and denser collagen fibril arrangements were detected in Cd-exposed

groups, while Hg groups showed an increase in elastin fibril formation. This study showed that Cd exposure can result in cellular damage, inflammation and fibrosis of lung tissue, which increases the risk of respiratory diseases (Naidoo *et al.*, 2019).

Venter *et al.* (2017a) conducted an *ex vivo* study to investigate the ultrastructural, confocal and viscoelastic characteristics of whole blood and plasma after exposure to Cd and Cr, alone and in combination. The aim was to determine if Cr synergistically increases the effect of Cd on blood coagulation. Scanning electron microscopy analysis of the exposed groups showed alterations in the erythrocyte morphology as well as thickening of fibrin fibres. Confocal laser scanning microscopy (CLSM) of all exposed groups (exposed to Cd and Cr, alone and in combination) revealed the presence of phosphatidylserine on erythrocyte membranes, indicating that eryptosis took place. Viscoelastic analysis showed unstable and fragile clot formation when exposed to Cd and Cr in combination. The authors concluded that the coagulation system is a target for heavy metal toxicity (Venter *et al.*, 2017a).

Cigarette smoke is well known for its disease-causing capabilities and has been linked to serious illnesses like cardiovascular diseases, cancer, diabetes and strokes. The constant exposure to trace amounts of heavy metals found in tobacco products have become a concerning health issue and the mechanisms through which they cause toxicity is still poorly understood. Although many studies have been undertaken to determine the effect of heavy metal exposure on tissue and organ damage at toxic concentrations, very few focussed on metal exposure in combination and their effect on the coagulation system. Therefore, this study attempted to address the lack of knowledge regarding the effects of Cd, Pb and Cr, alone and in combination.

2.6. Aim and objectives

The aim of this study was to investigate the effects of Cd, Pb and Cr, alone and in combination on erythrocytes and fibrin networks as well as the coagulation system in human blood. In addition, the ability of these metals to produce ROS and NO were determined.

The aim of this study was achieved through the following research objectives:

1. Investigating the effects of the metals alone and in combination on the morphology of fibrin networks and erythrocytes by using scanning electron microscopy (SEM).
2. Investigating the effects of the metals alone and in combination on the parameters of coagulation over time using thromboelastography (TEG®).
3. Investigating the effects of the heavy metals, alone and in combination on the formation of reactive oxygen species (ROS) molecules using the DCFH-DA assay in the blood.
4. Investigating the effects of the heavy metals, alone and in combination on nitrite levels in the blood using the Griess assay.

These objectives were achieved using the experimental strategy presented in Figure 2.4.

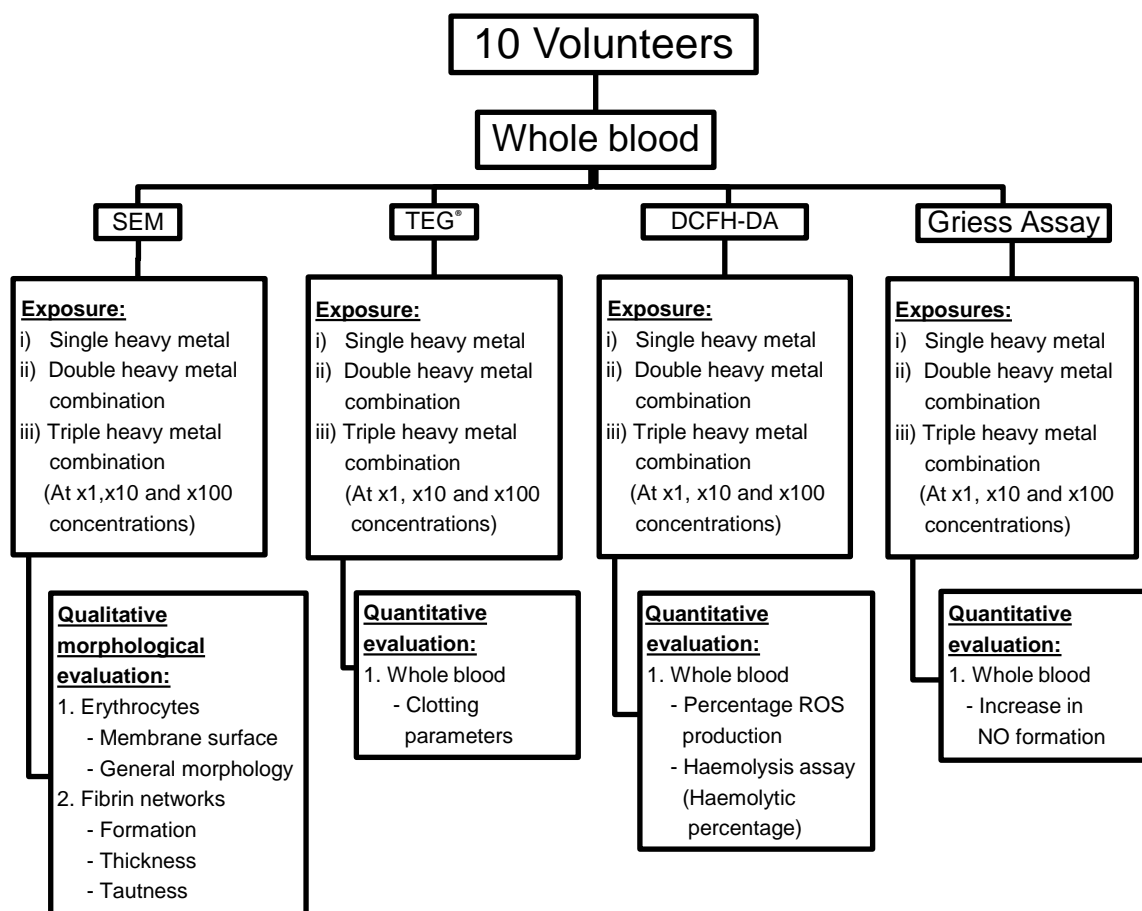


Figure 2.4: Flow diagram of the objectives of this research project.

2.7. Ethical consideration

The protocol for this study was submitted to the Research Ethics Committee of the Faculty of Health Science at the University of Pretoria to obtain ethical approval (Ethics Reference Number: 377/2020). Informed consent was obtained from each person that volunteered to donate blood for the study. A number was assigned to each sample to ensure anonymity. No personal information of any patient was published or presented in any way.

2.8. Data management

Collected data were stored electronically on the investigator's computer, and periodically backed up onto a designated Google Drive folder owned by the supervisor. All raw and processed data were uploaded to the Google Drive folder before final submission of the dissertation.

2.9. Funding

This project was supported and funded by the supervisor, Prof HM Oberholzer. All additional costs were covered by the Department of Anatomy, Faculty of Health Sciences of University of Pretoria.

Chapter 3

Chapter 3: The effect of cadmium, lead and chromium alone and in combination on fibrin networks and erythrocyte morphology

3.1. Introduction

Red blood cells (RBCs) are present in almost all vertebrates and play an important role in oxygen transportation (Mesarec *et al.*, 2019). The human cardiovascular system facilitates blood circulation throughout the body, provide cells with oxygen and nutrients and in return dispose of metabolic waste. Humans are exposed to different concentrations of heavy metals every day, depending on their environment, lifestyle and duration of exposure. One of the main heavy metals sources is cigarette smoke and with the growing rate of nicotine addiction, it is of key importance to determine how exposure affects RBC morphology (Caruso *et al.*, 2013). Previous studies have shown that Cd and Cr targets the circulatory system (Arbi *et al.*, 2017; Barrett *et al.*, 2018; Swanepoel *et al.*, 2015). Scanning electron microscopy analysis showed alterations in the erythrocyte morphology as well as thickening of fibrin fibres. Exposure to these heavy metals also affected clot formation and CLSM analysis revealed the presence of phosphatidylserine on erythrocyte membranes (Venter *et al.*, 2017a). In addition, oxidative stress can induce eryptosis which is characterised by cell shrinkage and blebbing (Lang *et al.*, 2012b).

In order for the cardiovascular system to function properly, the shape and stability of erythrocytes are of key importance. Healthy RBCs are 7.5 to 8.7 μm in diameter, 1.7 to 2.2 μm in thickness and bi-concave (discocyte) in shape (Pretorius *et al.*, 2016). Reversible elastic deformation, facilitated by membrane flexibility with a high surface-to-volume ratio, plays a significant role in RBC functionality and how efficiently they pass through vessels and capillaries. The morphology of RBCs can vary in shape (target cell, spherocyte, ovalocyte, stomatocyte, sickle cell, acanthocyte, teardrop, schistocyte, helmet cell and burr cell) and size (normal, microcyte, and macrocyte) (Diez-Silva *et al.*, 2010). With some capillaries being as small as 3 μm wide, RBCs need to have the ability to change shape in order to squeeze through the tiniest blood vessels. If the cell membrane composition (fatty acids, carbohydrates and proteins) is abnormal, RBCs can become rigid or fragile, slowing the flow of blood (Mesarec *et al.*, 2019).

The RBC membrane is comprised of a phospholipid bilayer that maintains the cell surface area and aids in elasticity. Underneath this bilayer is a two-dimensional network of spectrin molecules (cytoskeleton) that contributes towards the shear elastic properties of RBCs. Vertical interactions connect the integral proteins or peripheral proteins with the lipid bilayer and spectrin network, while horizontal interactions refer to the bindings involved in the spectrin network formation (Diez-Silva *et al.*, 2010). A disruption in any of these interactions can change the density of the spectrin network and cause membrane fluctuations. The structure, mechanical integrity and overall shape of RBCs are influenced by three factors: 1) the sheer stress on the membrane, 2) the nature of binding between the vertical interactions and 3) changes in metabolic activity that facilitates remodelling (Diez-Silva *et al.*, 2010).

Fibrin fibres are a major structural component in blood clots and play an important role in haemostasis. Fibrinogen, which is activated by thrombin, is polymerised into a meshwork of fibrin fibres (Pretorius and Lipinski, 2013). In the event of injury or trauma, the fibrin meshwork will stem blood flow and aid in wound healing (Undas and Ariëns, 2011). Examining the ultrastructural morphology may prove as an important tool for studying the effects of metal exposure. Fibrinogen's scavenging properties makes it more susceptible to oxidation and in turn protects other proteins from oxidation. *In vitro* evidence suggests that fibrinogen oxidation may impair or enhance clot formation depending on the oxidant (Undas and Ariëns, 2011).

In 2019, Yaprak and Yolcubal conducted a pilot study to test whether smoking increases the level of heavy metal concentrations found in platelet-rich fibrin (PRF). The authors were able to measure the exact concentration of each heavy metal and found a significant increase in Cd, Pb and Cr levels. For this chapter, the blood of ten healthy individuals were exposed to three different concentrations (x1, x10 and x100 the original concentration found in PRF for each respective metal) of Cd (0.21 µg/L), Pb (4.1 µg/L) and Cr (224 µg/L), alone and in combination. Scanning electron microscopy was used to analyse the morphology of erythrocytes and fibrin networks. The group exposed to isoPBS was used as a control group and compared to all the other metal exposed groups. The micrographs of a healthy individual without any exposure would typically showcase normal biconcave shaped erythrocytes with a smooth membrane and normal cell diameter. The fibrin networks would also appear organized without any sticky masses. This method is ideal to use because it generates high resolution, three-dimensional images that provide a detailed surface image of the cellular structure.

3.2. Materials and Methods

3.2.1. Metal preparations

Stock solutions (concentrations equal to X1000 the pre-determined values for each respective heavy metal) for the various heavy metals (CdCl_2 , PbCl_2 and CrCl_2) (Merck, Darmstadt, Germany) were made using isotonic phosphate-buffered saline (isoPBS) (Sigma-Aldrich, St Louis, MO, USA). Working solutions were made from the stock solutions. Whole blood was then exposed to the different concentrations of heavy metals as indicated in Table 3.1.

Table 3.1: The concentrations and volume of whole blood exposed to different heavy metals.

GROUP	CONCENTRATION (X1)	CONCENTRATION (X10)	CONCENTRATION (X100)	VOLUME
Control	0 µg/L *	0 µg/L	0 µg/L	5 mL
Cd	0.21 µg/L *	2.1 µg/L	21 µg/L	5 mL
Pb	4.1 µg/L *	41 µg/L	410 µg/L	5 mL
Cr	224 µg/L *	2 240 µg/L	22 400 µg/L	5 mL
Cd + Pb	0.21 µg/L + 4.1 µg/L *	2.1 µg/L + 41 µg/L	21 µg/L + 410 µg/L	5 mL
Cd + Cr	0.21 µg/L + 244 µg/L *	2.1 µg/L + 2 240 µg/L	21 µg/L + 22 400 µg/L	5 mL
Pb + Cr	4.1 µg/L + 244 µg/L *	41 µg/L + 2 240 µg/L	410 µg/L + 22 400 µg/L	5 mL
Cd + Pb + Cr	0.21 g/L + 4.1 µg/L + 244 µg/L *	2.1 µg/L + 41 µg/L + 2 240 µg/L	21 g/L + 410 µg/L + 22 400 µg/L	5 mL

* Obtained from: (Yaprak and Yolcubal, 2019).

3.2.2. Blood collection

Ethical clearance was obtained from the Research Ethics Committee of the Faculty of Health Sciences, University of Pretoria to collect blood from ten healthy, consenting donors (377/2020). Informed consent was obtained from each person volunteering to participate in the study. A number was assigned to each sample to ensure anonymity. No personal information of any patient was published or presented in any way.

The volunteers for this study were selected from the staff and students on Prinshof campus, at the Faculty of Health Sciences, University of Pretoria, South Africa. Each volunteer was asked to complete a questionnaire to determine their smoking (never smoked / stopped smoking 10 years ago / occasional smoker), as well as second-hand smoking status (level of exposure to second-hand smoke). Only non-smokers, whom have never smoked before with low levels of second-hand exposure, within the age range of 20 to 50 years, without any scheduled drug use, medical condition or disease that affects the cardiovascular system were included in this study. Volunteers that classified themselves as occasional smokers (1 cigarette

per month), and smoked a cigarette within one month of blood collection was also excluded. Approximately 15 mL of blood was collected from each participant in three citrate tubes. This procedure was done by a phlebotomist or a qualified medical doctor. The experiments were conducted within the first four hours after drawing blood.

3.2.3. Sample preparation for SEM

The effect of the metals, alone and in combination, on the morphological changes to erythrocyte membranes and fibrin networks were investigated using SEM. Whole blood was exposed to different concentration ranges of the various metal groups as indicated in Table 3.1 and incubated for 30 minutes (min) at room temperature. The samples were prepared by following the standard SEM procedure described by Arbi *et al.* (2017). Blood smears were made on glass coverslips (LASEC, South Africa) with the use of thrombin [20 U/mL (Sigma-Aldrich, St Louis, MO, USA)]. The coverslips were left to air dry for 10 min and then washed in isoPBS (0.075 M Na₂HPO₄, 0.2 M NaH₂PO₄.H₂O, and 0.2 M NaCl) for 20 min. The samples were fixed in 2.5% glutaraldehyde/formaldehyde (GA/FA) (Sigma-Aldrich, St Louis, MO, USA) solution [5 mL 0.075 M PBS, 0.5 mL 50% GA and 1 mL 25% FA in 3 mL distilled water (dH₂O) pH=7.4] for 30 min and washed with the same buffer three times. Osmium tetroxide (1%) (Sigma-Aldrich, St Louis, MO, USA) was used as a secondary fixative for 15 min and the samples were then washed again as explained in the previous step. After fixation, the samples were dehydrated using increasing concentrations (30%, 50%, 70%, 90%) of ethanol (EtOH, Merck, Darmstadt, Germany) followed by three changes of absolute EtOH. After the 100% EtOH was removed, the samples were dried with 100% hexamethyldisilazane (HMDS) (Merck, Darmstadt, Germany). The coverslips were left to air dry overnight, and then mounted on aluminium stubs and coated with carbon. A Zeiss Ultra Plus FEG SEM (Oberkochen, Germany) was used to study the morphology of the red blood cells and fibrin networks (Arbi *et al.*, 2017).

In order to ensure repeatability and accuracy of morphological analysis, micrographs were taken at a low magnification of the two cover slips created for each participant. This ensured that an accurate depiction of erythrocytes and fibrin network formation were captured. This procedure was repeated when capturing micrographs at a higher magnification to study individual erythrocytes. The membrane morphology and overall shape of the erythrocytes were characterised in three categories: 1) normal morphology (biconcave shape with uniform membrane), 2) slightly affected (loss of biconcave shape with some membrane alteration e.g., bleb formation) and 3) significantly affected (eryptotic cells).

A blind analysis of the SEM samples was performed by the principal investigator and all data/results were monitored and confirmed by the supervisor and co-supervisors.

3.3. Results

Erythrocyte morphology and fibrin network formation of whole blood (Figure 3.1 and Table 3.2) were evaluated using SEM. Whole blood was exposed to Cd, Pb and Cr alone and in combination at different concentrations for 30 min. Thrombin was added to stimulate clot formation. The changes in erythrocyte morphology and changes due to fibrin fibre interactions (Figure 3.2 and Table 3.3) were also evaluated.

Figure 3.1A is a representative image of the control group (isoPBS) that shows predominantly healthy biconcave erythrocytes with a smooth membrane and normal cell diameter ($\pm 8 \mu\text{m}$) (similar to erythrocyte in Figure 3.2A). A fibrin network of major thick (green arrow) and minor thin (orange arrow) fibres can be seen between and around the erythrocytes. Figure 3.1B – V shows erythrocytes exposed to x1, x10 and x100, the concentration found in PRF, of the metals Cd, Pb and Cr, alone and in combinations (Yaprak and Yolcubal, 2019).

In Figure 3.1B, the erythrocytes from the Cd x1 exposed group are similar to that of the control group with the presence of a sticky mass of fibrin fibres (blue arrow). Major thick (green arrow) and minor thin (orange arrow) fibres can be seen. Some of the thick fibres appears to be bent and less taut (pink arrows). Some areas of fused fibres are also visible (yellow arrow). In Figure 3.1C some of the erythrocytes from the Cd x10 exposed group appear to fold around the fibrin networks (similar to erythrocytes in Figure 3.2K and L) which appear organised with minimal bending and less taut fibres (pink arrow). Major thick (green arrow) and minor thin (orange arrow) fibres are also present. Some of the erythrocytes in Cd x100 exposed group (Figure 3.1D) are deformed (purple arrow) with many of the fibres appearing to be bent and less taut (pink arrows). Some of the fibres fused together to form thick strands (yellow arrow) and sticky mass areas (blue arrows).

In Figure 3.1E, the erythrocytes in the Pb x1 exposed group have an abnormal morphology. They are semi-spherical in shape and have a slightly swollen appearance with less smooth cell membranes (circled erythrocytes) (similar to erythrocytes in Figure 3.2E and J). A thin densely arranged fibrin network is present with sticky masses (blue arrows) being formed in some areas. Some of the fibres appear to be less taut (pink arrow) and in other areas, they fuse together (yellow arrow). Major thick (green arrow) and minor thin (orange arrow) fibres

are also present. In Figure 3.1F (Pb x10 exposed group) some of the erythrocyte membranes formed pointed extensions (maroon arrow) (similar to erythrocyte in Figure 3.2H), which resulted in a pinched appearance. The fibrin network appears less organised with more convoluted fibres (yellow arrows) and clumps of sticky masses (blue arrows). Major thick (green arrow) and minor thin (orange arrow) fibres are also present. In Figure 3.1G (Pb x100 exposed group) the formation of primary echinocytes (purple arrow) can be seen (similar to erythrocyte in Figure 3.2B), as indicated by the nodule like spicules. Thin regularly arranged fibrin (orange arrow) networks are present with some sticky masses (blue arrow) and fused fibrin areas (yellow arrow). Some of the fibres are thicker (green arrow) and less taut (pink arrows).

In Figure 3.1H the erythrocytes from the Cr x1 exposed group, appear to be flatter in shape and larger in diameter (similar to erythrocytes in Figure 3.2F), compared to a typical discocyte (as seen in Figure 3.2A). The fibrin network formation also appears less organized with more sticky masses (blue arrow) and less taut fibres (pink arrow). Major thick (green arrow) and minor thin (orange arrow) fibres are also present. In the Cr x10 and x100 exposed groups (Figure 3.1I and J) the presence of echinocytes (purple arrow) became more prominent and membrane folding around the fibrin strands became more apparent. The thick fibrin strands appear to be bent and less taut (pink arrows), forming clumps of sticky masses (blue arrow) and fused areas (yellow arrow). Major thick (green arrow) and minor thin (orange arrow) fibres are also present.

The Cd + Pb exposed groups at x1 and x10 are shown in Figure 3.1K and L respectively. In the x1 exposed group, erythrocyte clumping was observed (white line marked area). The erythrocytes in both groups are semi-spherical in shape, have a slightly swollen appearance and the cell membranes are rough and irregular (circled erythrocytes). The fibrin network in the x10 exposed group appeared to be denser and thicker individual fibres (green arrows) than that of the x1 exposed group with more fused areas (yellow arrow). The fibres are also bending and less taut (pink arrows). In Figure 3.1M the erythrocytes of the Cd + Pb x100 group are clumped together and trapped under a mesh like fibrin network that has an unorganized, haphazard arrangement. In some areas, the individual fibres cannot be clearly distinguished (red arrows). Major thick (green arrow) and minor thin (orange arrow) fibres are present, with some of the fibres appearing to be bent and less taut (pink arrow).

The Cd + Cr exposed groups at x1, x10 and x100 are shown in Figure 3.1N, O and P respectively. The erythrocytes in Figure 3.1N are slightly deformed with a bulging and swelling

appearance. Some of the erythrocytes formed nodule like projections on the membranes (purple arrow), which is an indication of echinocyte formation. Many of the thick fibrin fibres appear to be bent and less taut (pink arrows) with some fibres forming sticky masses (blue arrows). At the x10 and x100 concentrations (Figure 3.1O and P, respectively) the presence of echinocytes became more apparent, suggesting an increased loss of membrane integrity. In Figure 3.1O thick major fibres (green arrow) appear to be forming fused fibrin areas (yellow arrow) with clumps of sticky masses (blue arrows). Some of the fibres are bent and less taut (pink arrow). Minor thin (orange arrow) fibres are also present. In Figure 3.1P large areas of net-like coverings (red arrows) are formed by the thin fibres (orange arrow) with areas of fused fibrin fibres (yellow arrow). Major thick (green arrow) fibres are also present.

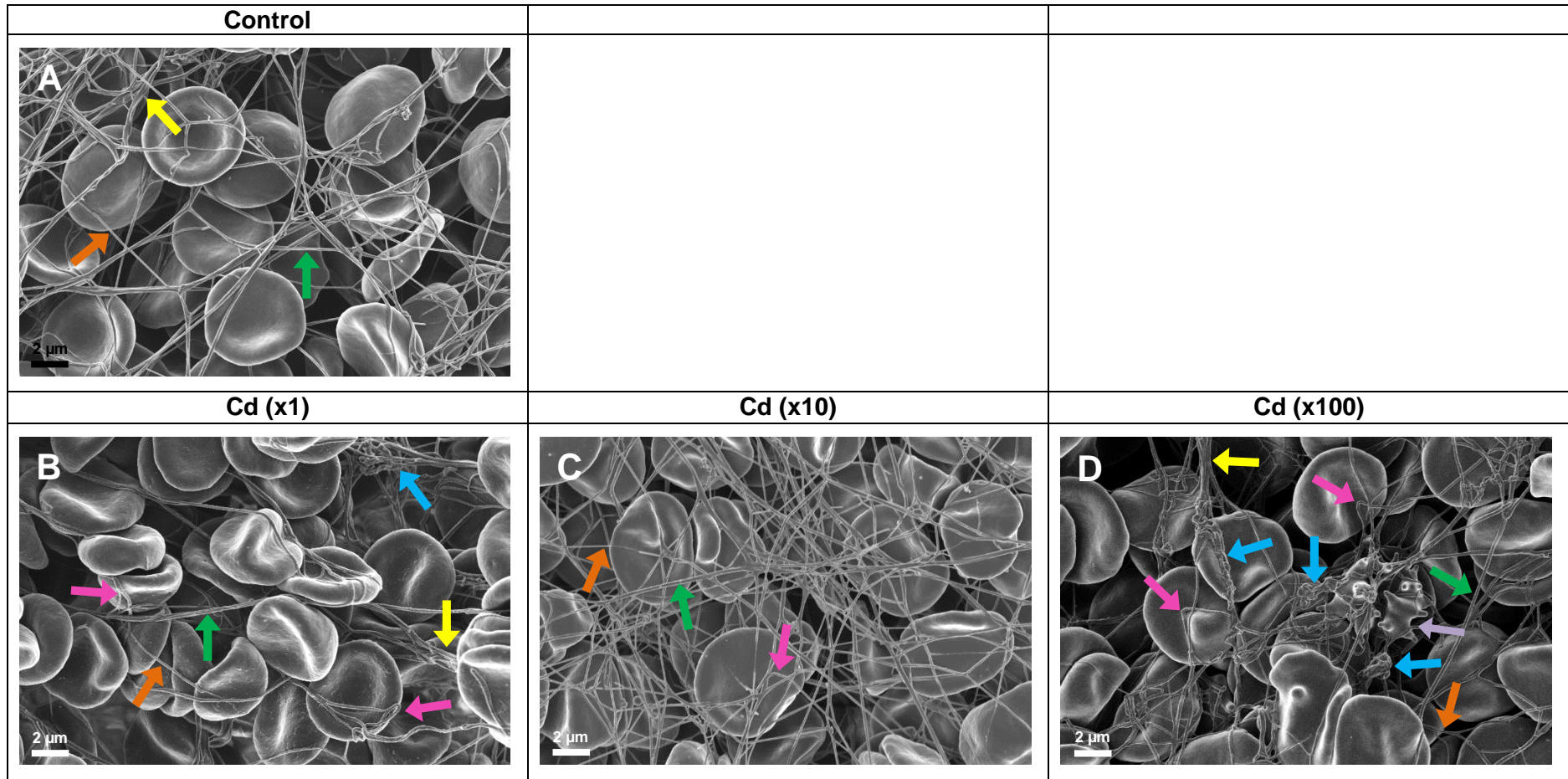
Figure 3.1 Q, R and S are representative of erythrocytes from the Pb + Cr combination group at x1, x10 and x100 respectively. The erythrocytes in the x1 and x10 exposed groups (Figure 3.1 Q and R respectively) appear to be flatter in shape and larger in diameter, compared to the typical discocyte (as seen in Figure 3.2A). Overall, the fibres appeared less taut (pink arrows) with some fibres forming sticky masses (blue arrows) and fused areas (yellow arrows). Major thick (green arrow) and minor thin (orange arrow) fibres are also present. In Figure 3.1S some of the erythrocyte membranes in the Pb + Cr x100 group formed nodule like projections (purple arrow), which is an indication of echinocyte formation. Overall, the fibrin network is dense and unorganized with a haphazard structure. This net-like covering (red arrows) of fibres in which cells become trapped appear mesh-like with some individual fibres not being clearly distinguished from one another. Major thick (green arrow) and minor thin (orange arrow) fibres are also present.

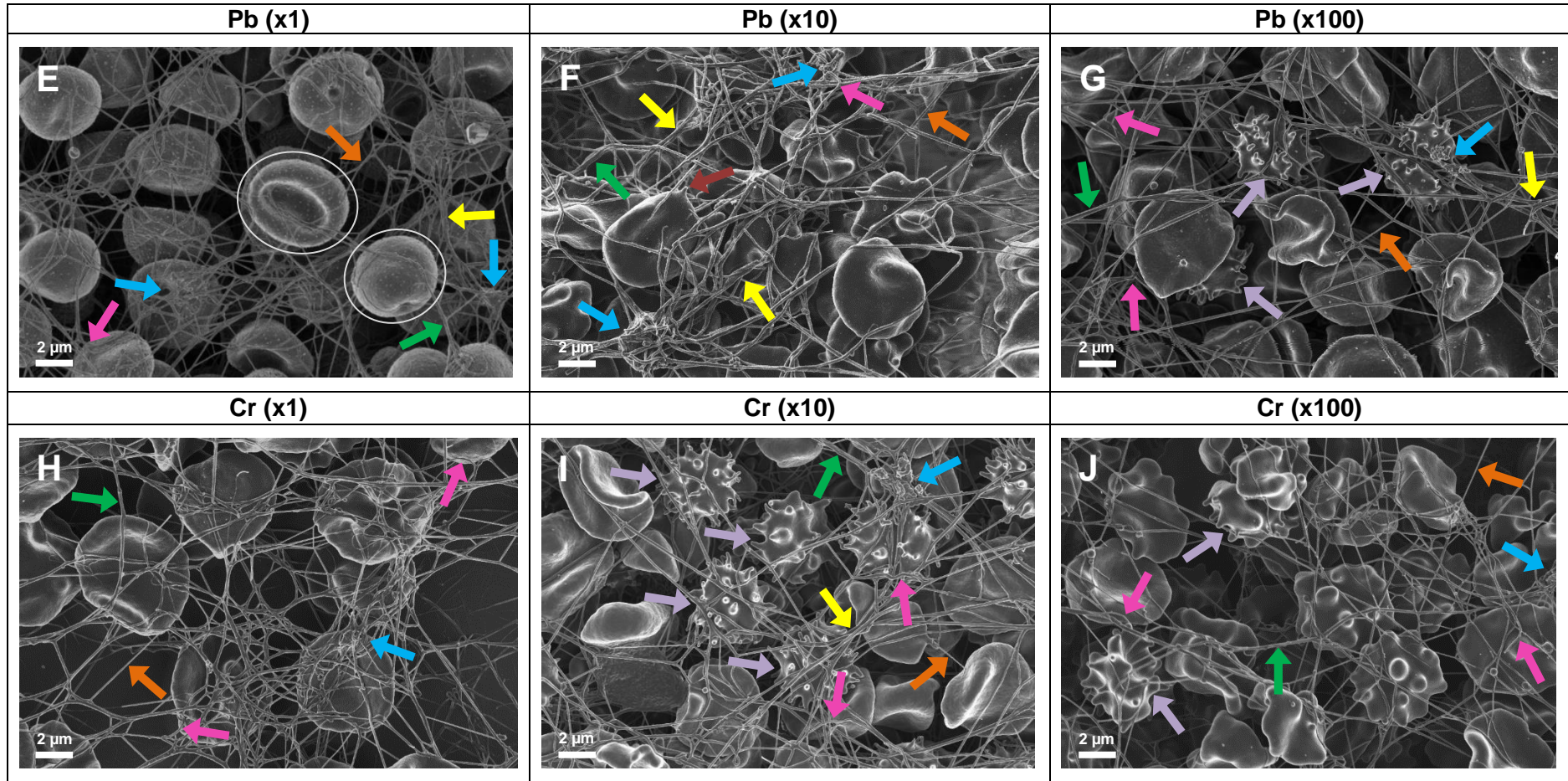
In Figure 3.1T the erythrocytes from Cd + Pb + Cr x1 exposed group are semi-spherical in shape, have a slightly swollen appearance and the cell membranes appear rough and irregular (circled erythrocyte). Pores (maroon arrow) can be seen in some of the membranes (similar to erythrocyte in Figure 3.2I). The fibrin network appears less organised with more convoluted fibres (pink arrows) and areas of fused fibres (yellow arrows). Major thick (green arrow) and minor thin (orange arrow) fibres are also present. The fibrin network in the Cd + Pb + Cr x10 exposed group, has major thick (green arrow) and minor thin (orange arrow) fibres that are haphazardly arranged with large sticky masses of fibrin fibres (blue arrows) visible. The fibres are bent and less taut (pink arrows) and fuse together (yellow arrow). In Figure 3.1V (Cd + Pb + Cr x100 exposed group) normal discocytes and echinocytes (purple arrow) are trapped within the thick mesh-like fibrin network. Large amounts of net-like coverings (red arrows) are formed

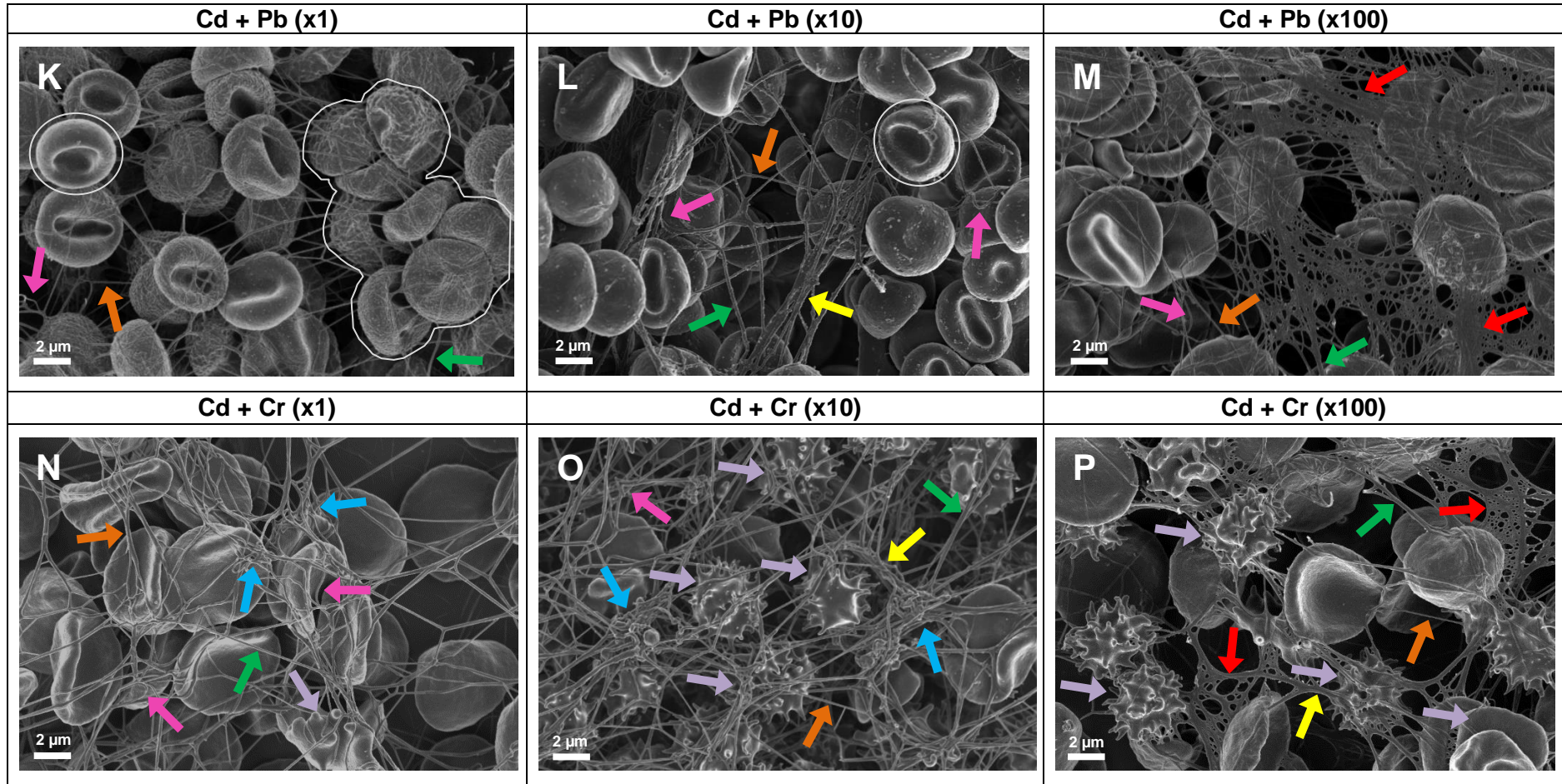
by thin fibres (orange arrow) with an underlying layer of fused fibrin fibres (yellow arrow). Major thick (green arrow) fibres are also present.

A summary of the findings is shown in Table 3.2 below and the severity of the changed erythrocyte morphology and changes due to fibrin fibre interactions is shown in Table 3.3.

Figure 3.2A – G are representative images of the various different erythrocyte shapes that was observed in the different experimental groups, indicated by the white arrows. In the control group (Figure 3.2A) the typical concaved morphology of an erythrocyte (discocyte) can be seen, with echinocytes present in the x100 Pb group (Figure 3.2B). The occasional microspherocyte was observed in the x10 Pb + Cr combination (Figure 3.2C) as well as knizocytes in the x1 Pb group (Figure 3.2D) and stomatocytes in the x10 Cd + Cr combination (Figure 3.2E). In the x100 Cd + Pb + Cr combination group, leptocytes were observed (Figure 3.2F) with dacryocytes present in the x100 Cr group (Figure 3.2G). Similarly, Figure 3.2H – L, represents erythrocytes that showed membrane irregularity, as indicated by the maroon arrows. In Figure 3.2H, the membranes formed pointed extensions in the x10 Pb group. Pores were seen in the erythrocyte membranes of the x1 Cd + Pb + Cr combination group (Figure 3.2I) and the x10 Cd exposed group (Figure 3.2J) showed erythrocytes with a rough and irregular looking appearance. In Figure 3.2K and L, membrane folding around the fibrin strands are visible in the x100 Pb + Cr exposed groups.







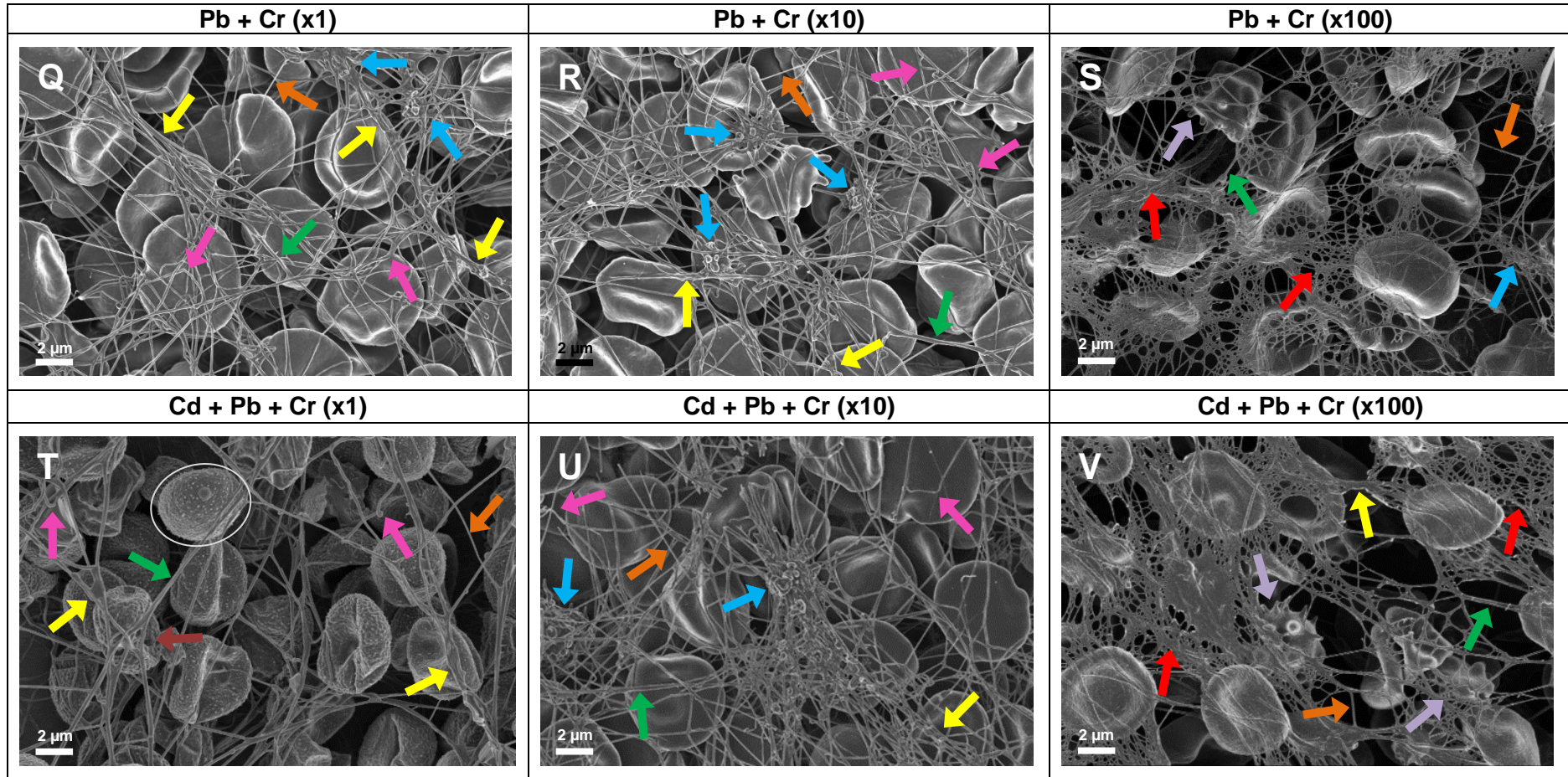


Figure 3.1: Scanning electron micrographs of whole blood with thrombin exposed to Cd, Pb and Cr, alone and in combination at concentrations x1, x10 and x100 showing fibrin network formation together with erythrocytes; Scale bars = 2 μ m. (A): Control; (B – D): Cd; (E – G): Pb; (H – I): Cr; (K – M): Cd + Pb; (N – P): Cd + Cr; (Q – S): Pb + Cr; (T -V): Cd + Pb + Cr. **Orange arrows:** thin minor fibres; **green arrows:** thick major fibres; **yellow arrows:** fused fibrin fibre areas; **blue arrows:** sticky mass fibrin fibres; **red arrows:** net-like coverings of thin fibres; **pink arrows:** bending less taut fibres; **purple arrows:** deformed erythrocyte and **maroon arrows:** membrane pores. **Circled cells:** altered erythrocyte shape and **white line marked area:** erythrocyte clumping.

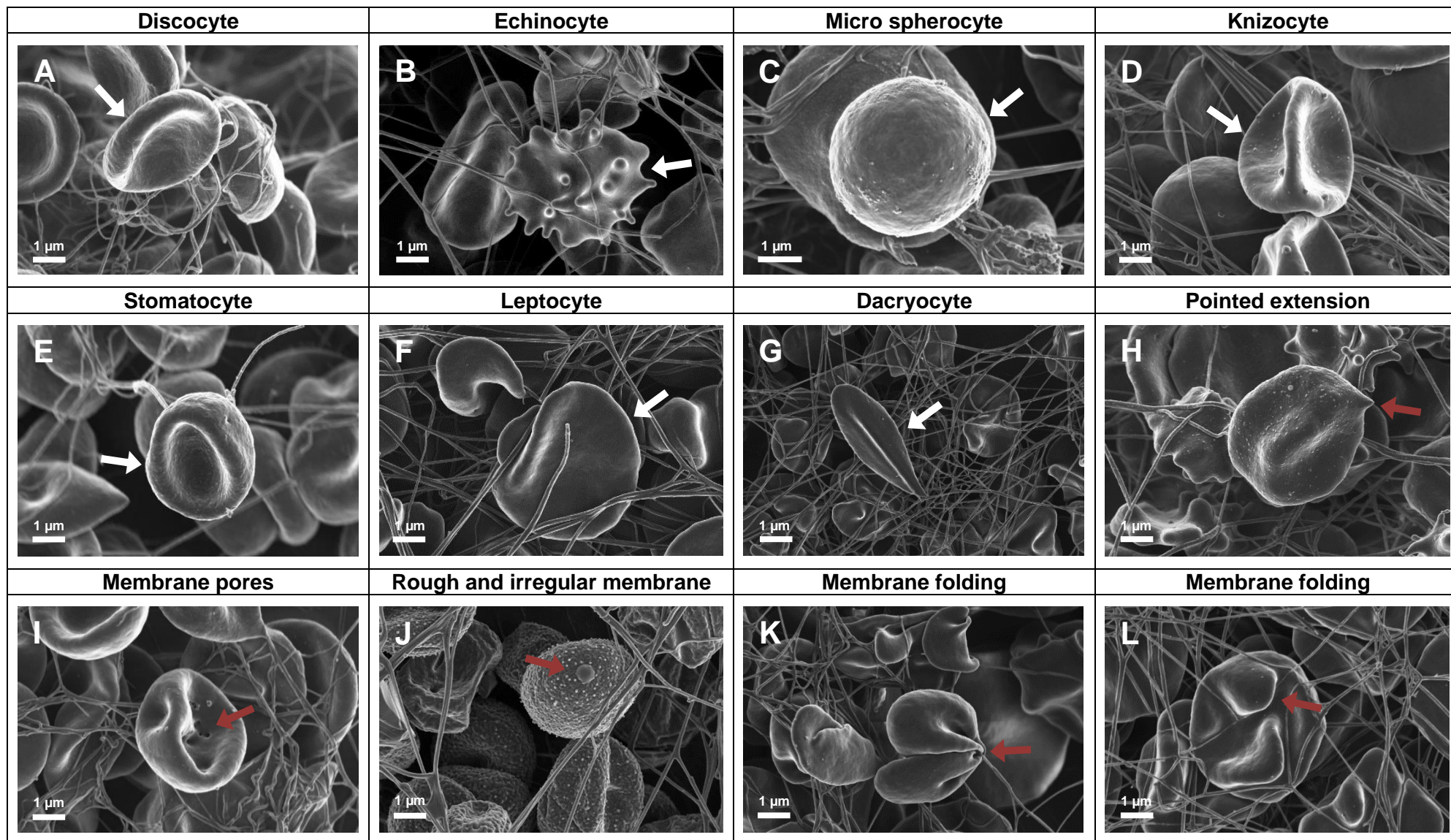


Figure 3.2: Representative SEM micrographs of erythrocytes prepared from whole blood with added thrombin, exposed to metals; scale bars: 1 μ m. **Fig A:** Control; **Fig B:** x100 Pb; **Fig C:** x10 Pb + Cr; **Fig D:** x1 Pb; **Fig E:** x10 Cr; **Fig F:** x100 Cd + Pb + Cr; **Fig G:** x100 Cr; **Fig H:** x10 Pb; **Fig I:** x1 Cd+ Pb + Cr; **Fig J:** x10 Cd and **Fig K and L:** x100 Pb + Cr. **White arrows** indicate erythrocyte variation and **maroon arrows** indicate membrane alteration.

Table 3.2: Summary of the changes observed in whole blood with added thrombin, exposed to metal combinations at different concentrations.

	Deformed erythrocytes	Presence of major thick and minor thin fibres	Less taut fibres	Net-like coverings of minor thin fibres	Sticky masses of thick fibres	Fused areas
Control						
	---	X	---	---	---	X
Cd						
X1	---	X	X	---	X	X
X10	---	X	X	---	---	---
X100	X	X	X	---	X	X
Pb						
X1	---	X	X	---	X	X
X10	---	X	X	---	X	X
X100	X	X	X	---	X	X
Cr						
X1	---	X	X	---	X	---
X10	X	X	X	---	X	X
X100	X	X	X	---	X	---
Cd + Pb						
X1	---	X	X	---	---	---
X10	---	X	X	---	---	X
X100	X	X	X	---	---	---
Cd + Cr						
X1	X	X	X	---	X	X
X10	X	X	X	---	X	X
X100	X	X	---	X	---	X
Pb + Cr						
X1	---	X	X	---	X	X
X10	---	X	X	---	X	X
X100	X	X	---	X	X	---
Cd + Pb + Cr						
X1	---	X	X	---	---	X
X10	---	X	X	---	X	X
X100	X	X	---	X	---	X

'X' indicates the presence of a particular feature and '---' indicates the absence of a particular feature.

Table 3.3: Summary of SEM analysis in whole blood with added thrombin, exposed to metal combinations at different concentrations.

	Altered erythrocyte morphology	Changes due to interactions with fibrin fibres
	<u>Control</u>	
	+	+
	<u>Cd</u>	
X1	+	+
X10	+	+
X100	++	+
	<u>Pb</u>	
X1	+	+
X10	++	+
X100	++	+
	<u>Cr</u>	
X1	+	+
X10	+++	++
X100	+++	+++
	<u>Cd + Pb</u>	
X1	+	+
X10	++	+
X100	++	++
	<u>Cd + Cr</u>	
X1	++	+
X10	+++	+++
X100	+++	+++
	<u>Pb + Cr</u>	
X1	+	+
X10	++	++
X100	++	+++
	<u>Cd + Pb + Cr</u>	
X1	++	++
X10	++	++
X100	+++	+++

-: none; +: minimal; ++: mild; +++: severe

3.4. Discussion

It is well known that tobacco smoke contains trace amounts of heavy metals, which can negatively impact human health if accumulated over long periods of time. Red blood cell and fibrin network morphology can be used as a model to study the mechanisms underlying heavy metal toxicity, including the effect of Cd, Pb and Cr. Not only is blood a preferential site for heavy metal accumulation, but it also acts as a vehicle for these exogenous molecules to reach all tissue. Red blood cells play an important role in haemostasis and blood coagulation. Both qualitative and quantitative changes can affect bleeding or thrombosis (Notariale *et al.*, 2021).

The precise mechanisms through which heavy metals cause toxicity is still poorly understood but it has been linked to the formation of radicals, inhibition of antioxidant enzymes and binding to antioxidant elements that causes oxidative stress. Metal ions can cause oxidative damage in two ways: i) they act as a catalyst of the Fenton reaction by producing ROS and ii) they reduce the level of antioxidants such as GSH, by binding to enzymes that are involved in the antioxidant pathways. This, along with ROS production can result in lipid peroxidation, protein alterations, DNA damage and cell death (Notariale *et al.*, 2021).

Erythrocytes can act as an important health marker due to their highly specialized and organized cell membrane which is very sensitive to change. Interactions with inflammatory oxidizing agents and mediators can lead to membrane changes that are visible in the morphology. Metal ions cause oxidative stress and thus expose the outer part of the erythrocyte membrane to phosphatidylserine (PS), which facilitates RBC adhesion to the endothelium of blood vessels, decreasing microcirculation and contributing towards thrombosis (Lang *et al.*, 2012a). Phosphatidylserine also signals for eryptosis in order to remove defective erythrocytes before membrane rupturing or haemolysis can occur (Notariale *et al.*, 2021). Erythrophagocytosis of aged RBCs helps regulate the life span of mature cells and remove damaged cells. Furthermore, the increase of intracellular calcium ion concentration will lead to micro-vesicle formation, which are responsible for the change in shape from a biconcave discocyte to an echinocyte with regularly spaced projections or spicules (Greenwalt, 2006).

Erythrocytes do not have a nucleus and lack all the typical intracellular organelles found in other cell types (Notariale *et al.*, 2021). They are deformable due to their biconcavity and can take on various different shapes (Figure 3.2) which include discocytes (biconcave erythrocytes), echinocytes (erythrocytes with regular spaced short projections or spicules), spherocytes (swollen spherical erythrocytes), knizocytes (elevated or elongated pinched off area in the centre of erythrocytes with two or more invaginations on the membrane), stomatocytes (cup shaped erythrocytes with a slit-like central area and swollen cell periphery), leptocytes (flattened erythrocytes) and dacryocytes (teardrop-shaped erythrocytes) (Swanepoel and Pretorius, 2012).

Scanning electron microscopy analysis showed some ultrastructural changes to the erythrocytes and fibrin network after heavy metal exposure. The groups that were exposed to Cd, Pb and Cr, alone and in combination showed a higher prevalence of altered erythrocyte morphology compared to the control (isoPBS) group. The majority of erythrocytes observed in this study had a typical biconcave shape. The predominant altered erythrocyte shape observed was echinocytes with the occasional leptocyte and knizocyte.

Overall, the micrographs seem to depict a trend that different groups at different concentrations all showed an increase in erythrocyte deformation which can occur due to oxidative stress, generated by heavy metal exposure (Cimmino *et al.*, 2015). The metal exposed groups were different from the control and showed an increase in erythrocyte deformation from swelling to bulging to the formation of nodule-like spicules/projections. Erythrocyte deformation seem to increase when blood was exposed to Cr, alone and in combination as compared to singular metals, with Cd + Cr group appearing to cause the highest degree of echinocyte formation. This may be due to Cr being a strong redox agent (Cimmino *et al.*, 2015). These results are similar to results found in previous studies where Cd exposure caused increased levels of echinocyte formation in Wistar rats and common carp (Ghosh and Indra, 2018; Witeska *et al.*, 2011). Cadmium had the same effect on human blood, along with increased membrane rigidity (Kerek *et al.*, 2018). Any alteration in erythrocyte morphology will reduce their lifespan (usually 120 days) and result in their removal from the circulatory system via phagocytosis, or destruction in the spleen by haemolysis (Lang *et al.*, 2012a).

Red blood cell morphology is not the only component affected by heavy metal exposure. Oxidative stress also plays an important role in platelet activation and thus influences the fibrin fibre morphology (De Maat and Verschuur, 2005). Reactive oxygen species have been shown to induce platelet activation, suggesting that these highly reactive molecules can interfere with

the thrombotic process at multiple steps (Cimmino *et al.*, 2015). Blood clotting is dependent on interactions between fibrinogen and thrombin to ultimately form polymerized fibres that holds the platelet plug together (Van Rooy *et al.*, 2015). Apart from oxidative stress, other mechanisms like phosphodiester inhibition, enzymatic changes and membrane interference should also be investigated as a possible explanation for the alterations observed in the fibrin networks.

After comparing different groups at different concentrations, the micrographs showed an increase in potential clot formation. The presence of sticky thick fibres (green arrows) that are haphazardly organized may be an indication of inadequate clot retraction. This can potentially influence the clot lysis time and increase the risk of thrombosis. The group with the least toxic effect appeared to be the Cd group, while the Cd + Cr combination appeared to be the most toxic group with the fibres being bent and less taut (pink arrows) and forming sticky masses (blue arrows) at the lowest concentration. At the higher concentrations, fibrin fibres fused together (yellow arrows) and formed net-like coverings (red arrows) that can have detrimental effects on coagulation. At higher concentrations, the fibrin network became less organized and appeared mesh-like. This caused the erythrocytes to become trapped in the fibrin network and contributed to their altered erythrocyte morphology. The results are similar to what was observed by Venter *et al.* (2017a) in an *ex vivo* study after Cd and Cr exposure in whole blood. Based on Yaprak and Yolcubal (2019), Cr (224 µg/L) accumulates at a much higher concentration in PRF than the other two metals (Cd: 0.21 µg/L and Pb: 4.4 µg/L) and might explain the general tendency for Cr to have a much larger effect. It is also important to keep in mind that some of the morphological features mentioned above (sticky fibrin masses, fused areas of the fibrin network and the tautness of the fibres) are not dose-dependent and could have been caused by errors during sample preparation.

3.5. Conclusion

Exposure to Cd, Pb and Cr, alone and in combination causes changes in the morphology of erythrocytes as well as the fibrin networks. Erythrocyte deformation seem to increase when blood is exposed to Cr, whether it is alone or in combination. The Cd + Cr combination group appears to be the most toxic group since it caused the highest degree of echinocyte formation. These findings correlate with the unorganized, haphazard structure of the fibrin network. Even at the lowest concentration, sticky fibrin masses were formed and at the higher concentrations, fibrin fibres fused together and formed net-like coverings. Novel findings were that heavy metal

exposure, especially Cr can potentially influence clot formation and increase the risk of thrombosis.

Chapter 4

Chapter 4: Thromboelastography: The effect of metals on coagulation parameters

4.1. Introduction

Thromboelastography (TEG[®]) is a haemostatic assay that measures the viscoelastic properties of whole blood clot formation (Nickson, 2020). The data obtained from such an assay can accurately be quantified, providing researchers with a new method of determining the effects of heavy metal exposure in blood. TEG[®] is advantageous compared to morphological techniques because quantitative data is generated which allows researchers to test a specific hypothesis, using different statistical tests (Da Luz *et al.*, 2013).

TEG[®] is commonly used by doctors to determine the necessity of a blood transfusion in trauma cases and high-risk procedures like liver transplantation or heart surgery (Nickson, 2020). This assay has also been used in the development of new drugs (Nickson, 2020). For this study, the data obtained from the TEG[®] was used to determine if there was any adverse effect on the coagulation parameters of blood after exposure to Cd, Pb and Cr, alone and in combination.

The physical properties of blood clot formation are measured via a pin suspended in a heated (37°C) cup filled with blood. As the clot develops, it rotates the pin containing a torsion wire connected to a mechanical-electrical transducer. The elasticity and strength of the developing clot changes the rotation of the pin, which is then converted into electrical signals. A computer algorithm is then used to create a graphical and numerical output which can be subjected to statistical testing (Nickson, 2020).

The TEG[®] is convenient because it only takes approximately 30 min to perform and can easily be repeated and compared (Nickson, 2020). A disadvantage of the TEG[®] is that the machine needs to be calibrated on a daily bases and should only be operated by trained personnel. The process is also susceptible to technical variations such as a delay in processing that can alter the accuracy of the results (Da Luz *et al.*, 2013). Figure 4.1 is the graphical waveform obtained from a normal TEG[®] tracing, indicating the different parameters. Table 4.1 provides a description of the different coagulation parameters that can be measured with the TEG[®].

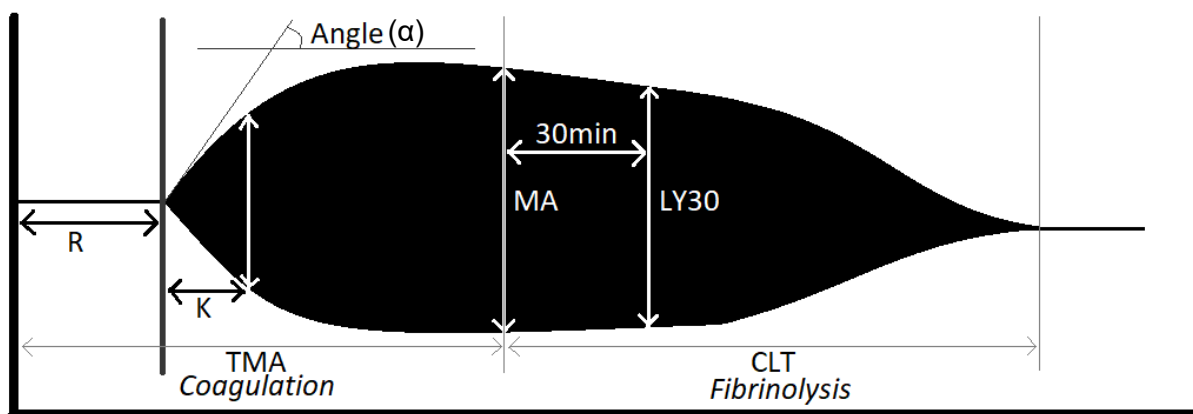


Figure 4.1: The graphical waveform representation of a normal TEG[®] tracing (Nickson, 2020). R: reaction time; K: clotting time; α : slope between R and K; MA: maximum amplitude; LY30: amplitude at 30 min; TMA: time to maximum amplitude; CLT: clot lysis time.

Table 4.1: Whole blood parameters, measured by the TEG[®] (Nickson, 2020).

<u>Abbreviation</u>	<u>Parameter</u>	<u>SI Unit</u>	<u>Description</u>
R	Reaction time	min	Time of latency from start of test to initial fibrin formation (amplitude 2mm).
K	Clotting time	min	Time taken to achieve a certain level of clot strength (amplitude of 20mm).
α	Angle (Slope between R and K)	degrees	Measures the speed at which fibrin build up and cross-linking takes place, hence assesses the rate of clot formation.
MA	Maximum amplitude	mm	Represents the ultimate strength of the fibrin clot; i.e., overall stability of the clot.
G	Clot strength	dynes / cm ²	Final clot strength.
A30	Amplitude at 30 min	mm	Percentage lysis at 30 min (standard measure of fibrinolysis)
CI	Coagulation index		Mathematical compilation of other TEG [®] outcome variables (R, K, α and MA)
TMA	Time to maximum amplitude(s)	min	The time it takes for the clot to reach ultimate strength.
SP	Split point	Dynes / cm ²	Initial fibrin formation (conversion of fibrinogen to first detachable fibrin)

4.2. Materials and Methods

4.2.1. Metal preparation

The method for preparing stock and working solutions for the various metals were the same as described in Section 3.2.1. Due to time and financial constraints, only the x100 exposure group was subjected to TEG analysis. Whole blood was exposed to x100 the heavy metal concentration found in cigarette smoke, as indicated in Table 3.1 (Yaprak and Yolcubal, 2019).

Blood was exposed to Cd (21 µg/L), Pb (410 µg/L) and Cr (22400 µg/mL) individually as well as in combination.

4.2.2. Blood collection

The process of blood collection was the same as described in Section 3.2.2.

4.2.3. Sample preparation for TEG®

Whole blood was exposed to different concentrations of heavy metals, alone and in combination (Table 3.1) and incubated for 30 min at room temperature. Two samples were run simultaneously in the channels of the TEG® (TEG® 5000 computer-controlled device, Haemoscope Corp., Niles, USA). In order to start the coagulation process, 20 µL of calcium chloride (CaCl₂) (Sigma-Aldrich, St Louis, MO, USA) was added to 340 µL of whole blood in the oscillating cup of the TEG®. This process was run until LY30 was reached (Janse Van Rensburg *et al.*, 2019).

4.2.4. Statistical Analysis

The D'Agostino & Pearson normality test (Graph Pad version 6.1) was used to determine normality of the data. After normality was determined, the One-Way ANOVA and Tukey's multiple comparison test was performed on all parametric data. The Kruskal-Wallis test was performed on all non-parametric data. Multiple comparisons were done between the coagulation parameters (Table 4.1) of each individual experimental group to determine the significance. Statistical analysis was performed with a 95% confidence interval and a p-value of < 0.05 was considered significant.

4.3. Results

Blood clot formation was monitored using TEG® after a 30 min exposure to x100 concentration of Cd, Pb and Cr, alone and in combination. Figure 4.2 is a graphical waveform representation of all the whole blood parameters, with their respective normal ranges indicated below. Figure 4.2B is a superimposed version of Figure 4.2A and shows the representative tracings for the control group and Cd, Pb or Cr combination groups. As seen in Figure 4.2A the tracings of the groups containing Cr (orange, purple, green and blue) all have a shorter R-time (min) compared to the control group (white tracing) which can be indicative of a potential increase in coagulability. Both Table 4.2 and 4.3 summarize the effects of x100 metal exposure on the

coagulation parameters of whole blood and in Figure 4.3A – I, compare the mean value of each parameter to the control using graphs.

Statistical analysis was performed on the coagulation parameters to determine if there were any significant ($p > 0.05$) differences between each experimental group and the control. After performing a normality test, either the One-way ANOVA (parametric data) along with Tukey's multiple comparison test or Kruskal-Wallis (non-parametric data) test was used to determine significance.

Table 4.2 shows a five-point summary of the data collected from the TEG[®] runs. When comparing the mean value of each coagulation parameter to the control group (isoPBS), analysis revealed that only two parameters had statistical relevance, more specifically the R-time and SP-value (d/sc) for the groups exposed to Cr, alone and in combination (Cd + Cr, Pb + Cr and Cd + Pb + Cr).

The graph in Figure 4.3A shows a clear decrease in R-time for the Cr, Cd + Cr, Pb + Cr and Cd + Pb + Cr groups. It was also noted that the Cd + Pb combination had the highest R-value compared to the other groups and Pb has similar values to the control. A shorter R-time suggests a decrease in the time it takes for clot to start forming. In Figure 4.3B, it can be seen that all the metal groups show a decrease in k-time (min) as compared to the control. An overall trend could not be distinguished, but the Cd group had the highest k-value, compared to the other metal groups. Figure 4.3C and Table 4.2 reveal that all the metal groups, except Cd + Cr, show an increase in α -angle as compared to the control. This might be due to the Cd + Cr group having a higher degree of standard deviation than the rest of the groups, suggesting that the data obtained from the TEG[®] are more spread out in relation to the mean.

In Figure 4.3D and Table 4.2, it can be seen that all the metal groups, except Cd show a slight increase in MA (mm), with all of the values being close to the control. Figure 4.3E shows that all the metal groups, except Cd and Cd + Cr have a higher G-value (d/sc) compared to the control. In Table 4.2, it can be seen that the Cd + Cr combination is the closest in value to the control and Cd is lower. All the metal groups show an increase in A30 (mm) compared to the control, except Cd and Cd + Pb (Figure 4.3F). None of the values are statistically significant, with the Cd + Cr combination being the closest to the control (Table 4.2).

In Figure 4.3G, all the metal groups except Cd, show an increase in the CI-value as compared to the control. Even though none of the values are significantly different from the control, it is

noteworthy that the Pb + Cr combination show the largest CI-value with the biggest difference in value compared to the control. Lastly, in Figure 4.3H and I, it can be seen that all the metal groups except the Cd + Pb combination, show a decrease in TMA (min) and SP values as compared to the control. The groups with Cr, alone and in combination, show a lower TMA-value than the rest of the groups, including the control (Table 4.2). The graph in Figure 4.3I shows a clear decrease in the SP-value for the Cr, Cd + Cr, Pb + Cr and Cd + Pb + Cr groups as compared to the control. These differences are statistically significant and correspond with the findings found for the R-time parameter.

Table 4.2: Summary of the effects of Cd, Pb and Cr, alone and in combination, at x100 concentration found in cigarette smoke (Yaprak and Yolcubal, 2019) on the parameters of whole blood.

Parameters	<u>R (min)</u>		<u>K (min)</u>		<u>α (deg)</u>		<u>MA (mm)</u>		<u>G (d/sc)</u>		<u>A30 (mm)</u>	
	Normal Ranges		Normal Ranges		Normal Ranges		Normal Ranges		Normal Ranges		Normal Ranges	
	9 - 27		2 - 9		22 - 58		44 - 64		36000 - 85000			
	Mean ± SD	Range	Mean ± SD	Range	Mean ± SD	Range	Mean ± SD	Range	Mean ± SD	Range	Mean ± SD	Range
Control	4,80 ± 1,02	3,7 - 6,5	2,80 ± 1,97	1,6 - 8,3	69,40 ± 3,25	64,4 - 75,4	52,10 ± 9,38	29,5 - 63,0	5,75 ± 1,79	2,1 - 8,5	52,31 ± 9,27	29,9 - 62,9
Cd	4,54 ± 1,08	3,2 - 6,1	2,44 ± 1,13	1,4 - 5,2	70,57 ± 5,13	61,7 - 76,3	51,40 ± 7,81	42,0 - 65,0	5,55 ± 1,83	3,6 - 9,3	51,48 ± 7,71	42,3 - 65,0
Pb	4,81 ± 1,27	3,4 - 6,4	2,17 ± 0,50	1,6 - 3,1	70,62 ± 3,55	64,0 - 75,8	53,80 ± 6,30	40,5 - 60,0	5,98 ± 1,36	3,4 - 7,5	53,77 ± 6,31	40,2 - 60,1
Cr	2,13 ± 0,49 *	1,3 - 2,8	1,82 ± 0,70	0,8 - 3,0	75,57 ± 3,99	67,4 - 82,9	53,14 ± 7,45	42,0 - 67,0	5,96 ± 1,89	3,8 - 10,2	53,52 ± 7,33	43,0 - 67,4
Cd + Pb	5,27 ± 1,46	2,9 - 7,0	1,98 ± 0,32	1,5 - 2,4	71,67 ± 3,94	65,3 - 77,5	53,66 ± 8,02	41,0 - 69,1	6,14 ± 2,20	3,5 - 11,2	48,50 ± 18,8	0,10 - 69,2
Cd + Cr	2,27 ± 0,39 *	1,5 - 2,8	2,28 ± 1,50	0,8 - 5,6	67,22 ± 21,79	7,30 - 81,8	52,25 ± 8,10	35,5 - 60,0	5,73 ± 1,61	2,8 - 7,5	52,37 ± 8,15	35,6 - 60,4
Pb + Cr	2,11 ± 0,49 *	1,3 - 2,8	1,99 ± 0,85	1,1 - 4,2	73,25 ± 5,62	58,5 - 78,3	54,00 ± 8,49	37,5 - 66,5	6,20 ± 2,01	3,0 - 9,9	54,18 ± 8,70	37,2 - 66,8
Cd + Pb + Cr	2,24 ± 0,67 *	1,2 - 3,4	2,08 ± 1,48	1,0 - 6,1	73,64 ± 5,24	60,8 - 78,6	52,72 ± 8,97	33,5 - 66,0	5,91 ± 2,04	2,5 - 9,7	52,91 ± 8,96	33,8 - 66,1

Parameter	<u>CI</u>		<u>TMA (min)</u>		<u>SP (d/sc)</u>	
	Normal Ranges		Normal Ranges		Normal Ranges	
	-3 - 3				1,5	
	Mean ± SD	Range	Mean ± SD	Range	Mean ± SD	Range
Control	0,81 ± 1,46	-2,6 - 2,3	27,74 ± 3,23	21,8 - 33,5	4,24 ± 0,88	3,1 - 5,8
Cd	0,72 ± 1,26	-0,9 - 2,6	26,67 ± 4,43	22,0 - 33,3	3,87 ± 1,31	1,3 - 5,3
Pb	1,03 ± 1,02	-0,9 - 2,3	27,35 ± 3,99	21,8 - 34,2	4,01 ± 1,23	2,2 - 5,8
Cr	1,50 ± 1,12	0,1 - 3,8	21,83 ± 3,62	16,2 - 28,0	1,69 ± 0,75 *	0,2 - 2,7
Cd + Pb	0,88 ± 1,47	-1,6 - 3,6	27,76 ± 7,34	2,60 - 46,8	4,70 ± 1,46	2,6 - 6,9
Cd + Cr	1,35 ± 1,24	-1,2 - 2,6	23,54 ± 5,66	16,9 - 35,2	1,91 ± 0,66 *	0,3 - 2,6
Pb + Cr	1,67 ± 1,35	-0,7 - 3,7	24,41 ± 5,06	19,3 - 36,8	1,70 ± 0,50 *	0,8 - 2,4
Cd + Pb + Cr	1,40 ± 1,39	-1,3 - 3,7	24,35 ± 5,24	15,4 - 32,3	2,06 ± 0,68 *	1,2 - 3,4

* Statistical significance: p-value of ≤ 0.05. **SD**: Standard Deviation. **R** = Reaction time; **K** = Clotting time; **α** = Angle; **MA** = Maximum amplitude; **G** = Clot strength; **A30** = Amplitude at 30 min; **CI** = Comprehensive coagulation index; **TMA** = Time to maximum amplitude; **SP** = Split point (initial fibrin formation).

Table 4.3: Summary of the effects of Cd, Pb and Cr, alone and in combinations, at the x100 concentration of each respective metal, on the various parameters of whole blood. The data represents the average of ten volunteers.

	<u>Cd</u> (x100)	<u>Pb</u> (x100)	<u>Cr</u> (x100)	<u>Cd + Pb</u> (x100)	<u>Cd + Cr</u> (x100)	<u>Pb + Cr</u> (x100)	<u>Cd + Pb + Cr</u> (x100)
<u>R (min)</u>							
<u>Average</u>	↓	↔	↓*	↑	↓*	↓*	↓*
<u>K (min)</u>							
<u>Average</u>	↓	↓	↓	↓	↓	↓	↓
<u>α (deg)</u>							
<u>Average</u>	↑	↑	↑	↑	↓	↑	↑
<u>MA (mm)</u>							
<u>Average</u>	↓	↑	↑	↑	↑	↑	↑
<u>G (d/sc)</u>							
<u>Average</u>	↓	↑	↑	↑	↓	↑	↑
<u>A30 (mm)</u>							
<u>Average</u>	↓	↑	↑	↓	↑	↑	↑
<u>CI</u>							
<u>Average</u>	↓	↑	↑	↑	↑	↑	↑
<u>TMA (min)</u>							
<u>Average</u>	↓	↓	↓	↑	↓	↓	↓
<u>SP (d/sc)</u>							
<u>Average</u>	↓	↓	↓*	↑	↓*	↓*	↓*

R = Reaction time; **K** = Clotting time; **α** = Angle; **MA** = Maximum amplitude; **G** = Clot strength; **A30** = Amplitude at 30 min; **CI** = Comprehensive coagulation index; **TMA** = Time to maximum amplitude; **SP** = Split point (initial fibrin formation). ↑: Increase the value, ↓: decrease the value and ↔: similar to the value as compared to the control values. The **shaded blocks** do not follow the trend of the majority groups. * Statistically significant, p-value of ≤ 0.05; 95% confidence interval.

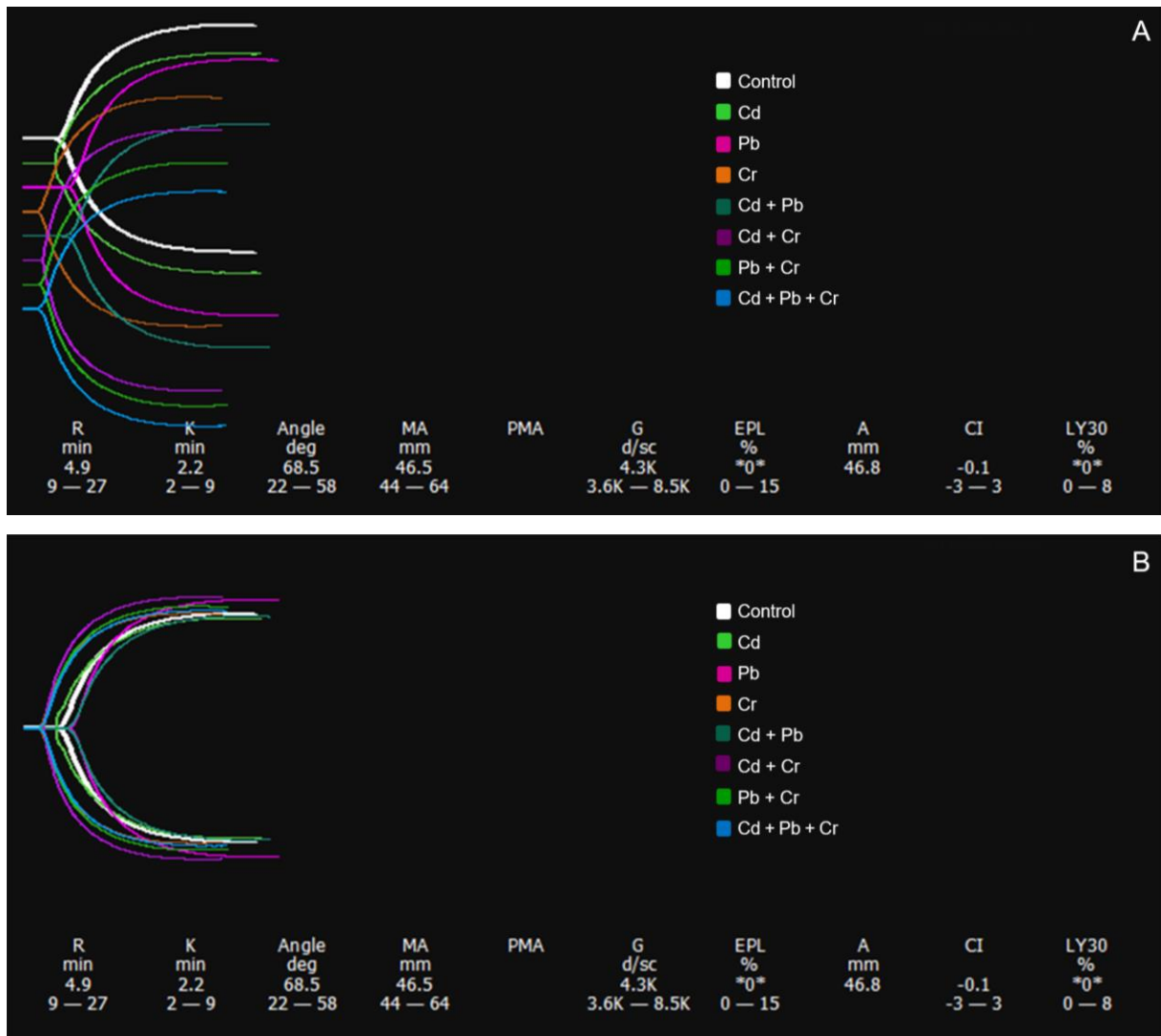
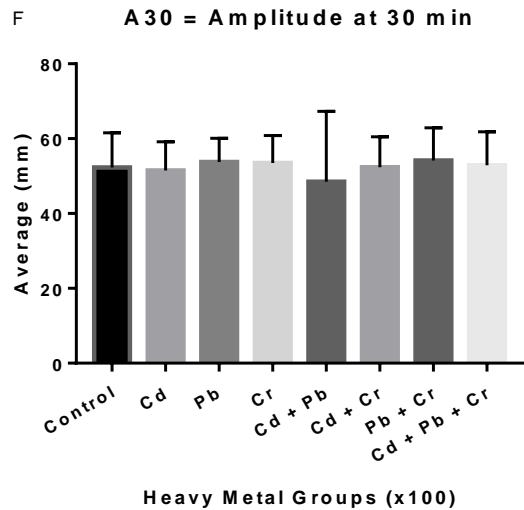
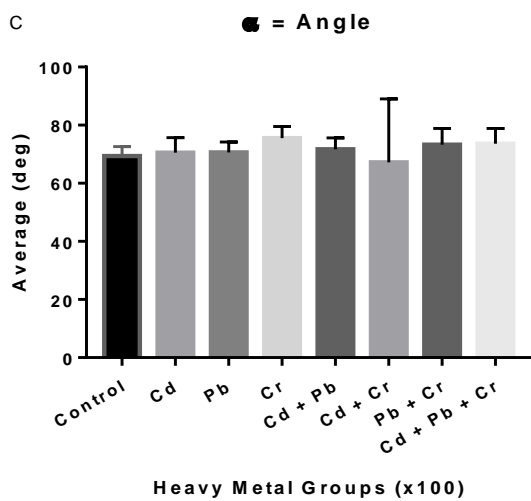
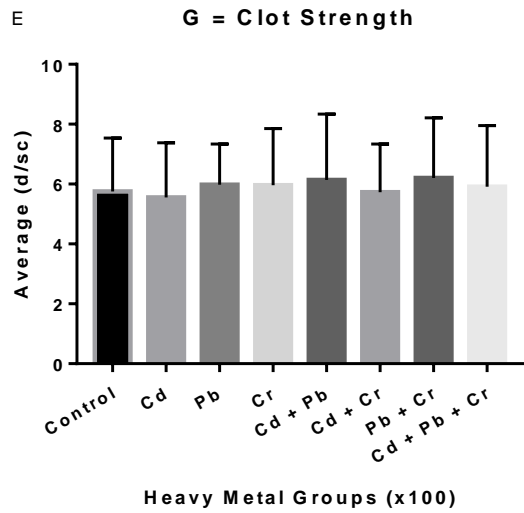
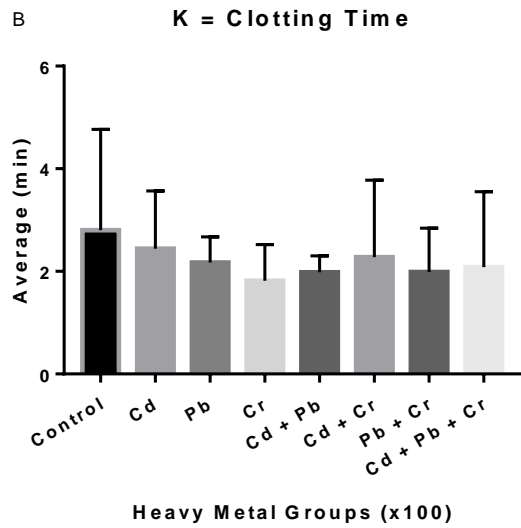
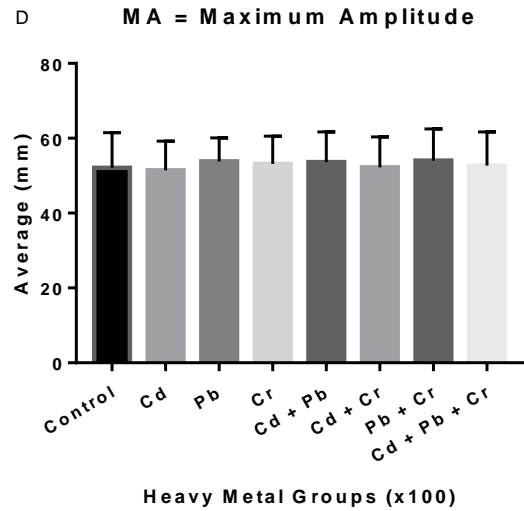
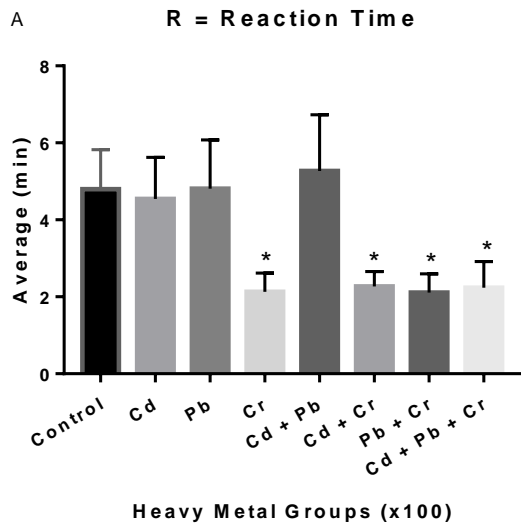


Figure 4.2: Representative TEG[®] viscoelastic traces of the control and metal groups. Control: **white**; Cd: **lime green**; Pb: **pink**; Cr: **orange**; Cd + Pb: **moss green**; Cd + Cr: **purple**; Pb + Cr: **green** and Cd + Pb + Cr: **blue**. A: not superimposed, B: superimposed.



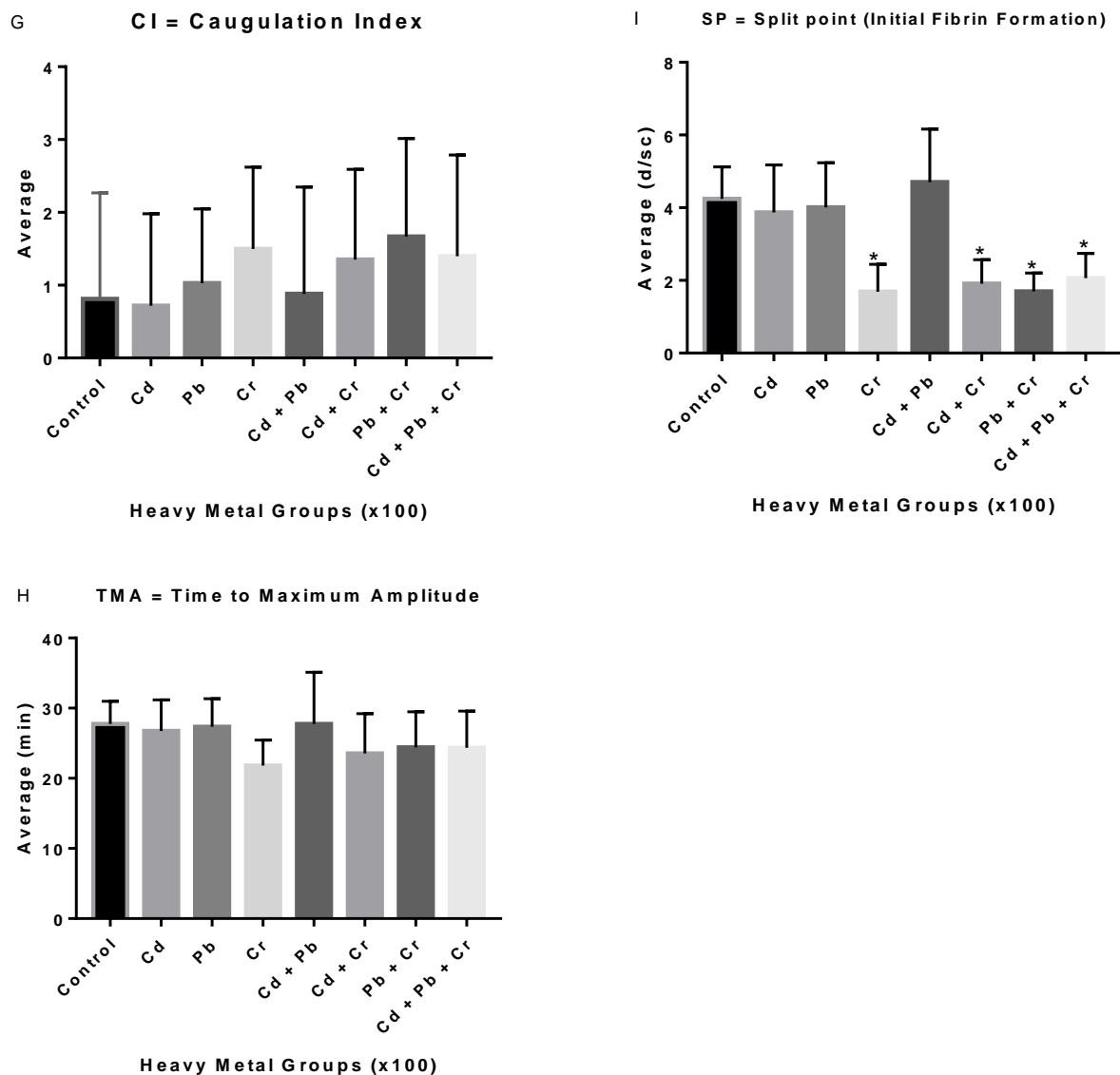


Figure 4.3: Graphical representation of the mean and standard deviation (error bars) for the coagulation parameters * Statistically significant, p-value of ≤ 0.05 ; 95% confidence interval.

4.4. Discussion

The haemostatic system in the body has the ability to control clot formation and clot lysis in order to prevent haemorrhages and aid in the healing process of damaged blood vessels (Venter *et al.*, 2017a). This is achieved by regulating platelet activation together with the coagulation cascade. Vasoconstriction, along with adhesion and aggregation of platelets helps to form a platelet plug at the site of injury, which is then stabilized by fibrin formation (Thakur and Ahmed, 2012). The whole process is regulated in such a way that it doesn't cause thrombosis elsewhere in the body. Conventional testing, like fibrinogen levels, the number of

platelets and thrombin time can be used to quantify clot formation (Ruttmann, 2006). Although these traditional methods still provide useful information, they are seen as isolated tests because they only test parts of the coagulation cascade. Coagulation is an intricate process with multiple interactions between factors, proteins, platelets, activators and inhibitors. This can lead to an inaccurate reflection of what actually happens in the patient because measurements of static endpoints do not necessarily reflect the dynamics of the system (Ruttmann, 2006).

TEG[®] is a method that was developed by Dr Hellmut Hartert, in 1948 that enabled doctors and researchers to accurately study whole blood parameters. This convenient method provides a global assessment of the haemostatic function by monitoring and evaluating the parameters and elastic properties of whole blood (Thakur and Ahmed, 2012). The principle of TEG[®] is based on the fact that the end product of haemostasis is a clot. Depending on the physical properties (stability, rate and strength) of the clot, doctors can accurately predict if the patient will have normal haemostasis or develop thrombosis (Ruttmann, 2006). TEG[®] is sensitive to the interactions between cellular and plasmatic components because it measures the physical and elastic properties of the blood clot. This in turn affects the rate and structure of clot formation and lysis (Ruttmann, 2006).

Various parameters are captured by the numerical and graphical output of the TEG[®] analysis. The time it takes for the clot to start to develop (at an amplitude of 2 mm in TEG[®] tracing) is called the reaction time (R-time). This is achieved through fibrin formation. Factor deficiencies and anticoagulants will prolong the R-time, whereas hypercoagulable conditions will shorten the time (Ruttmann, 2006). The trend seen in the viscoelastic results (Figure 4.2) indicate that the R-time significantly decreased for all the groups containing Cr when compared to the control group. A decrease in the R-time is a result of advanced fibrin formation, which is catalysed by thrombin and stabilized by thrombin-catalysed factor XIII (FXIII) (Kell and Pretorius, 2017). Calcium acts as a co-factor in the formation of thrombin and FXIII during coagulation (Kell and Pretorius, 2017; Swanepoel *et al.*, 2015). The methodologies used in this study isn't specific enough to determine the mechanism through which Cr impacts the enzymatic pathways of coagulation. However, heavy metals like Cr are known to interact with the Ca-binding sites and can cause an increase in Ca-levels and ROS. A decrease in R-time, indicated by a shorter initiation time for clot formation, would suggest an increase in platelet activation. This can lead to hypercoagulable states and potentially thrombosis (Ruttmann, 2006). Thrombin helps to form clots by cleaving fibrinogen to form fibrin, which is then polymerised to form fibrin fibres. These fibres, along with activated platelets form the clot.

Scanning electron microscopy analysis of the metal exposed groups revealed considerable fibrin formation. The groups containing Cr, especially the Cd + Cr combination showed sticky mass formation with fibrin strands fusing together and forming net-like coverings. These findings support the fact that heavy metals, particularly Cr have the ability to influence clot formation and increase the risk of thrombosis.

The k-time is a representation of the time it takes for the clot to reach a fixed level of firmness (between 2 mm and 20 mm amplitude in the TEG[®] tracing). Increased fibrinogen levels and platelet function will shorten the k-time and anticoagulants will prolong it (Ruttmann, 2006). A slight decrease in the k-time was observed in all the metal groups (Figure 4.2B) which might suggest an increase in thrombin. This can lead to higher fibrinogen levels and platelet activation which would in turn decrease the time it takes for the clot to amplify (k-time). A short k-time is an indication of hypercoagulability and may stimulate thrombosis in the blood (Ruttmann, 2006; Thakur and Ahmed, 2012). A considerable increase in thrombin will lead to clot formation. High levels of thrombin typically induce fibrinogen cleavage, producing fibrin that can be polymerised. Polymerised fibres along with activated platelets will form blood clots (Ruttmann, 2006).

The k-time and α -angle are closely related because they are both functions of the rate of polymerisation. Similar to k-time, increased fibrinogen levels and platelet function will increase the α -angle and anticoagulants will decrease it. The α -angle measures the speed at which clot strengthening takes place and therefore evaluates the rate of clot formation (Thakur and Ahmed, 2012). The α -angle is generally more comprehensive in hypocoagulable conditions because the k-time will be undefined (the final clot firmness doesn't reach an amplitude of 20 mm) (Ruttmann, 2006). Although, no significance was observed, the data obtained in the current study showed a slight overall increase (except the Cd + Cr combination which is lower than the control) of the α -angle when compared to the control group (Table 4.3).

The MA-value is a measurement of the maximum strength and stiffness of the developed clot and influenced by platelet (80%) and fibrin (20%) function. A deficiency in coagulation factors can lead to decreased MA, whereas hypercoagulable states will increase MA (Thakur and Ahmed, 2012). There were no significant differences in the MA for all the experimental groups compared to the control (Figure 4.2 D) suggesting that the maximum strength of the developing clot for all the metal groups are similar to that of the control group. Another measurement of clot strength is G, which is a computer-generated value that reflects the strength of the clot from the initial fibrin formation to fibrinolysis. The G-parameter takes into account the roles that

platelets and enzymes play in clot formation, making it a better measurement than MA (Da Luz *et al.*, 2013). Most of the metal groups showed a slight increase in G-value, except the Cd and Cd + Cr combination. Although not significant (Figure 4.2 E), the data still suggest that a stronger and more stable clot was formed, as compared to the control. Stronger clot strength can contribute to thrombosis and also affect fibrinolysis (Van Rooy *et al.*, 2015).

The coagulation index (CI) is a mathematically calculated value that is an overall indication of coagulation. It takes into account the relative contribution of each of the four parameters (r-time, k-time, α -angle and MA) and predicts the state of coagulation (hypo-, normal- or hypercoagulable) (Thakur and Ahmed, 2012). The normal CI-value range for humans are between minus three and plus three. Values higher than three are considered hypercoagulable and values lower than minus three are considered hypocoagulable. All the metal exposed groups with the exception of Cd, showed a slight increase in CI-value compared to the control but still within the normal range. It is noteworthy that the index values are the highest in groups containing Cr, suggesting that this heavy metal has the potential to increase overall coagulability in blood.

One of the main limitations of TEG[®] is that it has never been standardized in comparison to the more conventional tests. The TEG[®] procedure is time sensitive and a delay in processing can alter the test results (Thakur and Ahmed, 2012). Although the experimental results for this study show a certain trend, they only explain acute exposure for short periods of time. In reality, the general smoking population is chronically exposed to these heavy metals, for long periods of time. Other factors like lifestyle choices, living conditions, type of occupation and genetics can also play a role in thrombus formation. Therefore, TEG[®] can only be used as an investigative tool to analyse the effects of Cd, Pb and Cr, alone and in combination, on the coagulation parameters of blood, for a short period of time, at fixed exposures.

Conclusion

No statistically significant changes were observed in all but two of the measured coagulation parameters. The viscoelastic results indicated that the R-time and SP-values significantly decreased for all the groups containing Cr when compared to the control group, indicating a shorter initiation time for clot formation. Other trends were observed when metal exposed groups were compared to the control. These include a decrease in k-time and an overall increase (with the exception to some groups) in α -angle, MA, G and CI. These trends are an indication that Cd, Pb and Cr, alone and in combination have the potential to increase the coagulability of blood, leading to more hypercoagulable states and potentially thrombosis.

Chapter 5

Chapter 5: The effect of cadmium, lead and chromium, alone and in combination on ROS formation

5.1. Introduction

Red blood cells have a key function of transporting oxygen to all tissue by deforming and squeezing through narrow capillaries to reach every cell. If RBCs are continuously exposed to sources of ROS, membrane damage can occur, which will impair deformability (Venter *et al.*, 2017a). This will contribute to the elimination of aged or damaged RBCs from blood circulation and impair oxygen delivery. Although RBCs have an extensive antioxidant system to minimize the effects of oxidative stress caused by ROS, the oxidation of haemoglobin attached to the membrane is relatively inaccessible by this system (Mohanty *et al.*, 2014).

Various toxicological studies have shown strong associations between heavy metal exposure and increased risks of health-related issues (Barrett *et al.*, 2018; Caruso *et al.*, 2013; Venter *et al.*, 2017a; Venter *et al.*, 2015). The mechanisms through which Cd, Pb and Cr cause adverse effects are still poorly understood, but oxidative stress from ROS is believed to be one of the main contributors to these health issues (Huang *et al.*, 2016). Heavy metals in general, have electron sharing affinities that can form covalent bonds with sulfhydryl groups found in proteins. Damage to the antioxidant defence system or thiol depletion can lead to ROS production. Fenton-like reactions and the depletion of sulfhydryl reserves appear to play a major role in oxidative stress observed in metal toxicity which can lead to membrane damage, protein dysfunction, impaired DNA repair and eventual cell death (Ercal *et al.*, 2002).

A variety of methods have been developed for ROS detection, which includes spin trapping, chemiluminescent probing and fluorescent probing. While these methods are widely used, many of them are not specific, do not allow subcellular localization and can produce artefacts. Due to their high reactivity, the half-life of ROS is very short, ranging from nanoseconds to seconds and detection requires rapid acting probes that compete with antioxidants to produce stable products that are quantifiable (Dikalov and Harrison, 2014). For this study, the dichlorodihydrofluorescein diacetate (DCFH-DA) assay was used to detect cellular ROS production. DCFH-DA is a cell permeating ester that is hydrolysed to DCFH in the cytoplasm and then oxidized to form 2',7'-dichlorofluorocein (DCF), whose fluorescence can be measured at 522 nm using a spectrofluorometer (Huang *et al.*, 2016).

Isotonic phosphate buffered saline (isoPBS) and 2,2'-Azobis (2-amidinopropane) dihydrochloride (AAPH) were used as negative and positive controls respectively. The PBS solution is isotonic, non-toxic and has a pH of 7.4, which is similar to the cellular environment and will keep the cells from rupturing. In contrast, AAPH is a water-soluble compound with radical-generating abilities that is used to mimic the oxidative stress state. The half-life of AAPH is about 175 hours and directly generates peroxy radicals without generating hydrogen peroxide as an intermediate (Moreira Gomes *et al.*, 2016). The constant rate of free radical generation makes AAPH ideal to study the effects of Cd, Pb and Cr, alone and in combination on ROS formation in blood.

Although the DCFH-DA assay is widely used and has many advantages over other methods, there are still a few limitations. Factors such as the pH value, reagent concentration and incubation temperature can affect the performance of the assay (Huang *et al.*, 2016). In some cases, DCF has shown to react with oxygen to produce oxygen-ions and hydrogen peroxide, thus artificially elevating the very ROS that it is attempting to quantify (Dikalov and Harrison, 2014).

The haemolysis assay was also used as a rapid high-throughput screen for cytocompatibility by measuring the amount of haemoglobin released into the medium. Sodium dodecyl sulphate (SDS) was used as a positive control that causes cell lysis by incorporating into the membrane and denaturing proteins (Brown and Audet, 2008).

5.2. Materials and Methods

5.2.1. Metal preparation

The method for preparing stock and working solutions for the various metals were the same as described in section 3.2.1.

5.2.2. Blood collection

The process of blood collection was the same as described in section 3.2.2.

5.2.3. Sample preparation for DCFH-DA assay

A modified version of the method described by Janse van Rensburg *et al.* (2019) was used to measure the ROS production in erythrocytes. In order to isolate erythrocytes, whole blood was centrifuged at 200 x g for 30 min and washed twice with isotonic phosphate buffered saline (isoPBS: 0.137 M NaCl, 3 mM KCl, 1.9 mM NaH₂PO₄, 8.1 mM Na₂HPO₄, pH 7.4) (Sigma-Aldrich, St Louis, MO, USA). The collected erythrocytes were diluted to a 5% (v/v) dilution with isoPBS. A 96-well plate was prepared by pipetting 15 µL of the various heavy metal concentrations into the allocated wells along with 90 µL of the erythrocyte suspension. A negative control was exposed to 15 µL isoPBS and a positive control for ROS production was exposed to 15 µL of 2 mg/mL AAPH (Sigma-Aldrich, St Louis, MO, USA). A 75 µM DCFH-DA solution (Sigma-Aldrich, St Louis, MO, USA) was prepared beforehand and 15 µL was added to each well. The plate was incubated for 20 hrs at 37°C. The change in fluorescence was measured using the FLUOstar OPTIMA plate reader (BMG Labtech, Offenburg, Germany) with an excitation wavelength of 485 nm and emission wavelength of 520 nm (Janse Van Rensburg *et al.*, 2019). The results were expressed as percentage ROS production, using the formula below.

$$\% \text{ ROS production} = (F_{\text{sample}} - F_{0\%} / F_{100\%} - F_{0\%}) \times 100$$

- F_{sample} = Fluorescence of erythrocytes exposed to metals alone and in combination
 $F_{0\%}$ = Fluorescence of erythrocytes exposed to isoPBS (0% haemolysis)
 $F_{100\%}$ = Fluorescence of erythrocytes exposed to 2 mg/mL AAPH (100% haemolysis).

5.2.4. Sample preparation for the haemolysis assay

The samples were prepared by following the standard haemolysis protocol described in Tabart *et al.* (2009). In order to isolate erythrocytes, whole blood was centrifuged at 200 x g for 30 min and washed twice with isotonic phosphate buffered saline (isoPBS: 0.137 M NaCl, 3 mM KCl, 1.9 mM NaH₂PO₄, 8.1 mM Na₂HPO₄, pH 7.4) (Sigma-Aldrich, St Louis, MO, USA). The collected erythrocytes were diluted to a 5% (v/v) dilution with isoPBS. Sodium dodecyl sulphate (2% SDS) was used as a positive control that represents 100% haemolysis and isoPBS was used as a negative control that represents 0% haemolysis. The 5% blood solution was then exposed to the different metals, alone and in combination at x100 concentration and incubated for 24 hrs at 37°C. After incubation, the samples were centrifuged at 1200 x g for 2 min and the supernatant transferred in triplicate to a 96-well plate (Tabart *et al.*, 2009). Absorbance was measured at 570 nm. The results were expressed as percentage haemolysis, using the formula below.

$$\% \text{ Haemolysis} = (A_{\text{sample}} - A_{0\%} / A_{100\%} - A_{0\%}) \times 100$$

- A_{sample} = Absorbance of erythrocytes exposed to metals alone and in combination
 $A_{0\%}$ = Absorbance of erythrocytes exposed to isoPBS (0% haemolysis)
 $A_{100\%}$ = Absorbance of erythrocytes exposed to 2% SDS (100% haemolysis).

5.2.5. Statistical analysis

The percentage relative to the control was calculated for each sample. AAPH was taken as 100% and isoPBS as 0%. All the data was presented as the mean \pm standard error of the mean (SE). Both the D'Agostino & Pearson normality test and Shapiro-Wilk normality test (Graph Pad version 6.1) were used to determine normality of the data. After normality was determined, the One-Way ANOVA and Tukey's multiple comparison test was performed on all parametric data. Multiple comparisons were done between the different concentrations of each individual experimental group to determine the significance. Statistical analysis was performed with a 95% confidence interval and a p-value of < 0.05 was considered significant.

5.3. Results

5.3.1. The effect of heavy metals on ROS production

The DCFH-DA assay was used to determine the ability of Cd, Pb and Cr alone and in combination to induce ROS formation at x1, x10 and x100 the concentration found in PRF exposed to cigarette smoke (Yaprak and Yolcubal, 2019). After whole blood was processed and exposed to the heavy metals, the erythrocyte suspension was incubated for 20 hours. Isotonic phosphate buffered saline was used as a negative control which represents 0% ROS production and AAPH was used as a positive control that represents 100% ROS production. The data was collected from ten volunteers and the mean, along with standard error of the mean was calculated from triplicate experiments. Significance was determined at p-value ≤ 0.05 and 95% confidence interval.

In Figure 5.1, the results obtained from each x1 metal exposed group in the DCFH-DA assay was compared to one another. The AAPH exposed group (positive control) showed 100% ROS production, compared to isoPBS (negative control group) with 0% ROS production. No significance was observed for any of the metal exposed groups, compared to the negative control (isoPBS) or other metal groups from the same concentration. It is worth mentioning that the Cd + Pb + Cr combination group showed the highest level of ROS production (16.78%), compared to the Cd + Cr (7.53%), Pb + Cr (4.91%) and Cd + Pb (4.62%) groups (Table 5.1). The standard error of the mean for all the metal exposed groups were high, ranging from 6.27 (Pb) to 11.02 (Cd + Pb + Cr), suggesting that the fluorescent reading obtained for some of the samples were not representative of the general population.

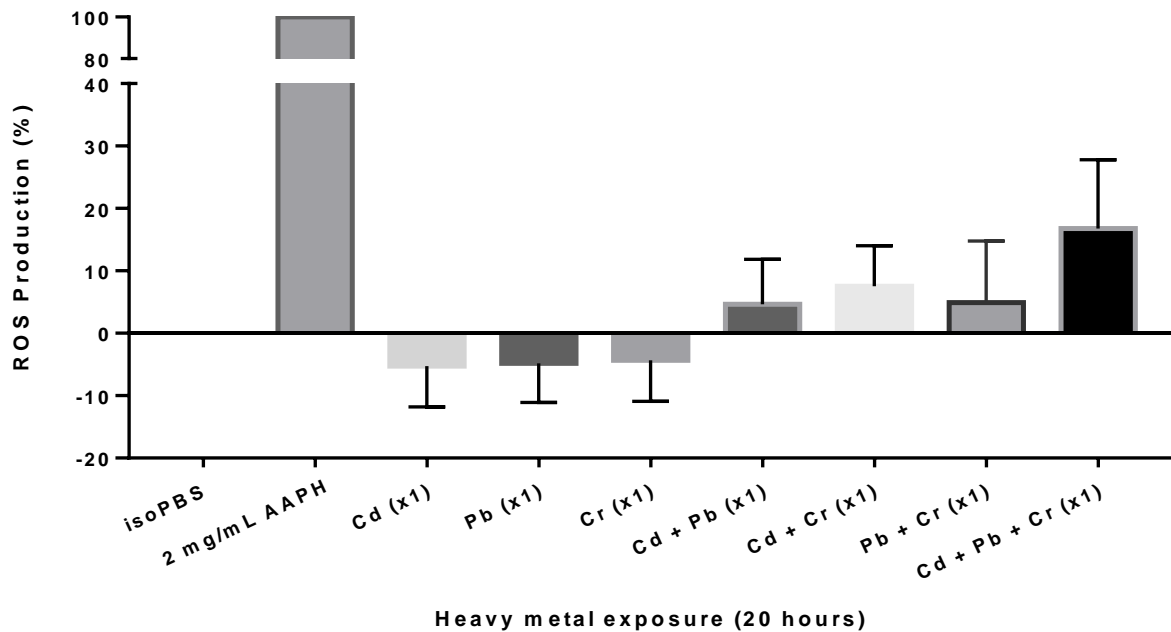


Figure 5.1: The effects of Cd, Pb and Cr alone and in combination on ROS production (%) evaluated at x1 the concentration found in PRF exposed to cigarette smoke. The data is expressed as the mean \pm standard error of the mean for ten independent triplicate experiments. **Positive control:** AAPH and **Negative control:** isoPBS.

Figure 5.2 compared each x10 metal exposed group to one another, as well as to the positive (AAPH) and negative (isoPBS) control. The groups exposed to isoPBS or AAPH showed 0% and 100% ROS production, respectively. The x10 Cd and x10 Pb exposed groups were the only groups that showed significance when compared to the negative control (isoPBS) and other metal groups. The Pb group showed the highest level of ROS production (45.45%), compared to the rest of the metal groups, which showed no ROS production except for the x10 Cd exposed group (30.62%) (Table 5.1). The standard error of the mean for the x10 exposed groups were not as high, compared to the x1 exposed groups, ranging from 3.70 (Cd) to 6.80 (Cr). The two groups that showed significance (Cd and Pb), had smaller standard error of mean values, in relation to the other groups (3.70 and 5.39 respectively) suggesting that the fluorescent readings were more clustered around the population mean and these results may be a better representation of the population.

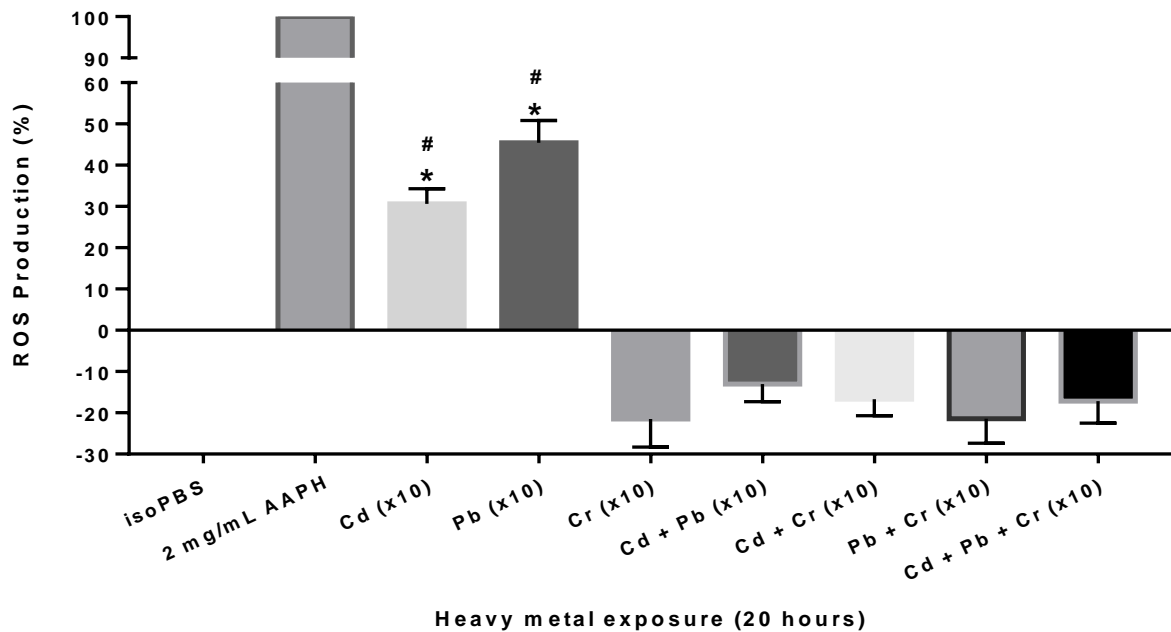


Figure 5.2: The effects of Cd, Pb and Cr alone and in combination on ROS production (%) evaluated at x10 the concentration found in PRF exposed to cigarette smoke. * Indicates significance compared to the negative control and # indicates significance compared to other metal groups. The data is expressed as the mean \pm standard error of the mean for ten independent triplicate experiments. **Positive control:** AAPH and **Negative control:** isoPBS.

In Figure 5.3, the results obtained from the x100 metal exposed groups were compared and no significance was observed for any of the individual metal groups or those in combination. The AAPH exposed group showed 100% ROS production, compared to isoPBS with 0% ROS production. It is noteworthy that the x100 Cd + Pb combination group showed the most ROS production (6.8%) compared to the x100 Pb (6.73%) and Cd (5.75%) groups (Table 5.1). The standard error of the mean for the metal exposed groups, ranges from 2.03 (Pb) to 7.18 (Pb + Cr) suggesting that the fluorescent readings for some of the groups Cd (3.44), Pb (2.03) and Cd + Pb (5.12) were clustered around the population mean and others were more spread out.

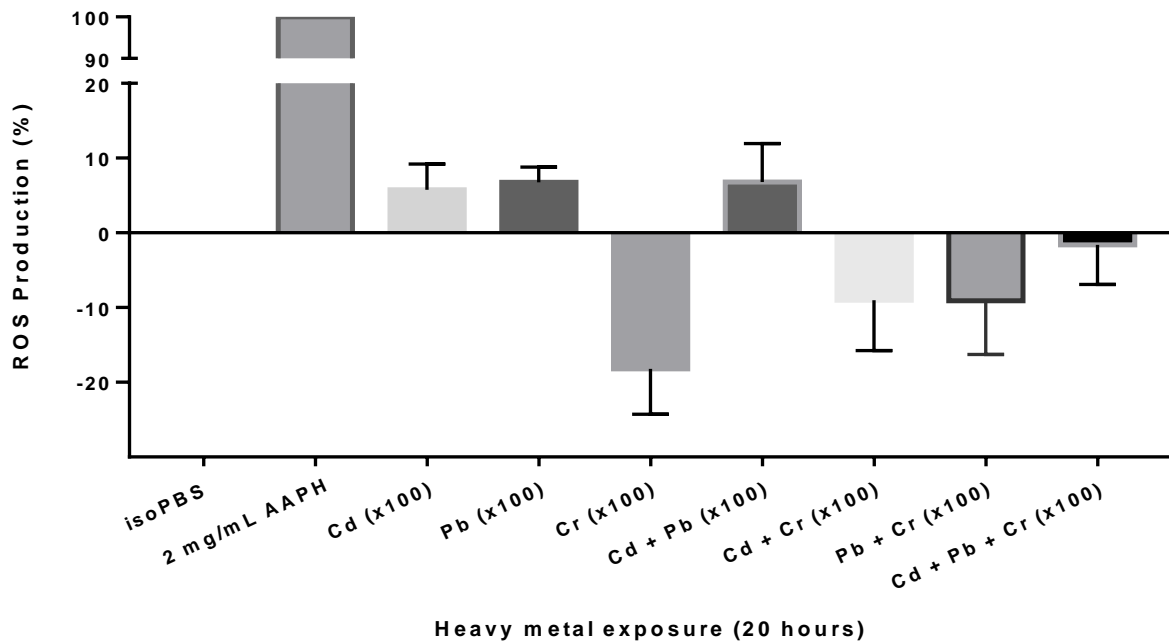


Figure 5.3: The effects of Cd, Pb and Cr alone and in combination on ROS production (%) evaluated at x100 the concentration found in PRF exposed to cigarette smoke. The data is expressed as the mean \pm standard error of the mean for ten independent triplicate experiments. **Positive control:** AAPH and **Negative control:** isoPBS.

In Figure 5.4A, the ROS production of Cd (dark grey bars) and Pb (light grey bars) exposed groups at different concentrations were compared to one another. Both the groups showed varied significance and it became apparent that the only significant ROS production was observed at the x10 concentration. The rest of the groups either showed small amounts of ROS production (x100 Cd and x100 Pb) or none at all (x1 Cd and X1 Pb). It was also noted that the standard error of the mean for each group seems to decrease as the concentrations increased suggesting that the samples better represent the population at higher concentrations (Table 5.1).

Figure 5.4B is a summary of the effect that Cd, Pb and Cr alone and in combination has on ROS production (%) evaluated at x1, x10 and x100 the concentration found in PRF of cigarette smoke. Overall, only a small amount of ROS production was observed in some of the groups. Although a trend could not be established, Cd and Pb, alone and in combination seem to be the cause of all the ROS production observed, except for the Cr combination groups in the x1 concentration. The standard error of the mean for the majority of the groups were large, which would suggest more widely spread data around the population mean.

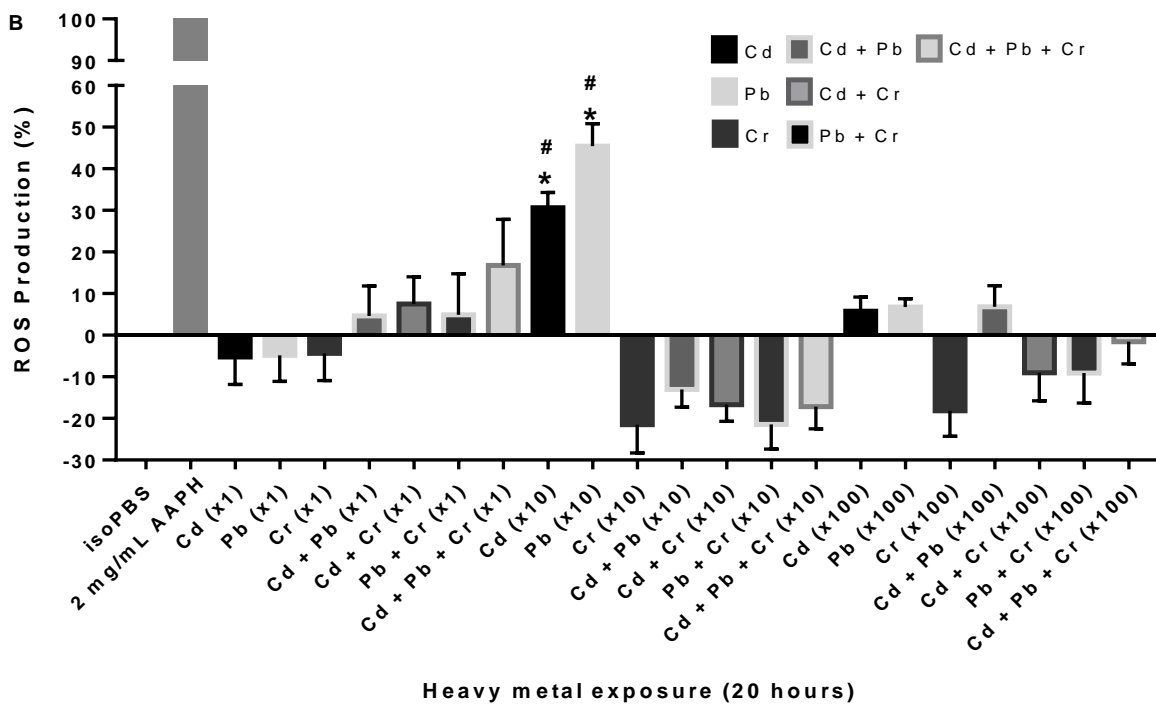
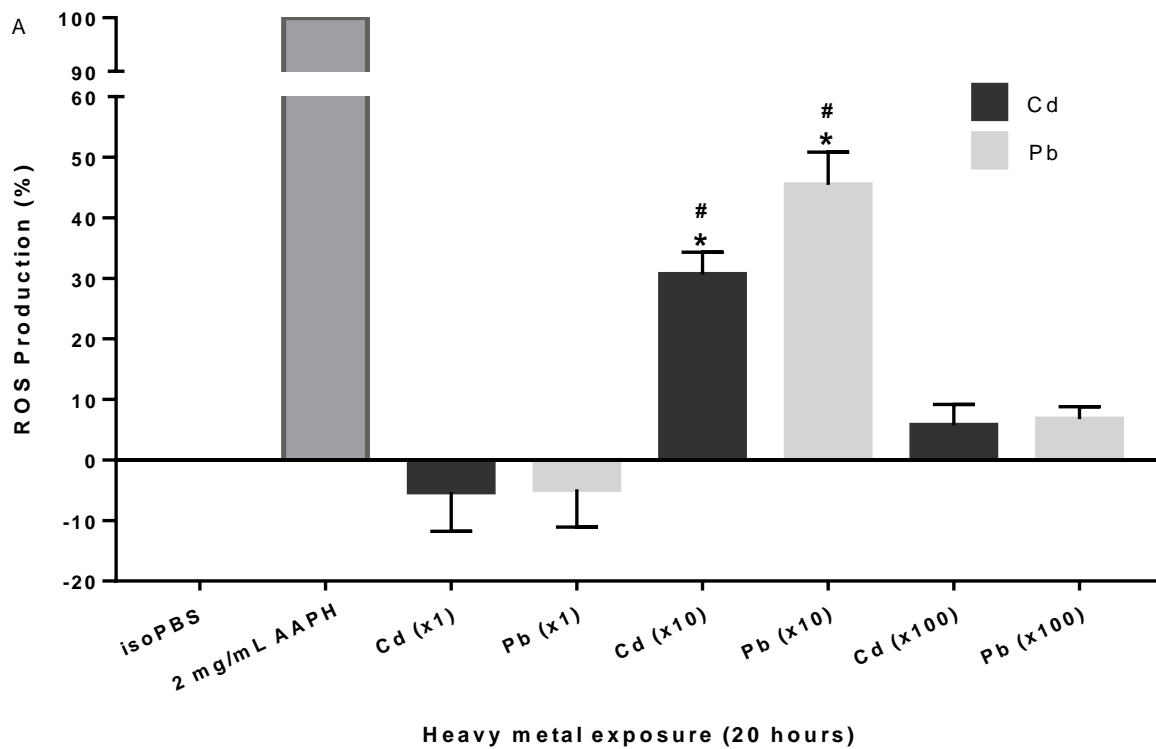


Figure 5.4: Effect of heavy metals on ROS production (%), evaluated at x1, x10 and x100 the concentration found in PRF exposed to cigarette smoke. **A)** Cd vs Pb and **B)** Cd, Pb and Cr alone and in combination. The data is expressed as the mean \pm standard error of the mean for ten independent triplicate experiments. * Indicates significance compared to the negative control and # indicates significance compared to other metal groups. **Positive control:** AAPH and **Negative control:** isoPBS.

A five-point summary of the findings regarding ROS production is shown in Table 5.1 below. The minimum and maximum values, as well as the mean and standard error of the mean of each group are tabulated in the table and corresponds with Figure 5.1 to 5.5.

Table 5.1: Summary of the effect of Cd, Pb and Cr, alone and in combination on ROS production at x1, x10 and x100 the concentration found in cigarette smoke (Yaprak and Yolcubal, 2019)

<u>Concentrations</u>	<u>X1</u>		<u>X10</u>		<u>X100</u>	
	<u>Mean ± SEM</u>	<u>Range</u>	<u>Mean ± SEM</u>	<u>Range</u>	<u>Mean ± SEM</u>	<u>Range</u>
Control	0.00 ± 0.00	0.00 – 0.00	0.00 ± 0.00	0.00 – 0.00	0.00 ± 0.00	0.00 – 0.00
AAPH (2mg/mL)	100 ± 0.00	100 – 100	100 ± 0.00	100 – 100	100 ± 0.00	100 – 100
Cd	-5.26 ± 6.54	-36.23 – 15.44	30.62 ± 3.7*#	13.04 – 45.99 **	5.75 ± 3.44	-12.41 – 24.26
Pb	-4.83 ± 6.27	-40.05 – 19.3	45.45 ± 5.39*#	26.80 – 81.21 **	6.73 ± 2.03	-5.71 – 17.66
Cr	-4.35 ± 6.58	-51.22 – 19.22	-21.47 ± 6.80	-67.77 – 3.25	-18.2 ± 6.09	-43.71 – 16.64
Cd + Pb	4.62 ± 7.21	-35.75 – 47.04	-13.02 ± 4.25	-36.77 – 4.22	6.81 ± 5.12	-24.54 – 26.54
Cd + Cr	7.53 ± 6.49	-24.42 – 36.13	-16.71 ± 4.00	-32.48 – 4.33	-9.02 ± 6.73	-43.80 – 34.99
Pb + Cr	4.91 ± 9.87	-39.59 – 55.74	-21.41 ± 5.94	-59.63 – 6.021	-9.11 ± 7.18	-30.01 – 37.38
Cd + Pb + Cr	16.78 ± 11.02	-34.62 – 61.39	-17.14 ± 5.34	-39.91 – 12.95	-1.60 ± 5.33	-22.28 – 23.92

Statistically significant compared to the * negative control (isoPBS) and # other metal groups (p-value of ≤ 0.05; 95% confidence interval). SEM: Standard error of the mean. **Cd x1**: 0.21 µg/mL; **Pb x1**: 4.1µg/mL and **Cr x1**: 224 µg/mL. **Cd x10**: 2.1 µg/mL; **Pb x10**: 41µg/mL and **Cr x10**: 2 240 µg/mL. **Cd x100**: 21 µg/mL; **Pb x100**: 410µg/mL and **Cr x100**: 22 400 µg/mL.

5.3.2. The haemolytic effect of heavy metals

The ability of Cd, Pb and Cr alone and in combination, to induce haemolysis in erythrocytes was evaluated at x1, x10 and x100 the concentration found in PRF of cigarette smoke (Figure 5.5). Sodium dodecyl sulphate (SDS) was used as a positive control to induce 100% haemolysis and isoPBS as a negative control for 0% haemolysis. None of the metal exposed groups showed any significant signs of haemolysis across concentrations, ranging from 0.36% (x10 Cd + Pb) to 1.04% (x100 Cd). Upon closer investigation, Cd caused the most haemolysis out of the three metals, with Pb in second and Cr in third. These differences were statistically insignificant. One of the double combinations (Cd + Cr) (x1: 0.66%, x10: 0.68% and x100: 0.78%) and the triple combination (Cd + Pb + Cr) (x1: 0.64%, x10: 0.72% and x100: 0.80%) also showed higher levels of haemolysis compared to the other metal combination groups at various concentrations.

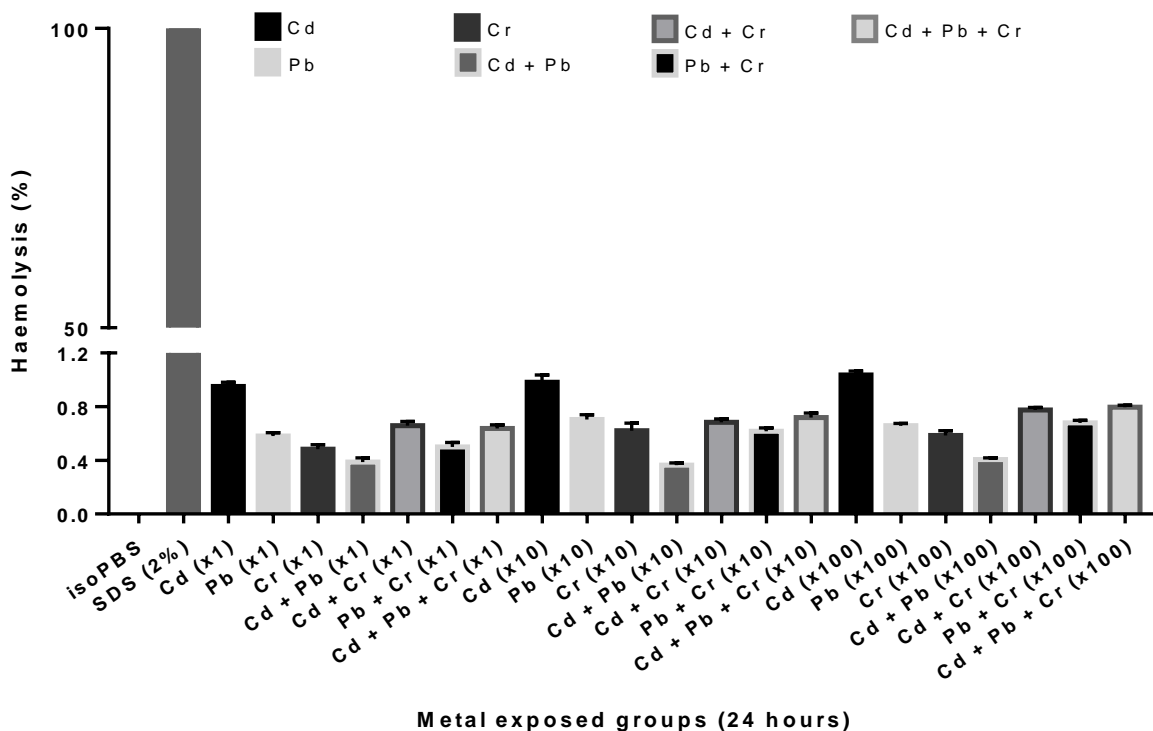


Figure 5.5: The haemolytic effects of Cd, Pb and Cr alone and in combination at x1, x10 and x100 the concentration found in PRF exposed to cigarette smoke. The data is expressed as the mean \pm standard error of the mean for ten independent triplicate experiments. **Positive control:** 100% haemolysis induced by 2% SDS; **Negative control:** 0% haemolysis induced by isoPBS.

5.4. Discussion

Smoking is one of the major risk factors that contribute to the annual number of deaths in South Africa. It is well known that tobacco smoke contains trace amounts of heavy metals, which can accumulate in the vascular system and spread throughout the body. Red blood cells, in particular, are a prominent site for heavy metal accumulation and the precise mechanism through which they cause toxicity is still poorly understood (Notariale *et al.*, 2021). Heavy metal exposure has been linked to the formation of radicals, inhibition of antioxidant enzymes and binding to antioxidant elements that cause oxidative stress. Oxidative stress occurs when the concentration of ROS generation exceeds the antioxidant capability of the cell (Xi-Biao *et al.*, 1999).

Reactive oxygen species are often implicated in heavy metal toxicology. Studies clearly indicate that although different mechanisms lead to ROS production, the subsequent mechanisms and the types of oxidative tissue damage are similar (Stohs *et al.*, 2001). In this study the effect of Cd, Pb and Cr, alone and in combination on ROS production was evaluated

at x1, x10 and x100 the concentration found in PRF exposed to cigarette smoke. During optimization, the blood was exposed to heavy metals for different time intervals (4, 6, 8, 12, 16, 20 and 24) to try and increase sensitivity. No ROS production was observed for the zero-to-18-hour incubation periods and AAPH started to induce haemolysis after a 20-hour incubation period. It was decided that a 20-hour incubation period would yield the most promising results. Tobacco users are exposed to not just one, but a variety of different heavy metals that have the potential to interact with one another (Caruso *et al.*, 2013). These interactions between the metals can be additive, synergistic or antagonistic. A synergistic interaction implies that metal combinations will increase toxicity and an antagonistic interaction will decrease toxicity (Singh *et al.*, 2017).

A haemolysis assay was performed on the exposed blood to establish whether the heavy metals, alone or in combination, have any cell lysis ability after a 24-hour incubation period. Due to the nature of this study, it was important to make sure that no cell death occurred during the 20-hour incubation period for the DCFH-DA assay, as it would affect the fluorescent readings. No significant haemolysis was observed for any of the metal exposed groups when compared to the positive control (2% SDS) (Figure 5.5), which means that none of the ROS production detected in the DCFH-DA assay was due to the oxidation of cellular content after cell lysis.

The findings in this chapter suggest that Cd might be the most toxic out of the three heavy metals used in this study. Although not significant, Cd showed the highest haemolytic potential compared to the other metals (Figure 5.5). The Cd exposed group also showed a significant increase in ROS production (30.62%) (Figure 5.2) which can lead to oxidative stress and cell damage. These findings correlate with other *in vitro* and *in vivo* studies (Bagchi *et al.*, 1997; Hart *et al.*, 1999; Liu and Jan, 2000; Venter *et al.*, 2017b). Hart *et al.* (1999) reported signs of apoptosis after exposing a rat lung epithelial cell line to Cd for 72 hours and concluded that ROS production can: 1) up-regulate genes involved in the oxidative stress pathway, 2) activate redox transcription factors and 3) deplete GSH content. Similarly, Liu and Jan (2000) concluded that the DNA strand breaks observed in Cd-treated bovine aortic endothelial cells, resulted from the excision of oxidized bases on the DNA strand. Cadmium-induced ROS production has also been linked to increased lipid peroxidation, oxidative DNA damage and depletion of protein-bound sulfhydryl groups (Bagchi *et al.*, 1997).

Although the haemolytic potential of Pb at the experimental concentrations were less than 1% (Figure 5.5), the DCFH-DA analysis revealed that Pb has the greatest ability to cause oxidative

stress in erythrocytes via ROS production (Figure 5.4). The Pb group that was exposed to the x10 concentration showed significant levels of ROS production (45.45%) that can ultimately lead to cellular damage. A study conducted by Patra *et al.* (2001) showed that Pb exposure to rats resulted in increased lipid peroxide levels and non-protein bound thiol content in the liver and brain. Lead have also shown to deplete protein-bound sulfhydryl groups and GSH, which resulted in ROS generation (Xi-Biao *et al.*, 1999).

Chromium, alone and in combination, showed no significant ROS production or haemolytic potential at any of the experimental concentrations. On the contrary, this metal caused a decrease in ROS production at the x10 and x100 concentrations when combined with Cd and/or Pb (Figure 5.4). A study done on the toxicological interactions among Cr and other metals suggest that a higher exposure concentration might enhance the cellular defence mechanisms and in turn lower the toxicity (Bae *et al.*, 2001). Previous studies have demonstrated that Cr, at a higher concentration, has the potential to undergo redox cycling and enhance ROS production (Bagchi *et al.*, 2001; Bagchi *et al.*, 1997; Evans *et al.*, 2013; Xi-Biao *et al.*, 1999). This can result in radical formation, lipid peroxidation, DNA fragmentation, altered gene expression and apoptotic cell death (Bagchi *et al.*, 2001).

An overall trend could not be established for any of the metal exposed groups because most of them showed little to no ROS production. The reason as to why significant ROS production was observed in the x10 Cd and Pb exposed groups and not in the x100 concentration groups is still unclear (Figure 5.4A). Each salt used in this study has its own set of properties. Solubility is one of them and can have an influence on the final concentration. Cadmium(II)chloride is highly soluble in water (119.6 g/mL at 25°C) compared to lead(II)chloride (0.99 g/L at 20°C) (Cubicciotti, 1952). Undissolved CdCl₂ and PbCl₂ might be a possible explanation for the observation mentioned above. If some of the stock solutions underwent precipitation, the salt concentrations would have been lowered in order to increase the stability of the solution (Choi *et al.*, 2017). However, this is unlikely as the highest concentrations used in the current study were lower than the solubility levels reported. Another possible reason for the decreased level of ROS production observed at the highest concentration might be linked to ion aggregation. Even if the metals did dissolve properly, the salt ions might have formed cluster like structures that excluded the water molecules and as a result, decreased the concentration (Choi *et al.*, 2017). A decrease in concentration for the x100 solution might explain why the levels of ROS production observed at the x1 and x100 concentrations were similar for the Cd and Pb groups.

The high degree of standard error of the mean observed in all of the metal exposed groups might be due to interpersonal variation. The blood composition in individuals can differ from one another and is mainly determined by nutrient intake, body mass index, gender and age. Factors like intestinal microflora activity, antimicrobial use or smoking can also play a role (Hålldin *et al.*, 2019). To minimize the degree of interpersonal variation, all volunteers had to be non-smokers within the age range of 20 – 50 years old. Volunteers without any scheduled drug use, medical condition or disease that affects the cardiovascular system were included in this study. Another reason for the high degree of standard deviation might be attributed to laboratory errors like improper calibration, measurement estimation and inconsistent experimental techniques.

5.5. Conclusion

A small amount of ROS production was observed in some of the x1 and x100 exposed groups, with no significant difference compared to the negative control. The only significant findings were observed at the x10 concentration where the Cd and Pb exposed groups showed the highest level of ROS production, ranging from 30.62% to 45.45%, respectively. These readings differed significantly from that of the negative control and it is therefore likely that Cd and Pb causes oxidative damage in tissues exposed to them. A trend could not be established but the groups containing either Cd or Pb, alone and in combination seemed to cause most of the ROS production. Interpersonal variability amongst volunteers might be an explanation for the high degree of standard deviation observed and an *in vivo* study might be considered for further investigation.

Chapter 6

Chapter 6: The effect of cadmium, lead and chromium on nitrite levels

6.1. Introduction

The use of tobacco products have steadily been increasing all over the world and in turn the rate of nicotine addiction has also increased (Muhammad Waqar, 2012). Chronic smoking is a major risk factor for coronary and cerebral vascular diseases, atherosclerosis and hypertension (Toda and Toda, 2010). Although nicotine mediates most of the effects caused by tobacco smoke, other constituents like Cd, Pb and Cr may also play a significant role. Heavy metals can affect the haemodynamic control by acting directly on the synthesis and action of NO or by indirectly modifying the effects of nicotine (Pizzino *et al.*, 2017). Chronic smoking causes endothelial dysfunction by reducing NO formation and increasing the degradation of NO via the generation of free radicals (Toda and Toda, 2010). A radical is a highly reactive molecule or ion that is unstable and has at least one unpaired valence electron. They have a short lifetime and needs to react with other substances to become stable. In turn, this causes oxidative stress that can lead to cell damage (Pizzino *et al.*, 2017).

Nitric oxide helps to increase blood flow and lower blood pressure by stimulating vasodilation, inhibiting leukocyte and platelet adhesion, as well as reducing smooth muscle cell proliferation. It can also act to prevent atherosclerosis (Abeyakirithi, 2020). Nitric oxide is produced from an amino acid called L-arginine that is transformed to L-citrulline with the help of NOS in the presence of oxygen and cofactors. Nitric oxide synthase has three isoforms, of which endothelial NOS (eNOS) is constitutively expressed in endothelial cells (Adewoyin *et al.*, 2019; Brent, 2015). Due to its unstable nature, NO usually reacts with other molecules to form more stable products. In the blood, NO is oxidized to nitrite (NO_2^-) and then further to nitrate (NO_3^-), with the help of oxyhaemoglobin. Sometimes, NO_3^- is produced as a by-product when NO reacts directly with oxyhaemoglobin to form methaemoglobin (Abeyakirithi, 2020).

Red blood cells have always been considered to metabolize large quantities of NO due to their non-functional NOS-carrying capability and large haemoglobin content (Kleinbongard *et al.*, 2006). However, in a recent study RBCs have been identified as a possible vascular source of NOS-dependent NO formation by reversibly binding, transporting and releasing NO into the vascular system (Toda and Toda, 2010). The permeability of RBC membranes and the

lipophilic nature of NO creates a natural intrinsic barrier that prevents RBCs from consuming NO that are not produced by themselves (Kleinbongard *et al.*, 2006).

Heavy metal constituents found in cigarette smoke are known to generate free radicals that have the ability to oxidize NO into NO_2^- and NO_3^- . These compounds are more stable and can be measured using one of the following tests: Griess assay, Saville assay, electron paramagnetic resonance spectrometry and chemiluminescence (Giustarini *et al.*, 2008). In this study, the effect of Cd, Pb and Cr alone and in combination on NO_2^- production in erythrocytes was investigated using the Griess assay. This method was first invented by Johann Peter Griess in 1979, and has since then been used to quantify the major metabolites of NO in a variety of biological fluids like plasma, urine, serum and tissue culture medium (Tsikas, 2007). This assay relies on a diazotization reaction that uses sulfanilamide and N-1-naphthylenediamine dihydrochloride (NED) under acidic (phosphoric acid) conditions. Nitrites react with sulfanilic acid to form a diazonium cation, which subsequently couples to the aromatic amine 1-naphthylamine to produce a violet-coloured water-soluble azo dye that absorbs radiation at 540 nm (Tsikas, 2007).

The Griess assay is an inexpensive method that can accurately quantify NO_2^- in biological samples by following a relatively standard protocol that is reliable and easily repeatable. Factors such as the pH, temperature and reagent concentrations that can influence the experimental conditions need to be monitored to prevent possible interferences with sulfanilamide and NED (Giustarini *et al.*, 2008).

6.2. Materials and methods

6.2.1. Metal preparation

The method for preparing stock and working solutions for the various metals were the same as described in section 3.2.1.

6.2.2. Blood collection

The process of blood collection was the same as described in section 3.2.2.

6.2.3. Sample preparation for the Griess assay

The *in vitro* synthesis of NO_2^- in whole blood exposed to different heavy metal concentrations for 24 hrs were measured using a modified version of the method described by Bryan and Grisham (2007). Due to the haemoglobin interference in whole blood, only the blood plasma was used for this assay. In order to isolate the plasma, whole blood was centrifuged at $3600 \times g$ for 10 min. A 96-well microtiter plate (Sigma-Aldrich, St Louis, MO, USA) was prepared by pipetting 100 μL plasma, and 100 μL of nitrite solution (0.2 – 0.1 mM NaNO_2) (Sigma-Aldrich, St Louis, MO, USA) into each well. A positive control was exposed to 100 μL lipopolysaccharide (LPS: 10 $\mu\text{g}/\text{mL}$) (Sigma-Aldrich, St Louis, MO, USA) and a negative control was exposed to 100 μL isoPBS (0.137 M NaCl, 3 mM KCl, 1.9 mM NaH_2PO_4 , 8.1 mM Na_2HPO_4 , pH 7.4) (Sigma-Aldrich, St Louis, MO, USA). The Griess reagent (sulphanilamide, 2% w/v, and N-(1-naphthyl) ethylenediamine dihydrochloride, 0.1% prepared in 5% hydrochloric acid) (Sigma-Aldrich, St Louis, MO, USA) was prepared beforehand and 50 μL was added to each sample. The plate was left to incubate in the dark for 45 min at room temperature. After incubation, the Omega multimode micro plate reader (BMG Labtech, Munich, Germany) was used to measure the absorbance of each sample at 540 nm (for each sample, the assay was performed in triplicate). The net absorbance formula mentioned below, was used to determine the nitrite concentration in each sample (Bryan and Grisham, 2007).

$$\text{Net absorbance} = (\text{Slope} \times \text{NO}_2^- \text{ concentration}) + \text{Y-intercept}$$

6.2.4. Statistical analysis

The nitrite formation (mM) relative to the control was calculated for each sample, using the NaNO_2 standard curve (absorbance equals slope times concentration plus the y-intercept absorbance value). Isotonic phosphate buffered saline was taken as 0% and LPS was taken as 100%. All the data was presented as the mean \pm standard error of the mean. Both the D'Agostino & Pearson normality test and Shapiro-Wilk normality test (Graph Pad version 6.1) were used to determine normality of the data. After normality was determined, the One-Way ANOVA and Tukey's multiple comparison test was performed on all parametric data. Multiple comparisons were done between the different concentrations of each individual experimental group to determine significance. Statistical analysis was performed with a 95% confidence interval and a p-value of < 0.05 was considered significant.

6.3. Results

6.3.1. The effect of heavy metals on nitrite formation

The Griess assay was used to determine the ability of Cd, Pb and Cr alone and in combination to induce NO_2^- formation at x1, x10 and x100 the concentration found in PRF exposed to cigarette smoke (Yaprak and Yolcubal, 2019). After the whole blood was processed and exposed to heavy metals, the erythrocyte suspension was incubated for 24 hours. Lipopolysaccharide was used as a possible positive control that induce NO_2^- formation and isoPBS was used as a negative control, which represents the normal physiological blood NO_2^- concentration. The data was collected from 10 volunteers and the mean, along with standard error of the mean was calculated from triplicate experiments. Significance was determined at p-value ≤ 0.05 and 95% confidence interval.

In Figure 6.1 the results obtained from each x1 metal exposed group was compared to one another. Both of the groups exposed to LPS (positive control) and isoPBS (negative control) showed very low levels of NO_2^- formation (0.064 mM and 0.067 mM respectively). No significance was observed for any of the metal exposed groups, compared to the negative control or other metal groups from the same concentration. It is worth mentioning that all the groups showed similar or slightly more NO_2^- formation compared to the negative control, except for the Cd + Cr combination groups, which showed slightly less NO_2^- formation (0.063 mM). The standard error of mean for all the x1 exposed groups were very low, ranging from 0.011 to 0.012. The low standard error of mean suggests that the absorbance readings obtained from each sample was a good representation of the general population.

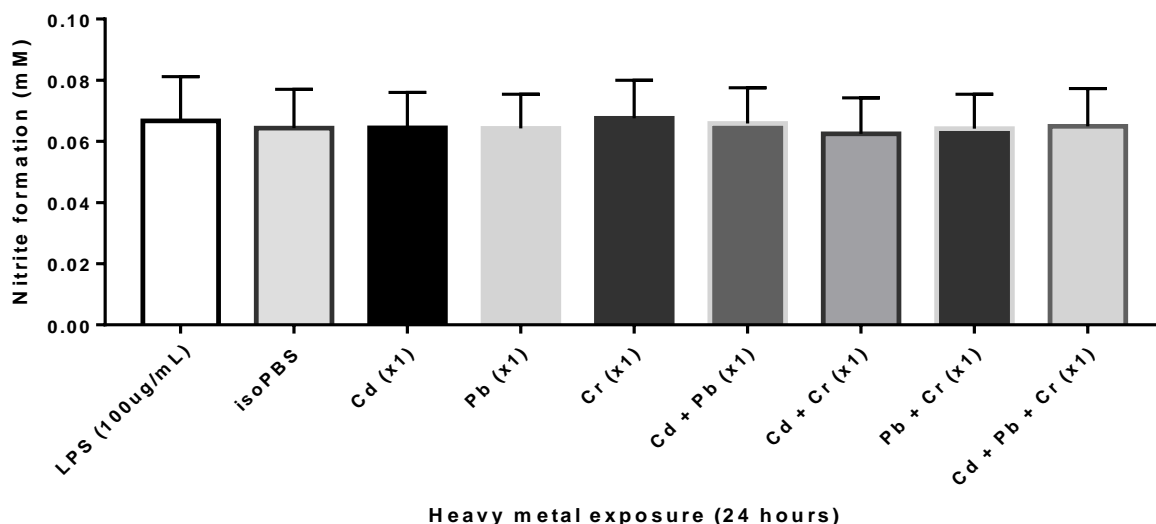


Figure 6.1 The effects of Cd, Pb and Cr alone and in combination on nitrite production (%) evaluated at x1 the concentration found in PRF exposed to cigarette smoke. The data is expressed as the mean \pm standard error of the mean for ten independent triplicate experiments. **Positive control:** 100 μ g/mL LPS and **Negative control:** isoPBS.

In Figure 6.2, the results obtained from the x10 metal exposed groups were compared. All the groups showed a slight increase in NO_2^- formation when compared to the negative control (0.065 mM), ranging from 0.065 mM to 0.069 mM. These differences, however was not statistically significant. A low standard error of mean, ranging from 0.011 to 0.013, suggest that the values obtained from each sample were clustered around the population mean and is therefore a good representation of the experimental population.

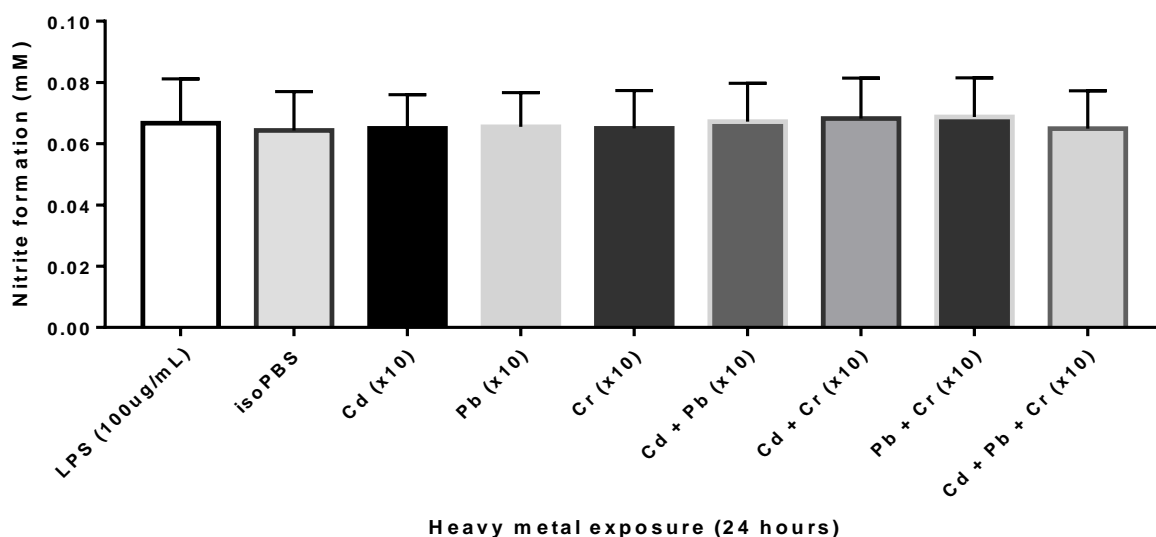


Figure 6.2: The effects of Cd, Pb and Cr alone and in combination on nitrite production (%) evaluated at x10 the concentration found in PRF exposed to cigarette smoke. The data is expressed as the mean \pm standard error of the mean for ten independent triplicate experiments. **Positive control:** 100 μ g/mL LPS and **Negative control:** isoPBS.

Figure 6.3 compared the x100 metal exposed group to one another, as well as to the positive (LPS) and negative (isoPBS) control. The groups exposed to LPS and isoPBS showed 0.067 mM and 0.064 mM NO_2^- formation, respectively. All of the groups showed similar or slightly higher levels of NO_2^- production compared to the negative control, except for the Cd + Pb (0.063 mM) and Pb + Cr (0.062 mM) combination groups. The standard error of mean for the metal exposed groups ranges from 0.010 to 0.013, suggesting that the sample means are closely distributed around the population mean.

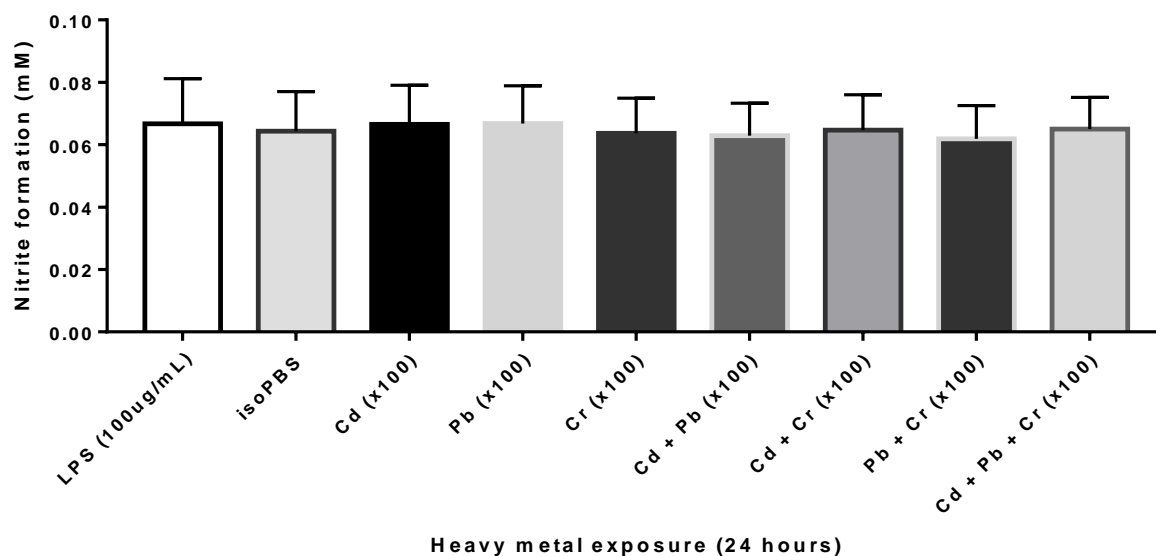


Figure 6.3: The effects of Cd, Pb and Cr alone and in combination on nitrite production (%) evaluated at x100 the concentration found in PRF exposed to cigarette smoke. The data is expressed as the mean \pm standard error of the mean for ten independent triplicate experiments. **Positive control:** 100 $\mu\text{g}/\text{mL}$ LPS and **Negative control:** isoPBS.

Figure 6.4 summarizes the effect of Cd, Pb and Cr alone and in combination on NO_2^- formation at x1, x10 and x100 the concentration found in PRF exposed to cigarette smoke. After comparing the results from each concentration to one another, the level of NO_2^- formation stayed the same even as the concentration increased. No significance was detected for any of the metal exposed groups, compared to the negative control.

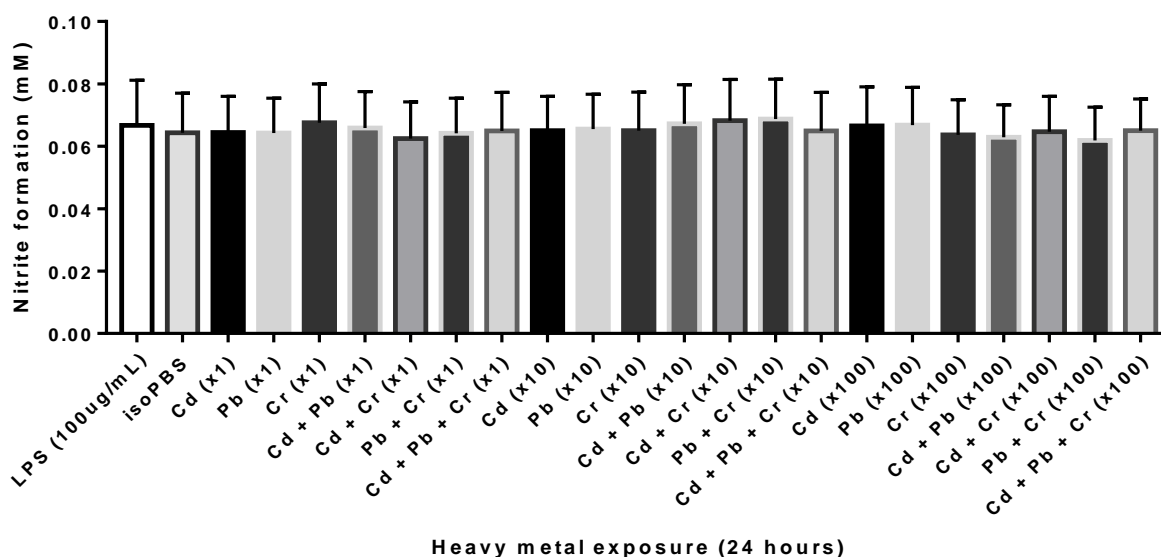


Figure 6.4: The effects of Cd, Pb and Cr alone and in combination on nitrite production (%) evaluated at x1, x10 and x100 the concentration found in PRF exposed to cigarette smoke. The data is expressed as the mean ± standard error of the mean for ten independent triplicate experiments. **Positive control:** 100 µg/mL LPS and **Negative control:** isoPBS.

A five-point summary of the findings regarding NO₂⁻ formation is shown in Table 6.1 below. The minimum and maximum values, as well as the mean and standard error of the mean of each group are tabulated and corresponds with Figure 6.1 to 6.3.

Table 6.1: Summary of the effect of Cd, Pb and Cr, alone and in combination on nitrite production at x1, x10 and x100 the concentration found in cigarette smoke (Yaprak and Yolcubal, 2019)

<u>Concentrations</u>	<u>X1</u>		<u>X10</u>		<u>X100</u>	
	<u>Mean ± SEM</u>	<u>Range</u>	<u>Mean ± SEM</u>	<u>Range</u>	<u>Mean ± SEM</u>	<u>Range</u>
Control (isoPBS)	0.064 ± 0.040	0.027 – 0.159	0.064 ± 0.040	0.027 – 0.159	0.064 ± 0.040	0.027 – 0.159
LPS (100 µg/mL)	0.067 ± 0.014	0.033 – 0.184	0.067 ± 0.014	0.033 – 0.184	0.067 ± 0.014	0.033 – 0.184
Cd	0.065 ± 0.012	0.029 – 0.146	0.065 ± 0.011	0.031 – 0.152	0.067 ± 0.013	0.030 – 0.165
Pb	0.064 ± 0.011	0.031 – 0.148	0.066 ± 0.011	0.031 – 0.152	0.067 ± 0.012	0.013 – 0.153
Cr	0.068 ± 0.012	0.032 – 0.162	0.065 ± 0.012	0.030 – 0.162	0.064 ± 0.011	0.029 – 0.148
Cd + Pb	0.065 ± 0.012	0.032 – 0.160	0.067 ± 0.013	0.028 – 0.162	0.063 ± 0.010	0.032 – 0.140
Cd + Cr	0.063 ± 0.012	0.026 – 0.157	0.068 ± 0.013	0.032 – 0.154	0.065 ± 0.011	0.029 – 0.147
Pb + Cr	0.064 ± 0.011	0.031 – 0.152	0.069 ± 0.013	0.032 – 0.164	0.062 ± 0.011	0.029 – 0.142
Cd + Pb + Cr	0.065 ± 0.012	0.028 – 0.162	0.065 ± 0.013	0.028 – 0.163	0.065 ± 0.010	0.031 – 0.140

SEM: Standard error of the mean. **Cd x1:** 0.21 µg/mL; **Pb x1:** 4.1µg/mL and **Cr x1:** 224 µg/mL. **Cd x10:** 2.1 µg/mL; **Pb x10:** 41µg/mL and **Cr x10:** 2 240 µg/mL. **Cd x100:** 21 µg/mL; **Pb x100:** 410µg/mL and **Cr x100:** 22 400 µg/mL.

6.4. Discussion

It is well known that tobacco smoke contains trace amounts of heavy metals, which can negatively impact human health if accumulated over long periods of time (Sitas *et al.*, 2017). Cellular signalling in general is very sensitive to environmental changes and excessive production of reactive nitrogen species can lead to oxidative stress and eventual cell death (Ercal *et al.*, 2002). Heavy metals such as Cd, Pb and Cr have the ability to indirectly form radicals in the blood stream that interfere with endothelial functioning by interacting with NO to form NO_2^- or NO_3^- in the presence of oxyhaemoglobin (Toda and Toda, 2010).

Before the Griess assay was used to measure the amount of NO_2^- formation in erythrocytes, a haemolytic test was done on whole blood to determine the cell lysis capability of each heavy metal on erythrocytes after a 24-hour incubation period (refer back to section 5.3.2 from Chapter 5). After confirming that no cell death occurred during that time (Figure 5.5), the Griess assay could safely be performed without any concern that the NO_2^- formation detected in the Griess assay was due to the oxidation of cellular content after cell lysis.

Isotonic phosphate buffered saline (isoPBS) and lipopolysaccharides (LPS) were used as negative and positive controls respectively. The PBS solution is isotonic, non-toxic and have a pH of 7.4, which is similar to the cellular environment and mimics physiological conditions. In contrast, LPS is a component found in the outer cell membrane of Gram-negative bacteria that induce cellular responses in the host to protect itself from bacterial infection (Simon and Fernandez, 2009). Studies have shown that exposure to large quantities of LPS in virtually all cell types (macrophages, dendrite cells, fibroblasts, chondrocytes, osteoclasts, astrocytes and epithelial cells) can result in ROS generation that react with NO to generate other NO radicals like NO_2^- and peroxynitrite (Virág *et al.*, 2003). The ability of LPS to constantly generate free radicals in a variety of different cells was the main reason it was used as a positive control in the Griess assay.

The results however, showed similar levels of NO_2^- formation in the LPS exposed group (0.067 mM), compared to the negative control and other metal exposed groups (Figure 6.4A). This means that the NO_2^- levels in blood plasma exposed to LPS was within normal ranges for a healthy individual. A possible explanation for this observation might be the fact that the NOS found in erythrocytes are non-functional and require various cofactors like calmodulin, tetrahydrobiopterin, nicotinamide adenine dinucleotide phosphate, heme, flavin adenine dinucleotide and flavin mononucleotide to be activated (Toda and Toda, 2010). During

optimization, different concentrations of LPS (10 µg/mL, 20 µg/mL and 100 µg/mL) were tested on whole blood, blood plasma and leukocyte suspensions at different time intervals (2, 4, 6, 8, 20 and 24 hours) to try and increase sensitivity, but the same results were obtained as mentioned above. Due to time constraints, other possible controls could not be tested and used as a substitute.

In this study the effects of Cd, Pb and Cr, alone and in combination on NO₂⁻ formation were evaluated at x1, x10 and x100 the concentration found in PRF exposed to cigarette smoke. The findings in this chapter showed that none of the metal exposed groups caused a significant increase in NO₂⁻ formation (ranging from 0.062 mM to 0.069 mM) compared to the negative control (0.064 mM). No synergistic, antagonistic or additive effect was observed for any of the metal combinations. Overall, the NO₂⁻ plasma levels resembled that of a healthy individual. Although the concentrations used in this study did not show a significant increase in NO₂⁻ formation, other studies suggest that heavy metal exposure at higher concentrations can have detrimental effects on the cell signalling pathway in endothelial cells (Briffa *et al.*, 2020; Majumder *et al.*, 2008; Pritchard *et al.*, 2000; Vaziri and Ding, 2001).

In 2008 a study was conducted by Majumder *et al.* (2008) to evaluate the effects of CdCl₂ (10 to 1000 nmol/L) on endothelial function. It was found that low levels of Cd exposure (100 nmol/L) block eNOS phosphorylation and inhibit NO production in endothelial cells. Similarly, in 2019 an animal study on ApoE^{-/-} mice showed that chronic exposure to Cd reduces NO bioavailability (Oliveira *et al.*, 2019). Lead-induced alterations in the cell signalling pathway of endothelial cells have shown to disrupt NO vasodilatory effects (Briffa *et al.*, 2020). These findings correlate with a study done by Vaziri and Ding (2001). They found that increased levels of ROS production due to Pb-induced hypertension in rats, enhance NO inactivation and decrease NO bioavailability, resulting in compensatory upregulation of NOS (Vaziri and Ding, 2001). In contrast, Cr exposure to endothelial cells have shown an increase in the production of superoxide anions without affecting the ability of endothelial cells to produce NO. However, the increased concentration of superoxide ions lead to NO being scavenged intracellularly to increase peroxynitrite formation (Pritchard *et al.*, 2000).

Due to the highly reactive nature of NO₂⁻ and the presence of haemoglobin in whole blood, NO₂⁻ is rapidly oxidized to NO₃⁻ to make it more stable. This makes it difficult to obtain accurate and reliable measurements of NO₂⁻ in the blood, which is why blood plasma is used in the Griess assay instead of whole blood (Giustarini *et al.*, 2008). Other factors like the type of acid used to prepare the Griess reagent can also influence the results. Giustarini *et al.* (2008)

experimented with different acids (hydrochloric, phosphoric, and acetic acid) and found that lower pH values resulted in a lower final absorbance (differences observed were not due to insufficient incubation time). They also mentioned that calibration curves are usually carried out in water or buffers (as recommended by kit manufacturers) but from an analytical point of view, it is better to prepare calibration curves in a matrix as similar to that where NO_2^- will be measured.

Possible future studies can focus on finding a suitable positive control that has the ability to constantly generate free radicals in blood plasma. Leukocyte isolation or the use of a cultured cell line can also be considered as a more sustainable way to study acute exposure (allows for longer exposure periods). The effects of heavy metals can also be tested at higher concentrations to represent long-term exposure.

6.5. Conclusion

No significant NO_2^- formation was observed in any of the metal exposed groups, when compared to the negative control (isoPBS). Due to haemoglobin interference, only the blood plasma was isolated and used in the Griess assay. This might explain why none of the groups showed an increase in NO_2^- formation because RBCs contain non-functional NOS. Endothelial cells however, contain active eNOS that will produce NO when stimulated and might yield better results if used in future studies.

Chapter 7

Chapter 7: Concluding discussion

7.1. Summarised results

Cigarette smoke is well known for its disease-causing capability and has been linked to serious illnesses like cardiovascular diseases, cancer, diabetes and strokes (Caruso *et al.*, 2013). Nicotine is one of the main constituents found in tobacco and is responsible for its addictive nature (Toda and Toda, 2010). Although efforts have been made by government institutions to try and reduce tobacco use, cigarette smoke is still considered to be the leading cause of preventable disease, disability and death in South Africa (Sitas *et al.*, 2017). Cigarette smoke contains trace amounts of heavy metals that accumulate in the vascular system and eventually spread throughout the body. Red blood cells, in particular, are a prominent site for heavy metal accumulation and the precise mechanisms through which they cause toxicity is still poorly understood (Notariale *et al.*, 2021). Many studies have been undertaken to determine the effect of heavy metal exposure on tissue and organ damage at toxic concentrations but very few focussed on metals in combination and their effect on the coagulation system (El-Safty *et al.*, 2004; Ghosh and Indra, 2018; Naidoo *et al.*, 2019; Witeska *et al.*, 2011). More data is needed on the combined effects of Cd, Pb and Cr at different concentrations.

This study has attempted to address the lack of knowledge regarding heavy metal toxicity associated with cigarette smoke by exposing whole blood to Cd, Pb and Cr alone and in combination to x1, x10 and x100 the concentration found in PRF exposed to cigarette smoke (Yaprak and Yolcubal, 2019). Scanning electron microscopy, TEG[®] and various assays were used as tests for toxicity. Whole blood was obtained from ten healthy non-smoking volunteers between the ages of 20 and 50 years old, without any medical condition or disease that might affect the cardiovascular system.

Scanning electron microscopy was used to assess the morphological changes. The results obtained showed that the Cd + Cr combination groups caused the highest degree of echinocyte formation. The fibrin fibres in these groups also took on a mesh like appearance and became less organized. Overall, the findings suggest that Cr, alone or in combination can potentially influence clot formation and increase the risk of thrombosis. These findings were supported by the TEG[®] results. Thromboelastography was used to measure the viscoelastic properties of whole blood clot formation and quantitatively support the micrograph analysis. Although most of the parameter changes were insignificant, the R-time and SP-values for all the groups containing Cr, showed a definite decrease in value compared to the control. These are

indications of advanced fibrin formation and supports the fact that Cr has the ability to increase the risk of thrombus formation.

The mechanisms through which these heavy metals altered the morphology and changed some of the coagulation parameters is still unclear. A few studies, however have suggested that ROS production and increased NO_2^- formation can lead to oxidative stress and induce morphological alterations (Bagchi *et al.*, 2001; Hart *et al.*, 1999; Liu and Jan, 2000; Venter *et al.*, 2017a). The DCFH-DA and Griess assays were used to investigate the radical generating ability of each heavy metal, alone and in combination. It was observed that the x10 Cd and Pb exposed groups produced significantly more ROS compared to the other metal groups and the negative control. In comparison, no significant increase in NO_2^- formation was observed in any of the metal exposed groups.

Increased ROS production, altered RBC and fibrin network morphology and a decrease in some of the coagulation parameters support the hypothesis that the coagulation pathway is a potential target for heavy metal toxicity. These changes can ultimately induce thrombosis and subsequently increase the risk of a stroke or heart attack (Gaziano, 2005). The results reported in this study will contribute to the pool of knowledge regarding the harmful effects of cigarette smoke and might increase awareness among consumers. In order to decrease the amount of heavy metal exposure caused by cigarette smoking, the manufacturing, marketing and distribution of tobacco products need to be better regulated by higher authorities.

7.2. Limitations and future prospective

One of the limitations of this study is that these *in vitro* experiments explain acute exposure for a short period of time and doesn't mimic the *in vivo* environment. The reality is that roughly 11% of tobacco users smoke around ten cigarettes a day (Sitas *et al.*, 2017), resulting in heavy metal accumulation over a longer time period. In a future study the effect of these heavy metals can be tested using an *ex vivo* model that allows investigators to assess the toxicity in a controlled environment. Animal studies (*in vivo*) can also be considered as it would generate more accurate results that reflect chronic heavy metal exposure.

Another limitation for this study is that SEM analysis mainly focussed on erythrocyte and fibrin network morphology but failed to address the possible side effects on platelet formation. Other methods like atomic force microscopy analysis can be used to evaluate erythrocyte and fibrin network elasticity to support and further explain the results observed in this study. Regarding

the blood clotting process, a TEG[®] machine was used to investigate clot formation. The results showed significant changes to some of the coagulation parameters but failed to address the possible influence of associated coagulation factors. Future studies can use other methods like the enzyme-linked immunosorbent assays to quantify the levels of coagulation factors or a clot lysis assay to evaluate fibrinolysis. The optimization process for the DCFH-DA and Griess assays proved to be very difficult because a suitable incubation period needed to be established that promoted maximum exposure without compromising cell viability. Another obstacle was finding a suitable positive control for the Griess assay to induce NO₂⁻ formation in RBCs.

Many studies have suggested that oxidative stress plays a key role in heavy metal toxicity but the mechanisms through which Cd, Pb and Cr cause adverse effects are still poorly understood (Cimmino *et al.*, 2015; De Maat and Verschuur, 2005; Ercal *et al.*, 2002; Janse Van Rensburg *et al.*, 2019; Lang *et al.*, 2012a). A new spectrophotometric method described by Ciuti and Liguri (2017) has been developed to measure the total antioxidant capacity (Atac *et al.*) of biological samples. This assay is based on a two-electron reduction of a reagent called 2,6-dichlorophenolindophenol (DCPIP) and its reaction with the antioxidants found in whole blood. This reaction is not influenced by haemoglobin and assesses the overall redox status of the sample (Ciuti and Liguri, 2017).

Chapter 8

Chapter 8: References

Abeyakirithi S. 2020. Nitric oxide [Online]. DermNet NZ. Available: <https://dermnetnz.org/topics/nitric-oxide> Accessed: [11 November 2021].

Adams SV, Newcomb PA, Shafer MM, *et al.*, 2011. Sources of cadmium exposure among healthy premenopausal women. *Science of the Total Environment*, 409: 1632-1637.

Adewoyin A, Adeyemi O and Davies N. 2019. Erythrocyte morphology and its disorders [Online]. IntechOpen. Available: <https://www.intechopen.com/chapters/67667> Accessed: [15 November 2020].

Adial A and Wiener SW. 2018. Heavy metal toxicity [Online]. Medscape. Available: <https://emedicine.medscape.com/article/814960-overview> Accessed: [20 February 2020].

Aggarwal V, Tuli HS, Varol A, *et al.*, 2019. Role of reactive oxygen species in cancer progression: Molecular mechanisms and recent advancements. *Biomolecules*, 9: 735-742.

Arbi S, Oberholzer HM, Van Rooy MJ, *et al.*, 2017. Effects of chronic exposure to mercury and cadmium alone and in combination on the coagulation system of Sprague-Dawley rats. *Ultrastructural Pathology*, 41: 275-283.

Atac MS, Sezen SC, Bilge M, *et al.*, 2015. Effect of acetaminofen versus lornoxicam administration on oxidative stress in rat hepatic and renal tissues. *Medical Science and Discovery*, 2: 244-253.

Bae DS, Gennings C, Carter WH, *et al.*, 2001. Toxicological interactions among arsenic, cadmium, chromium, and lead in human keratinocytes. *Toxicological Sciences*, 63: 132-142.

Bagchi D, Bagchi M and Stohs SJ. 2001. Chromium (VI)-induced oxidative stress, apoptotic cell death and modulation of p53 tumor suppressor gene. *Molecular Cell Biochemistry*, 222: 149-158.

Bagchi D, Vuchetich PJ, Bagchi M, *et al.*, 1997. Induction of oxidative stress by chronic administration of sodium dichromate (chromium VI) and cadmium chloride (cadmium II) to rats. *Free Radical Biology and Medicine*, 22: 471-478.

Bakshi A and Panigrahi AK. 2018. A comprehensive review on chromium induced alterations in fresh water fishes. *Toxicology Reports*, 5: 440-447.

Barrett CD, Hsu AT, Ellson CD, *et al.*,. 2018. Blood clotting and traumatic injury with shock mediates complement-dependent neutrophil priming for extracellular ROS, ROS-dependent organ injury and coagulopathy. *Clinical and Experimental Immunology*, 194: 103-117.

Bredt DS. 1999. Endogenous nitric oxide synthesis: Biological functions and pathophysiology. *Free Radical Research*, 31: 577-596.

Brent RL. 2015. Environmental causes of human congenital malformations. Available: <https://pdfs.semanticscholar.org/cead/1debcd6d6bbfd1af5a266a6f53745f8105a3.pdf> [Accessed March 07].

Briffa J, Sinagra E and Blundell R. 2020. Heavy metal pollution in the environment and their toxicological effects on humans. *Heliyon*, 6: 4691-4699.

Brown RB and Audet J. 2008. Current techniques for single-cell lysis. *Journal of the Royal Society*, 5: 131-138.

Bryan NS and Grisham MB. 2007. Methods to detect nitric oxide and its metabolites in biological samples. *Free Radical Biology and Medicine*, 43: 645-657.

Caruso RV, O'connor RJ, Stephens WE, *et al.*,. 2013. Toxic metal concentrations in cigarettes obtained from U.S. smokers in 2009: Results from the International Tobacco Control (ITC) United States survey cohort. *International Journal of Environmental Research and Public Health*, 11: 202-217.

Choi JH, Choi HR, Jeon J, *et al.*,. 2017. Ion aggregation in high salt solutions. VII. The effect of cations on the structures of ion aggregates and water hydrogen-bonding network. *The Journal of Chemical Physics*, 147: 154107-154114.

Cimmino G, Cirillo P, Ragni M, *et al.*,. 2015. Reactive oxygen species induce a procoagulant state in endothelial cells by inhibiting tissue factor pathway inhibitor. *Journal of Thrombosis and Thrombolysis : A Journal for Translation, Application and Therapeutics in Thrombosis and Vascular Science*, 40: 186-192.

Ciuti R and Liguri G. 2017. A novel assay for measuring total antioxidant capacity in whole blood and other biological samples. *Journal of Biomedical Science and Engineering*, 10: 60-76.

Cubicciotti D. 1952. The solubility of cadmium in mixtures of cadmium chloride with other chlorides. *Journal of the American Chemical Society*, 74: 1198-1200.

Da Luz LT, Nascimento B and Rizoli S. 2013. Thrombelastography (TEG®): Practical considerations on its clinical use in trauma resuscitation. *Scandinavian Journal of Trauma, Resuscitation and Emergency Medicine*, 21: 29-29.

De Maat MP and Verschuur M. 2005. Fibrinogen heterogeneity: Inherited and noninherited. *Current Opinion in Hematology*, 12: 377-383.

Di Bona KR, Love S, Rhodes NR, *et al.*,. 2011. Chromium is not an essential trace element for mammals: effects of a “low-chromium” diet. *Journal of Biological Inorganic Chemistry*, 16: 381-390.

Diez-Silva M, Dao M, Han J, *et al.*,. 2010. Shape and biomechanical characteristics of human red blood cells in health and disease. *Materials Research Society*, 35: 382-388.

Dikalov SI and Harrison DG. 2014. Methods for detection of mitochondrial and cellular reactive oxygen species. *Antioxidants and Redox Signaling*, 20: 372-382.

El-Safty AM, Afifi MH, Shouman E, *et al.*,. 2004. Effects of smoking and lead exposure on proximal tubular integrity among egyptian industrial workers. *Archives of Medical Research*, 35: 59-65.

Ercal N, Gurer-Orhan H and Aykin-Burns N. 2002. Toxic metals and oxidative stress part I: Mechanisms involved in metal induced oxidative damage. *Current Topics in Medicinal Chemistry*, 1: 529-539.

Evans BC, Nelson CE, Yu SS, *et al.*,. 2013. Ex vivo red blood cell hemolysis assay for the evaluation of pH-responsive endosomolytic agents for cytosolic delivery of biomacromolecular drugs. *Journal of Visualized Experiments*: 50166-50166.

Fang Z, Jiang C, Tang J, *et al.*,. 2016. A comprehensive analysis of membrane and morphology of erythrocytes from patients with glucose-6-phosphate dehydrogenase deficiency. *Journal of Structural Biology*, 194: 235-243.

Fthenakis VM. 2004. Life cycle impact analysis of cadmium in CdTe PV production. *Renewable and Sustainable Energy Reviews*, 8: 303-334.

Furie B and Furie BC. 2005. Thrombus formation in vivo. *The Journal of Clinical Investigation*, 115: 3355-3362.

Gaziano T. 2005. Cardiovascular disease in the developing world and its cost effective management. *Circulation*, 112: 3547-3553.

Ghosh K and Indra N. 2018. Cadmium treatment induces echinocytosis, DNA damage, inflammation, and apoptosis in cardiac tissue of albino Wistar rats. *Environmental Toxicological Pharmacology*, 59: 43-52.

Gidlow DA. 2004. Lead toxicity. *Occupational Medicine*, 54: 76-81.

Giustarini D, Rossi R, Milzani A, *et al.*,. 2008. Nitrite and nitrate measurement by Griess reagent in human plasma: evaluation of interferences and standardization. *Methods in Enzymology*, 440: 361-380.

Greenwalt TJ. 2006. The how and why of exocytic vesicles. *Transfusion*, 46: 143-152.

Gregg D, De Carvalho D and Kovacic H. 2004. Integrins and coagulation: A role for ROS/redox signaling? *Antioxidants and redox signaling*, 6: 758-764.

Hålldin E, Eriksen AK, Brunius C, *et al.*,. 2019. Factors explaining interpersonal variation in plasma enterolactone concentrations in humans. *Molecular Nutrition and Food Research*, 63: 1801159-1801167.

Hanfi MY, Mostafa MYA and Zhukovsky MV. 2019. Heavy metal contamination in urban surface sediments: Sources, distribution, contamination control, and remediation. *Environmental Monitoring and Assessment*, 192: 1-21.

Hans-Wedepohl K. 1995. The composition of the continental crust. *Geochimica et Cosmochimica Acta*, 59: 1217-1232.

Hart BA, Lee CH, Shukla GS, *et al.*,. 1999. Characterization of cadmium-induced apoptosis in rat lung epithelial cells: evidence for the participation of oxidant stress. *Toxicology*, 133: 43-58.

Huang W, Zhang Y, Zhang Y, *et al.*,. 2016. Optimization of the measurement of particle-bound reactive oxygen species with 2',7'-dichlorofluorescein (DCFH). *Water, Air and Soil Pollution*, 227: 164-176.

Janse Van Rensburg M, Van Rooy M, Bester MJ, *et al.*,. 2019. Oxidative and haemostatic effects of copper, manganese and mercury, alone and in combination at physiologically relevant levels: An ex vivo study. *Human and Experimental Toxicology*, 38: 419-433.

Jomova K and Valko M. 2011. Advances in metal-induced oxidative stress and human disease. *Toxicology*, 283: 65-87.

Kampa M and Castanas E. 2008. Human health effects of air pollution. *Environmental Pollution*, 151: 362-367.

Kell DB and Pretorius E. 2017. Proteins behaving badly. Substoichiometric molecular control and amplification of the initiation and nature of amyloid fibril formation: Lessons from and for blood clotting. *Progress in Biophysics and Molecular Biology*, 123: 16-41.

Kerek E, Hassanin M and Prenner EJ. 2018. Inorganic mercury and cadmium induce rigidity in eukaryotic lipid extracts while mercury also ruptures red blood cells. *Biochimica et Biophysica Acta*, 1860: 710-717.

Kleinbongard P, Schulz R, Rassaf T, *et al.*,. 2006. Red blood cells express a functional endothelial nitric oxide synthase. *Blood*, 107: 2943-2951.

Lang E, Qadri SM and Lang F. 2012a. Killing me softly – Suicidal erythrocyte death. *The International Journal of Biochemistry & Cell Biology*, 44: 1236-1243.

Lang F, Lang E and Föller M. 2012b. Physiology and pathophysiology of eryptosis. *Transfusion Medicine and Hemotherapy*, 39: 308-314.

Liu F and Jan KY. 2000. DNA damage in arsenite- and cadmium-treated bovine aortic endothelial cells. *Free Radical Biological Medicine*, 28: 55-63.

Lowe JS and Anderson PG 2008. *Blood and Lymphatic Circulatory Systems and Heart. Stevens & Lowe's Human Histology*. Philadelphia: Mosbey Publishers. pp 179-201

Majumder S, Muley A, Kolluru GK, *et al.*, 2008. Cadmium reduces nitric oxide production by impairing phosphorylation of endothelial nitric oxide synthase. *Biochemistry and Cell Biology*, 86: 1-10.

Mesarec L, Gózdź W, Iglič A, *et al.*, 2019. Normal red blood cells' shape stabilized by membrane's in-plane ordering. *Scientific Reports*, 9: 19742-19751.

Mohanty JG, Nagababu E and Rifkind JM. 2014. Red blood cell oxidative stress impairs oxygen delivery and induces red blood cell aging. *Frontiers in Physiology*, 5: 84-84.

Moini J 2016. *Cells. Anatomy and Physiology for Health Professionals*. United States of America: Jones & Bartlett Publishers. pp 46-66

Moreira Gomes MD, Carvalho GMC, Casquilho NV, *et al.*, 2016. 2,2'-Azobis (2-Amidinopropane) dihydrochloride is a useful tool to impair lung function in rats. *Frontiers in Physiology*, 7: 101-113.

Muhammad Waqar A. 2012. Levels of heavy metals in popular cigarette brands and exposure to these metals via smoking. *The Scientific World Journal*, 10: 729430-729438.

Naidoo SVK, Bester MJ, Arbi S, *et al.*, 2019. Oral exposure to cadmium and mercury alone and in combination causes damage to the lung tissue of Sprague-Dawley rats. *Environmental Toxicology and Pharmacology*, 69: 86-94.

Needleman HL, Gunnoe C, Leviton A, *et al.*, 1979. Deficits in psychologic and classroom performance of children with elevated dentine lead levels. *The New England Journal of Medicine*, 300: 689-695.

Nickson C. 2020. Thromboelastogram (TEG) [Online]. *Life in the fastlane: Life in the fastlane*. Available: <https://litfl.com/thromboelastogram-teg/> Accessed: [20 September 2021].

Nordberg GF. 2009. Historical perspectives on cadmium toxicology. *Toxicology and Applied Pharmacology*, 238: 192-200.

Notariale R, Infantino R, Palazzo E, *et al.*,. 2021. Erythrocytes as a model for heavy metal-related vascular dysfunction: The protective effect of dietary components. *International Journal of Molecular Sciences*, 22: 6604-6611.

Oliveira TF, Batista PR, Leal MA, *et al.*,. 2019. Chronic cadmium exposure accelerates the development of atherosclerosis and induces vascular dysfunction in the aorta of ApoE^{-/-} mice. *Biological Trace Element Research*, 187: 163-171.

Patra RC, Swarup D and Dwivedi SK. 2001. Antioxidant effects of alpha tocopherol, ascorbic acid and L-methionine on lead induced oxidative stress to the liver, kidney and brain in rats. *Toxicology*, 162: 81-88.

Pizzino G, Irrera N, Cucinotta M, *et al.*,. 2017. Oxidative stress: Harms and benefits for human health. *Oxidative Medicine and Cellular Longevity*, 2017: 8416763-8416763.

Pretorius E and Lipinski B. 2013. Differences in morphology of fibrin clots induced with thrombin and ferric ions and its pathophysiological consequences. *Heart Lung Circulation*, 22: 447-449.

Pretorius E, Olumuyiwa-Akeredolu OO, Mbotwe S, *et al.*,. 2016. Erythrocytes and their role as health indicator: Using structure in a patient-orientated precision medicine approach. *Blood Reviews*, 30: 263-274.

Pritchard KA, Ackerman A and Kalyanaraman B. 2000. Chromium (VI) increases endothelial cell expression of ICAM-1 and decreases nitric oxide activity. *Journal of Environmental Pathology, Toxicology and Oncology*, 19: 251-260.

Prozialeck W and Edwards J. 2012. Mechanisms of cadmium-induced proximal tubule injury: New insight with implications for biomonitoring and therapeutic interventions. *Journal of Pharmacology and Experimental Therapeutics*, 343: 2-12.

Rudolph C, Rudolph A, Hostetter M, *et al.*,. 2003. Effects of lead. *Rudolph's Pediatrics*. United States of America: McGraw-Hill Publishers. pp 181-266

Ruttmann T. 2006. Coagulation for the clinician. *South African Journal of Science*, 44: 22-37.

Sender R, Fuchs S and Milo R. 2016. Revised estimates for the number of human and bacteria cells in the body. *Public Library of Science Biology*, 14: 1002533-1002533.

Shaper AG, Pocock SJ, Walker M, *et al.*,. 1982. Effects of alcohol and smoking on blood lead in middle-aged british men. *British Medical Journal*, 284: 299-302.

Simon F and Fernandez R. 2009. Early lipopolysaccharide-induced reactive oxygen species production evokes necrotic cell death in human umbilical vein endothelial cells. *Journal of Hypertension*, 27: 1202-1216.

Singh N, Gupta VK, Kumar A, *et al.*,. 2017. Synergistic effects of heavy metals and pesticides in living systems. *Frontiers in Chemistry*, 5: 70-73.

Sitas F, Urban M, Bradshaw D, *et al.*,. 2017. Tobacco attributable deaths in South Africa. *Tobacco Control*, 13: 396-399.

Steven S, Frenis K, Oelze M, *et al.*,. 2019. Vascular inflammation and oxidative stress: Major triggers for cardiovascular disease. *Oxidative Medicine and Cellular Longevity*, 2019: 7092151-7092159.

Stohs SJ, Bagchi D, Hassoun E, *et al.*,. 2001. Oxidative mechanisms in the toxicity of chromium and cadmium ions. *Journal of Environmental Pathology, Toxicology and Oncology*, 20: 77-88.

Swanepoel AC, Nielsen VG and Pretorius E. 2015. Viscoelasticity and ultrastructure in coagulation and inflammation: Two diverse techniques, one conclusion. *Inflammation*, 38: 1707-1726.

Swanepoel AC and Pretorius E. 2012. Scanning electron microscopy analysis of erythrocytes in thromboembolic ischemic stroke: Erythrocytes in thromboembolic stroke. *International Journal of Laboratory Hematology*, 34: 185-191.

Tabart J, Kevers C, Pincemail J, *et al.*,. 2009. Comparative antioxidant capacities of phenolic compounds measured by various tests. *Food Chemistry*, 113: 1226-1233.

Thakur M and Ahmed A. 2012. A review of thromboelastography. *International Journal of Perioperative Ultrasound and Applied Technologies*, 1: 25-29.

Thor MY, Harnack L, King D, *et al.*,. 2011. Evaluation of the comprehensiveness and reliability of the chromium composition of foods in the literature. *Journal of Food Composition and Analysis*, 24: 1147-1152.

Toda N and Toda H. 2010. Nitric oxide-mediated blood flow regulation as affected by smoking and nicotine. *European Journal of Pharmacology*, 649: 1-13.

Tsikis D. 2007. Analysis of nitrite and nitrate in biological fluids by assays based on the Griess reaction: Appraisal of the Griess reaction in the L-arginine/nitric oxide area of research. *Journal of Chromatography B: Analytical Technologies in the Biomedical and Life Sciences*, 851: 51-70.

Undas A and Ariëns RA. 2011. Fibrin clot structure and function: A role in the pathophysiology of arterial and venous thromboembolic diseases. *Arteriosclerosis, Thrombosis and Vascular Biology*, 31: 88-99.

Van Rooy M-J, Duim W, Ehlers R, *et al.*,. 2015. Platelet hyperactivity and fibrin clot structure in transient ischemic attack individuals in the presence of metabolic syndrome: A microscopy and thromboelastography ® study. *Cardiovascular diabetology*, 14: 86-86.

Vaziri ND and Ding Y. 2001. Effect of lead on nitric oxide synthase expression in coronary endothelial cells: role of superoxide. *Hypertension*, 37: 223-226.

Vellios N. 2021. South Africa - Country Profile [Online]. *Tabacco Tactics*. Available: <https://tobaccotactics.org/wiki/south-africa-country-profile/> Accessed: [15 September 2021].

Venter C, Oberholzer HM, Bester MJ, *et al.*,. 2017a. Ultrastructural, confocal and viscoelastic characteristics of whole blood and plasma after exposure to cadmium and chromium alone and in combination: An ex vivo study. *Cellular Physiology and Biochemistry*, 43: 1288-1300.

Venter C, Oberholzer HM, Cummings FR, *et al.*,. 2017b. Effects of metals cadmium and chromium alone and in combination on the liver and kidney tissue of male Sprague-Dawley

rats: An ultrastructural and electron-energy-loss spectroscopy investigation. *Microscopy Research and Techniques*, 80: 878-888.

Venter C, Oberholzer HM, Taute H, *et al.*,. 2015. An in ovo investigation into the hepatotoxicity of cadmium and chromium evaluated with light- and transmission electron microscopy and electron energy-loss spectroscopy. *Journal of Environmental Science & Health*, 50: 830-838.

Venugopal B and Luckey TD 2013. Toxicologic Significance of the Physicochemical Properties of Metals. *Physiologic and Chemical Basis for Metal Toxicity*. United States of America: Springer Publishers. pp 103-128

Virág L, Szabó E, Gergely P, *et al.*,. 2003. Peroxynitrite-induced cytotoxicity: Mechanism and opportunities for intervention. *Toxicology Letters*, 140: 113-124.

W.H.O. 2016. Lead poisoning and health [Online]. World Health Organization. Available: <https://www.who.int/en/news-room/fact-sheets/detail/lead-poisoning-and-health> Accessed: [9 March 2020 2020].

Watt J, Ewart M-A, Greig FH, *et al.*,. 2012. The effect of reactive oxygen species on whole blood aggregation and the endothelial cell-platelet interaction in patients with coronary heart disease. *Thrombosis Research*, 130: 210-215.

Witeska M, Kondera E and Szczygielska K. 2011. The effects of cadmium on common carp erythrocyte morphology. *Polish Journal of Environmental Studies*, 20: 783-788.

Xi-Biao Y, Hua F, Jin-Liang Z, *et al.*,. 1999. A study on oxidative stress in lead-exposed workers. *Journal of Toxicology and Environmental Health, Part A*, 57: 161-172.

Yang X, Stoffella P and He Z. 2005. Trace elements in agroecosystems and impacts on the environment. *Trace Elements Medical Biology*, 19: 125-140.

Yaprak E and Yolcubal I. 2019. Presence of toxic heavy metals in platelet-rich fibrin: A pilot study. *Biological Trace Element Research*, 191: 363-369.

Chapter 9

Chapter 9: Appendices

9.1. Ethical clearance certificate



Faculty of Health Sciences

Institution: The Research Ethics Committee, Faculty Health Sciences, University of Pretoria complies with ICH-GCP guidelines and has US Federal wide Assurance.

- FWA 00002567, Approved dd 22 May 2002 and Expires 03/20/2022.
- IORG #: IORG0001762 OMB No. 0990-0279 Approved for use through February 28, 2022 and Expires: 03/04/2023.

Faculty of Health Sciences Research Ethics Committee

15 July 2021

Approval Certificate Annual Renewal

Dear Miss L Pretorius

Ethics Reference No.: 377/2020

Title: Investigating the effect of the heavy metals cadmium, lead and chromium, alone and in combination on the components of the coagulation system

The **Annual Renewal** as supported by documents received between 2021-06-24 and 2021-07-14 for your research, was approved by the Faculty of Health Sciences Research Ethics Committee on 2021-07-14 as resolved by its quorate meeting.

Please note the following about your ethics approval:

- Renewal of ethics approval is valid for 1 year, subsequent annual renewal will become due on 2022-07-15.
- Please remember to use your protocol number (377/2020) on any documents or correspondence with the Research Ethics Committee regarding your research.
- Please note that the Research Ethics Committee may ask further questions, seek additional information, require further modification, monitor the conduct of your research, or suspend or withdraw ethics approval.

Ethics approval is subject to the following:

- The ethics approval is conditional on the research being conducted as stipulated by the details of all documents submitted to the Committee. In the event that a further need arises to change who the investigators are, the methods or any other aspect, such changes must be submitted as an Amendment for approval by the Committee.

We wish you the best with your research.

Yours sincerely



On behalf of the FHS REC, Dr R Sommers

MBChB, MMed (Int), MPharmMed, PhD

Deputy Chairperson of the Faculty of Health Sciences Research Ethics Committee, University of Pretoria

The Faculty of Health Sciences Research Ethics Committee complies with the SA National Act 61 of 2003 as it pertains to health research and the United States Code of Federal Regulations Title 45 and 46. This committee abides by the ethical norms and principles for research, established by the Declaration of Helsinki, the South African Medical Research Council Guidelines as well as the Guidelines for Ethical Research: Principles Structures and Processes, Second Edition 2015 (Department of Health)

9.2. Patient informed consent documents

PATIENT OR PARTICIPANT'S INFORMATION & INFORMED CONSENT DOCUMENT

STUDY TITLE: Investigating the effect of the heavy metals cadmium, lead and chromium, alone and in combination on the components of the coagulation system.

Principal Investigators: Liselle Pretorius (Principle investigator)

Supervision: Prof HM Oberholzer (Supervisor)
Dr H Taute (Co-Supervisor)
Dr M van Rooy (Co-Supervisor)

Institution: University of Pretoria

DAYTIME AND AFTER-HOURS TELEPHONE NUMBER(S):

Daytime numbers: Ms. L Pretorius: 078 101 7939
Prof Oberholzer: 012 319 2533

Afterhours: Ms. L Pretorius: 078 101 7939

DATE AND TIME OF FIRST INFORMED CONSENT DISCUSSION:

dd	mm	y	Time

Dear Mr. / Mrs. date of consent procedure/...../.....

1) INTRODUCTION

You are invited to volunteer for a research study. This information leaflet is to help you to decide if you would like to participate. Before you agree to take part in this study you should fully understand what is involved. If you have any questions, which are not fully explained in this leaflet, do not hesitate to ask the investigator. You should not agree to take part unless you are completely happy about all the procedures involved. In the best interests of your health, it is strongly recommended that you discuss with or inform your personal doctor of your possible participation in this study, wherever possible.

2) THE NATURE AND PURPOSE OF THIS STUDY

You are invited to take part in a research study. The aim of this study is to investigating the effect of the heavy metals cadmium, lead and chromium, alone and in combination on the components of the coagulation system.

3) EXPLANATION OF PROCEDURES TO BE FOLLOWED

This study involves answering some questions with regard to your health status.

Question	Answer	
	Yes	No
Are you older than 18?		
Are you taking any medication?		
Do you smoke?		

If you are older than 18, are not taking any medication and are a non-smoker we would like to collect two 5 ml tubes of blood. The tubes of blood will not be labelled with your name but a number will be assigned. This is done to ensure anonymity. In the laboratory, the blood will be exposed to different concentrations of each metal. The effect on the cells and the coagulation system will then be measured. Any blood left over after these measurements will be destroyed as biohazardous material.

4) RISK AND DISCOMFORT INVOLVED.

The only possible risk and discomfort involved is the taking of blood from a vein. Small bruising or mild soreness at the puncture site may be experienced for several days. Any risk is minimized by using pre-packaged sterilized equipment and with careful attention to proper technique.

5) POSSIBLE BENEFITS OF THIS STUDY.

Although you will not benefit directly from the study, the results of the study will add on to the pool of knowledge regarding the adverse effects of heavy metal exposure.

6) I MAY AT ANY TIME WITHDRAW FROM THIS STUDY.

7) HAS THE STUDY RECEIVED ETHICAL APPROVAL?

This Protocol was submitted to the Faculty of Health Sciences Research Ethics Committee, University of Pretoria, telephone numbers 012 356 3084 / 012 356 3085 and written approval has been granted by that committee. The study has been structured in accordance with the Declaration of Helsinki (last update: October 2013), which deals with the recommendations guiding doctors in biomedical research involving human/subjects. A copy of the Declaration may be obtained from the investigator should you wish to review it.

VERBAL PATIENT INFORMED CONSENT (applicable when patients cannot read or write)

I, the undersigned, Dr, have read and have explained fully to the patient, named and/or his/her relative, the patient information leaflet, which has indicated the nature and purpose of the study in which I have asked the patient to participate. The explanation I have given has mentioned both the possible risks and benefits of the study and the alternative treatments available for his/her illness. The patient indicated that he/she understands that he/she will be free to withdraw from the study at any time for any reason and without jeopardizing his/her treatment.

I hereby certify that the patient has agreed to participate in this study.

Patient's Name _____
(Please print)

Patient's Signature _____ Date _____

Investigator's Name _____
(Please print)

Investigator's Signature _____ Date _____

Witness's Name _____ Witness's Signature _____ Date _____
(Please print)

(Witness - sign that he/she has witnessed the process of informed consent)

9.3. Originality report

DECLARATION OF ORIGINALITY UNIVERSITY OF PRETORIA

The Department of Anatomy places great emphasis upon integrity and ethical conduct in the preparation of all written work submitted for academic evaluation.

Academics teach you about referencing techniques and how to avoid plagiarism; it is your responsibility to act on this knowledge. If you are at any stage uncertain as to what is required, you should speak to your lecturer before any written work is submitted.

You are guilty of plagiarism if you copy something from another author's work (e.g. a book, an article or a website) without acknowledging the source and pass it off as your own. In effect you are stealing something that belongs to someone else. This is not only the case when you copy work word-for-word (verbatim) but also when you submit someone else's work in a slightly altered form (paraphrase) or use a line of argument without acknowledging it.

Students who commit plagiarism will not be given any credit for plagiarised work. The matter may also be referred to the Disciplinary Committee (Students) for a ruling. Plagiarism is regarded as a serious contravention of the University's rules and can lead to expulsion from the University.

The declaration which follows must accompany all written work submitted while you are a student of the Department of Anatomy No written work will be accepted unless the declaration has been completed and submitted.

Full names and surname of student: Lisele Pretorius

Student number: 16004273

Topic of work: Investigating the effects of the heavy metals cadmium, lead and chromium, alone and in combination on the components of the coagulation system.

Declaration

1. I understand what plagiarism is and am aware of the University's policy in this regard.
2. I declare that this dissertation (e.g. essay, report, project, assignment, dissertation, thesis, etc) is my own original work. Where other people's work has been used (either from a printed source, Internet or any other source), this has been properly acknowledged and referenced in accordance with departmental requirements.



SIGNATURE

15/12/2021

DATE